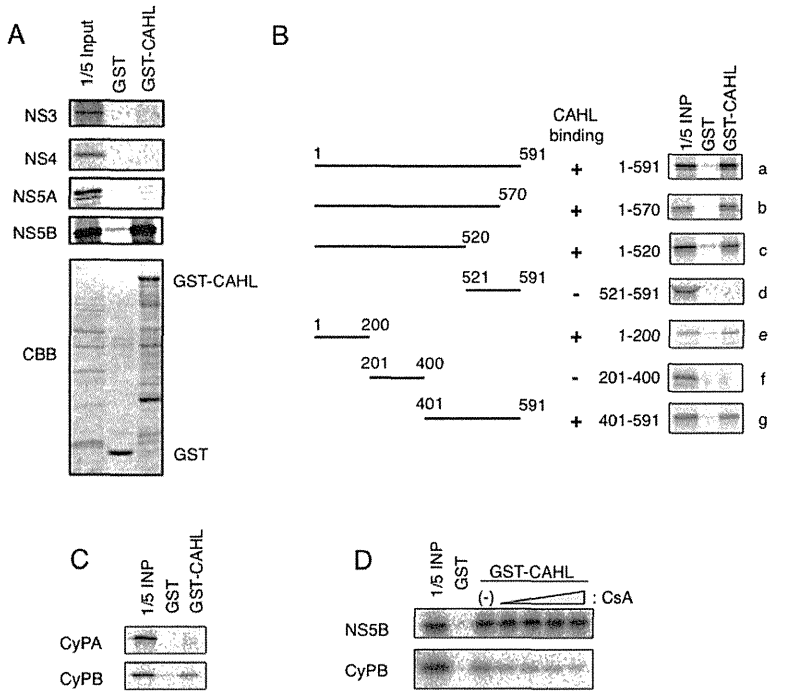

Figure 4. CAHL interacted with HCV NS5B and CyPB. (A) [^{35}S]-labeled in vitro translation products of HCV NS3, NS4B, NS5A, and NS5B were incubated with a recombinant GST fusion protein of CAHL (GST-CAHL) or GST as a negative control. "1/5 input" designates the signal for 1/5 the amount of the [^{35}S]-labeled product used in the pull-down assay. CBB staining patterns for the pulled-down proteins are shown in the bottom panel. (B) Mapping of the regions of NS5B responsible for the interaction with CAHL. At the left of the panel, schematic representations of the full-length and truncated mutants of NS5B are shown. The numbers indicate the amino acid residue numbers in NS5B. "CAHL binding" summarizes the results of the GST pull-down assay by +/−. GST pull-down data are presented as described in (A). (C) GST pull-down assay between GST-CAHL and in vitro translated CyPA or CyPB was performed as described in (A). (D) The interaction of CAHL with CyPB was disrupted by CsA treatment. GST pull-down assay between GST-CAHL and NS5B was performed in the absence and presence of CsA. The concentrations of CsA in lanes 4–7 are 1, 2, 8, and 20 μg/ml, respectively.
doi:10.1371/journal.pone.0018285.g004

specific for the CAHL gene (si-1, -2, -3, -4, and -5) were individually transfected into MH-14 cells to examine RNA sequence induced effectively down-regulation. When si-3 siRNA was transfected into cells, the endogenous CAHL gene expression reduced approximately 90% compared with si-control (treatment with siRNA for non-target gene) (Fig. S3), and among them, si-3 induced down-regulation of CAHL gene expression most effectively. Subsequently, we applied short hairpin RNA (shRNA) technology to stably knockdown CAHL gene expression in MH14 cells. We cloned DNA oligo coding the effective siRNA against CAHL gene into pLKO.1-puro shRNA vector. Lentivirus packed with shRNA against CAHL (sh-CAHL) or non-targeting shRNA (sh-control) were introduced into MH14 cells, and then these cells were cultured in the presence puromycin. As a result, we successfully obtained stably CAHL gene knockdown cell line, which reduced approximately to 6-fold compared with sh-control (Fig. 5A). In these sh-CAHL cells, HCV RNA was decreased approximately to 4-fold less than that in the sh-control cells (Fig. 5B). Furthermore, ectopic expression of CAHL increased the HCV replication level in a dose-dependent manner (Fig. 5C). These results suggest that CAHL positively plays in HCV replication.

To investigate the outcome of the interaction of CAHL with NS5B/CyPB, we performed RNA binding activity assay using sh-CAHL cells. NS5B is a viral RNA-dependent RNA polymerase and possesses RNA binding activity [11]. Indeed, NS5B formed a complex on RNA-immobilized sepharose together with CyPB and CAHL (lane 4 in Fig. 6A). However, shRNA-mediated depletion of endogenous CAHL dissociated CyPB from the NS5B/RNA complex (lane 6 in Fig. 6A), indicating that CAHL mediates the association of CyPB with NS5B/RNA. Moreover, when CsA was added to sh-CAHL cells, both CAHL and CyPB were dissociated from RNA (lane 6 in Fig. 6B). Thus, the possibility is suggested that the promotion of CyPB-NS5B complex association by CAHL is related with the stimulatory role of CAHL in HCV replication.

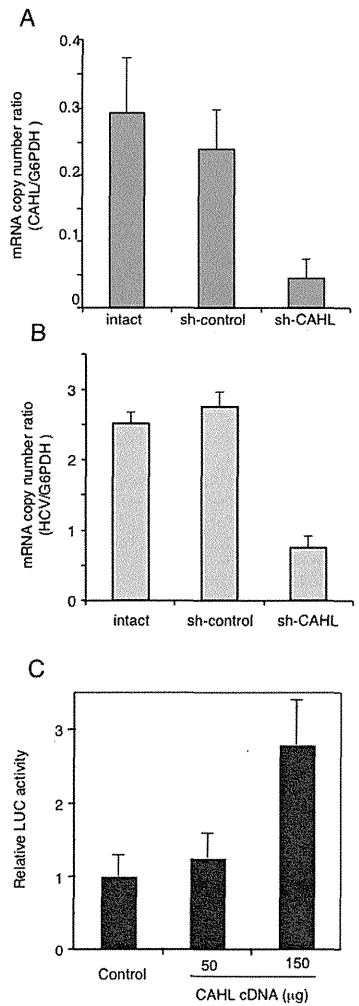

Figure 5. Establishment stably CAHL knockdown cell. (A) Lentivirus packed with shRNA against CAHL (sh-CAHL) or non-targeting shRNA (sh-control) were introduced into MH14 cells. Total RNAs were harvested and the absolute mRNA copy numbers of CAHL were examined by quantitative real time RT-PCR. (B) The same samples of total RNAs were used for the measurement of the absolute RNA copy number of the HCV genome by quantitative real time RT-PCR. (C) Cured MH-14 cells were transfected with LMH14 RNA reporter together with the expression plasmid for CAHL or the corresponding empty vector. At four days post-transfection, luciferase activities were measured. These results (A–C) represent the means of three independent experiments.
doi:10.1371/journal.pone.0018285.g005

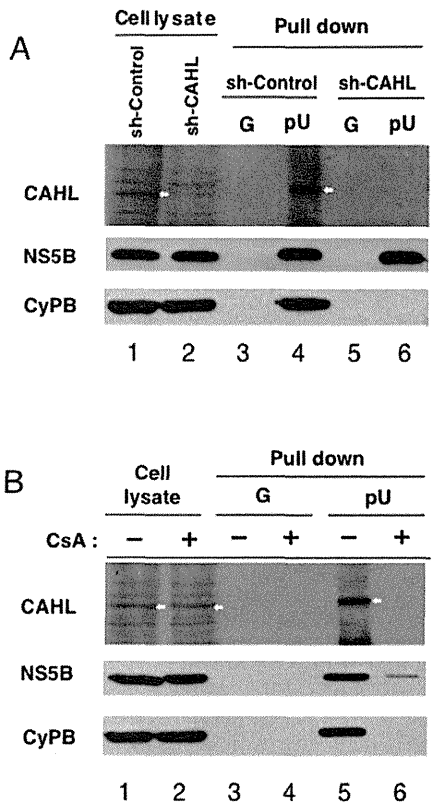

Figure 6. CAHL associated with the CyPB/NS5B complex plays critical roles in HCV replication. (A) Cells (sh-control or sh-CAHL cells) were harvested and analyzed protein expressions by using anti-CAHL, anti-NS5B, and anti-CyPB antibodies. White arrows indicate CAHL protein. (B) Cells were treated with or without 2 μg/ml CsA for 24 h, and then harvested and analyzed. These results were reproduced in three independent experiments. White arrows indicate CAHL protein.
doi:10.1371/journal.pone.0018285.g006

Discussion

Phage display, invented by Smith and Petrenko, is a versatile method for the detection of small molecule-binding proteins [14]. The technique can also be used to identify binding sites within the target protein itself. The combination of screening a library of phage-displayed peptides and analysis of affinity-selected peptides is anticipated to become a powerful tool for identifying drug-binding sites [15–19]. Screening phage display libraries generally entails immobilizing the drug onto a solid surface [20]. In the conventional method of phage display, small molecules should be converted into biotinylated derivatives and immobilized on a streptavidin-coated matrix. Conventional immobilization requires

the presence of desirable functional groups within the drug molecule as well as a multistep process to prepare the biotinylated derivatives. In contrast to biotinylation, photoimmobilization makes it possible to covalently immobilize drugs on a solid surface without the need for derivatization. We and Kanoh *et al.* have reported the affinity purification of proteins using affinity matrices, in which small molecules are photoimmobilized by photoreaction [12,21]. Because the photoreaction proceeds in a functional group-independent manner, the molecules are immobilized onto the solid surface in a nonoriented fashion. Thus, photoimmobilization can be a useful tool for the comprehensive analysis of drug-binding proteins.

Using this method, we identified CAHL as a novel target protein for CsA. CsA is a natural compound showing multiple biological activities, including an immunosuppressive function, anti-chaperone activity, inhibition of transporter activity and antiviral activity against human immunodeficiency virus and HCV. Thus far, p-glycoprotein and formyl peptide receptor, as well as CyPs, were reported as binding proteins for CsA [22], which enabled elucidation of the mechanism of the CsA-induced immunosuppressive function, anti-chaperone activity and anti-transporter activity, respectively. Although CyPA promotes HCV replication [11,23,24], we cannot fully explain the whole mode of action of CsA against HCV. CyPB is also reported to regulate HCV replication. It was reported that the HCV replicon showing resistance against the CsA-mediated anti-HCV effect possessed mutations in the coding region for NS5A and NS5B [25,26], indicating that NS5B was one of the determinants for the sensitivity to CsA. However, some such mutations within the NS5B coding region were dropped outside the region interacting with CyPA and CyPB [11,24], leading to the possibility that another cellular protein which is targeted by CsA, binds to NS5B and regulates HCV replication. The CAHL-NS5B regulation machinery is consistent with this idea. Deletion analysis for NS5B demonstrated that two separate regions (1-200aa and 401-520aa) of NS5B are likely to be involved in the interaction with CAHL. These regions are different from the NS5B domain interacting with CyPB (521-591aa) [11], suggesting that NS5B would interact with both CyPB and CAHL at the same time. Indeed, the mutations that induced resistant to CsA, the I432V in NS5B reside inside the regions interacting with CAHL (1-200 aa and 401-520 aa) [26], supported the relevance of CAHL in HCV genome replication. As another aspect, it is interesting that two CsA target molecules interact with each other and NS5B. Although we do not know in detail the implication of the interaction of these two CsA target molecules, CyPB and CAHL, there is a similar example already known: two FK506-binding proteins, P-glycoprotein (P-gp) and FKBP42, associate with each other [27]. In this situation, FKBP42 modulates P-gp function. We do not know in detail how these two target molecules of CsA, CyPB and CAHL both regulate NS5B function, which is a future subject of the study. Currently, a CsA derivative shows remarkable anti-HCV effect in chronic HCV-infected patients in the phase II clinical trial, and its mode of action needs to be fully clarified [28]. Our data suggest a new link of CAHL, in addition to CyP family, with CsA derivative's anti-HCV activity.

Cellular RNA helicases have been reported to be involved in HCV genome replication. DDX3 and DDX6 activate HCV genome replication through yet unknown mechanism [29,30]. RNA helicase p68 (DDX5) interacts with NS5B and supports HCV genome replication in a transient transfection assay [31]. Although the mechanism through which each RNA helicase regulates HCV genome replication may be different, the requirement of cellular RNA helicases for HCV genome replication is interesting for understanding HCV-cellular factors interaction.

CAHL expression in normal liver cells was much less than that in HCV infectious cells such as Huh-7 and MH-14. This is enigmatic since it is not clear how HCV replication start without CAHL, which positively plays HCV replication, at very beginning of HCV infection in normal liver cells. It was reported that a proinflammatory cytokine, TNF-α gene expression in hepatocytes and mononuclear cells derived from HCV carrier increased compared with healthy control [32]. As we here demonstrated CAHL induced by TNF-α, CAHL can express to some extent in the liver under chronic hepatitis C. We also show the association of CAHL with HCV replication. Taken together, CAHL may form a positive feedback loop for HCV replication: CAHL gene expression is induced by TNF-α that is highly upregulated by HCV infection, and CAHL in turn promotes HCV replication. Despite the low expression of CAHL in normal tissues, CAHL may have strong potential as a pharmaceutical target protein. In addition to CsA, isolation of specific inhibitors to the interaction of CAHL and NS5B could allow us to provide effective drug for HCV treatment.

In conclusion, we took advantage of strategy of chemical biology to isolate a cellular factor, CAHL, as CsA associated helicase-like protein, which would form trimer complex with CyPB and NS5B of HCV. These findings not only shed a light on new HCV treatment but also brought about great values of chemical biology to elucidate biological mechanisms of small-molecule and protein interactions.

Materials and Methods

Preparation of CsA-immobilized resins

CsA was purchased from Wako Pure Chemical Industries, Ltd. (Osaka, Japan). CsA-immobilized resins were prepared on photoaffinity resins as described previously [12]. Photoaffinity resins treated with UV irradiation in the absence of CsA were used for negative control.

Phage display screening

10 mg of CsA-immobilized resin was incubated in 1 ml of TBS (50 μM Tris-HCl [pH 8.0] and 150 mM NaCl) for 12 hours or longer before use. Phage screening conditions were performed as previously described [20]. For each panning step, 50 μl of CsA-immobilized resin slurry was added to 1 ml of the T7 phage ($>10^{11}$ pfu) followed by incubation for 8 hours at 4°C. After incubation, the bead slurry was washed 10 times by adding 1 ml of TBST (50 mM Tris-HCl [pH = 8.0], 150 mM NaCl, 0.1% Tween 20). To elute phage particles associated with resins, 100 μl of *Escherichia coli* ($OD_{600} = 0.6$) was added, and incubated for 10 min at 37°C. The phage infected *E. coli* were transferred into 1 ml of *E. coli* ($OD_{600} = 0.6$) and grown until lysed for three hours at 37°C with shaking. For titer check, 10 μl of infected *E. coli* was used.

RNA preparation and plasmid construction

To isolate the CAHL gene, we used total RNA derived from human liver. DNA cloning of the CAHL gene was carried out using a SMART-cDNA isolation kit following the manufacturer's instructions (Clontech Laboratories, CA, USA). In some cases, CAHL cDNA was reconstructed with pcDNA 3.1 myc-HisA (Invitrogen Corp., CA, USA) for overexpression experiments.

Surface plasmon resonance assay

SPR analysis was performed on a BIAcore 3000 (Biacore AB, Uppsala, Sweden). The bacterially expressed CAHL-C was immobilized covalently on a hydrophilic carboxymethylated dextran matrix on a CM5 sensor chip (Biacore AB) using a standard amine coupling reaction in 10 mM CH_3COONa [pH = 4.0]. Binding analyses were carried out in HBS-EP buffer (10 mM HEPES [pH = 7.4], 150 mM NaCl, 3.4 mM EDTA, 0.005% surfactant P20) containing 8% DMSO at a flow rate of 20 μl/min. Appropriate concentrations of CsA were injected over the flow cell. CyPA or CyPB was not used as a positive control because of two reasons: 1) those CyPs can be used for a positive control as CsA-CyP binding, but not for CsA-CAHL binding, and 2) FK506 doesn't bind CyPs, so that it is difficult to compare association behaviors between FK506 and CsA. The bulk effects of DMSO were subtracted using reference surfaces. To derive binding constants, data were analyzed by means of global fitting using BIAevaluation version 3.1 (Biacore AB).

Preparation of recombinant protein

CAHL-C cDNA encoding C-terminal 761 to1430 amino acids was constructed into pET21a prokaryotic expression vector (Merck, Darmstadt, Germany), which has a His-tag. pET21-CAHL-C construct was transformed into *E.coli* BL21(DE3) strain. After overnight induction with 0.1 mM IPTG at 20°C, recombinant CAHL-C was purified by nickel column chromatography with HisTrap (Amersham biosciences, Uppsala, Sweden) according to a manufacturer's procedure. To concentrate and exchange the buffer, purified CAHL-C was concentrated up to 40 times with PBS by using Amicon Ultra 30 (Millipore, EMD, Germany).

ATPase assay

ATPase activity was measured as described by Okanami *et al.* [33]. Briefly, CAHL-C protein (500 ng) was incubated in 50 μl of helicase/ATPase buffer containing 1 μl of [γ-^{32}P]ATP (1 Ci/μmol) in the presence or absence of 100 ng of total RNA derived from liver at 30°C for 30, 60, and 180 min. An aliquot (10 μl) was removed at the appropriate time and added to 200 ml of a solution containing 50 mM HCl, 5 mM H_3PO_4 and 7% activated charcoal. After the charcoal was precipitated by centrifugation to remove unreacted ATP, 10 μl of the supernatant was subjected to Cerencov counting to quantitate released [^{32}P]phosphate.

Northern blot analysis and reverse transcription PCR (RT-PCR) analysis

Tumor cell-derived total RNA was prepared using an RNeasy Mini Kit (QIAGEN Inc., Hilden, Germany) according to the manufacturer's instructions and then reverse-transcribed to cDNA with Transcriptor First Strand cDNA Synthesis Kit (Roche Applied Science, Mnnheim, Germany). A reverse-transcribed single strand DNA library of normal tissues was purchased from Clontec, Inc. (CA, USA). In Northern blot analysis, RNA samples were loaded to formaldehyde agarose gels and transferred onto a Hybond N membrane (GE Healthcare UK Ltd., Buckinghamshire, England). After UV-crosslinking, the membrane was hybridized with ^{32}P-labeled (Rediprime II, GE Healthcare) gene-specific probe, regions of $CAHL_{2913-4431}$ and human $G6PDH_{451-2016}$ and exposed to film for autoradiography. Measurement of CAHL gene expression by polymerase chain reaction (PCR) was performed using GoTaq Flexi DNA Polymerase (Promega, Co. WI, U.S.A.) and primer sets: forward primer, 5′-GACGGGAAAGGATTGGTCAA-3′ and reverse primer, 5′-CATCACTTCGTGCTTTTT-3′ for detection of CAHL, and forward primer, 5′-GACGAAGCGCAGACAGCGTCATGGCA-3′ and reverse primer, 5′-GCTTGTGGGGGTTCACCCACTTG-3′ for detection of G6PDH.

Quantitative real-time RT-PCR analysis

Total RNAs reverse-transcribed to cDNA were prepared as described above. Measurement of gene expression by quantitative analysis was performed using the LightCycler system (Roche Applied Science). Primers and hybridization probes were synthesized by Nihon Gene Research Laboratory Inc. (Sendai, Japan). Quantitative real time RT-PCR analyses of human glucose-6-phosphate dehydrogenase (G6PDH) and cyclosporin A associated helicase-like protein (CAHL, NM_022828) gene expression were performed using the LightCycler® FastStart DNA MasterPLUS SYBR Green I system (Roche Applied Science) with the following primer sets: forward primer, 5′-CTGCGTTATCCTCACCTTC-3′ and reverse primer, 5′-CGGACGTCATCTGAGTTG-3′ for detection of human G6PDH; forward primer, 5′-GTGT-CTGGACCCCATCCTTA-3′and reverse primer, 5′-CCCAT-CACTTCGTGCTTTTT-3′for detection of CAHL. Gene expression analysis of the HCV genome was performed using the LightCycler® FastStart DNA Master HybProbe system (Roche Applied Science) with the following primer set and probe: forward primer, 5′-CGGGAGAGCCATAGTGG-3′ and reverse primer, 5′-AGTACCACAAGGCCTTTCG-3′, and the fluorogenic probe, 5′-CTGCGGAACCGGTGAGTACAC-3′. PCR amplification of the housekeeping gene, G6PDH, was performed for each sample as control for sample loading and to allow normalization among samples. To determine the absolute copy number of the target transcripts, the fragments of G6PDH or target genes amplified by PCR using the above described primer set were constructed with pCR4®-TOPO® cloning vector (Invitrogen). The concentrations of these purified plasmids were measured by absorbance at 260 nm and copy numbers were calculated from concentration of samples. A standard curve was created by plotting the threshold cycle (Ct) versus the known copy number for each plasmid template in the dilutions. The copy numbers for all unknown samples were determined according to the standard curve using LightCycler version 3.5.3 (Roche Applied Science). To correct for differences in both RNA quality and quantity between samples, each target gene was first normalized by dividing the copy number of the target by the copy number of G6PDH, so that the mRNA copy number of the target was the copy number per the copy number of G6PDH. The initial value was also corrected for the amount of G6PDH indicated as 100% to evaluate the sequential alteration of the mRNA expression level.

Cell culture and transfection of siRNA and cDNA

The human tumor cell lines of breast adenocarcinoma MDA-MB-231, lung adenocarcinoma A-549, colon adenocarcinoma WiDr, hepatocellular carcinoma Huh-7, breast cancer SKBR3, cervical carcinoma HeLa, esophagus cancer KE-4, colon adenocarcinoma SW480, lung cancer Lu65, and esophagus squamous cell carcinoma TE-8 were obtained from Health Science Research Resources Bank (Sendai, Japan). These cells were cultured in Dulbecco's modified Eagle's medium (Huh-7, SKBR3, HeLa, KE-4, and SW480 cells), RPMI 1640 (A-549, WiDr, TE-8, and Lu65 cells) (SIGMA-ALDRICH, MO, USA), and Leibovitz's L15 (MDA-MB-231 cells) (Invitrogen) supplemented with 10% fetal bovine serum, MEM nonessential amino acids (Invitrogen), 200 unit/ml penicillin (Invitrogen), 200 μg/ml streptomycin (Invitrogen) and 2 mM L-glutamine (Invitrogen). MH-14 cells carrying the HCV subgenomic replicon [34] were cultured in the DMEM medium supplemented with 10% fetal bovine serum, MEM nonessential amino acids (Invitrogen), 200 unit/ml penicillin (Invitrogen), 200 μg/ml streptomycin (Invitrogen), 2 mM L-glutamine (Invitrogen) and 300 μg/ml G418 (Invitrogen). Five small interfering RNA (siRNA) duplexes containing 3′dTdT over

the hanging sequence were synthesized (Sigma-Aldrich, St. Louis, MO). These sequences were: si-1; 5′-GGACAUUCGCAUUGAUGAG-3′, si-2; 5′-CCUGUAAUUUGACUCAUAA-3′, si-3; 5′- GCCUUGGAUGUAAAUCUCUUU -3′, si-4; 5′- GGAGCUUUCAGUGACCAUA -3′, si-5; 5′-GGUCAAAUAAUAGUAGGAA-3′. A non-targeting siRNA (Sigma-Aldrich) was used as control. Plasmid and siRNA transfection was performed described previously [35]. In siRNA study, total RNAs from transfected cells were harvested after transfection for 5 days and examined mRNA copy number of CAHL by quantitative real-time RT-PCR.

Establishment of stable CAHL-knockdown cell by shRNA

Based on the siRNA data, we applied short hairpin RNA (shRNA) technology platform (Sigma Mission*RNAi*) to stably knockdown CAHL gene expression in MH14 cells. DNA oligo coding the effective siRNAs against each MH14-CAHL gene (5′-CCGGGCCTTGGATGTAAATCTCTTTCTCGAGAAAGAGATTTACATCCAAGGCTTTTTTG -3′) (sh-CAHL) was cloned into pLKO.1-puro shRNA vector. Plasmid DNA including non-targeting shRNA as control (sh-control) was transfected into MH14 cells along with Lentiviral Packaging Mix consisting of an envelope and packaging vector (Sigma-Aldrich) to produce lentivirus packed with shRNA cassettes using the standard procedure. After transfection, cells were cultured in the presence of 10 μg/ml puromycin.

Indirect immunofluorescence analysis

Anti-CAHL polyclonal antibody serum was generated in rabbits immunized with $CAHL_{1237\text{-}1251}$, ILHPKRGTEDRSDQS, according to our lab protocol [35]. Anti-NS3, NS4B, and NS5B, and NS5A were kindly provided from Dr. Kohara at The Tokyo Metropolitan Institute of Medical Science, Japan and Dr. Takamizawa at Osaka University, Japan, respectively. Cells were fixed with ice-cold acetone for 1 min, and then stained with anti-CAHL and anti-KDEL mAb (Santa Cruz Biotechnology, CA, USA) for ER antibodies followed by Alexa Fluor 488-conjugated goat anti-rabbit IgG and 594-conjugated goat anti-mouse IgG (Invitrogen), respectively, and visualized using a Bio-Rad MRC1024ES *laser confocal scanning microscopy system* (Bio-Rad Laboratories, CA, USA).

Immunoblot analysis

Immunoblot analysis was performed essentially as described previously [11,36].

RNA-protein binding precipitation assay

RNA-protein binding precipitation assay was essentially performed as described [11]. Briefly, to permeabilize plasma membrane, cells were treated 50 μg/ml digitonin (Nakarai Tesque Inc., Kyoto, Japan) in buffer B (20 mM HEPES-KOH [pH = 7.7], 110 mM KOAc, 2 mM MgOAc, 1 mM EGTA) at 25°C for 5 min. After treatment with 0.5 μg/ml proteinase K at 37°C for 5 min and washing with buffer B, cells were lysed in IP buffer (50 mM Tris-HCl [pH = 8], 150 mM NaCl, 0.5% NP-40, and protease inhibitory cocktail [Roche Applied Science]). After centrifugation, supernatants were incubated for 2 h with poly-U or protein G Sepharose resin (GE Healthcare). After four washes with IP buffer, precipitates were analyzed by immunoblot analysis. Supernatants after centrifugation were used as a positive control (designated Cell lysate in Fig. 4E and 4D).

GST-pull-down assay

GST-pull-down assay was performed as described previously [36].

Supporting Information

Figure S1 Predicted amino acid sequences of CAHL (NM_022828). Underlined residues (LLGQLRA) indicate identical sequence of phage clone #13.
(TIFF)

Figure S2 Indirect immunoflourescence analysis for colocalized with between CAHL and NS3, NS4A, NS4B, NS5A, and NS5B using Huh-7 (A) and MH-14 (B). The primary antibodies used were anti-CAHL (panels a, d, g, j, and m, green) and anti-NS proteins (panels b, e, h, k, and n, red) antibodies. Marge images of green and red signals are shown in panels c, f, i, l, and o.
(TIFF)

Figure S3 Determinant of knockdown efficiency against CAHL gene expression. Five siRNAs for the CAHL gene were individually transfected into MH-14 cells. After transfection, total RNAs of these cells were collected and examined mRNA copy number of CAHL by quantitative real-time RT-PCR.
(TIFF)

Table S1 List of phage clones and their encoding deduced peptide sequences screened by CsA biopanning. *Asterisk indicates the identical sequences.
(DOCX)

Author Contributions

Conceived and designed the experiments: KM HS KW K. Shimotohno SK K. Sakaguchi FS. Performed the experiments: KM HS KW KI TS KK KT HM AT. Analyzed the data: NS. Wrote the paper: KM HS KW FS.

References

1. Calne RY, White DJ, Thiru S, Evans DB, McMaster P, et al. (1978) Cyclosporin-A in patients receiving renal allografts from cadaver donors. Lancet 2: 1323–1327.
2. O'Keefe SJ, Tamura J, Kincaid RL, Tocci MJ, O'Neill EA (1992) FK-506- and CsA-sensitive activation of the interleukin-2 promoter by calcineurin. Nature 357: 692–694.
3. Clipstone NA, Crabtree GR (1992) Identification of calcineurin as a key signalling enzyme in T-lymphocyte activation. Nature 357: 695–697.
4. Liu J, Farmer JD, Jr., Lane WS, Friedman J, Weissman I, et al. (1991) Calcineurin is a common target of cyclophilin-cyclosporin A and FKBP-FK506 complexes. Cell 66: 807–815.
5. Fruman DA, Klee CB, Bierer BE, Burakoff SJ (1992) Calcineurin phosphatase activity in T lymphocytes is inhibited by FK 506 and cyclosporin A. Proc Natl Acad Sci U S A 89: 3686–3690.
6. Fischer G, Tradler T, Zarnt T (1998) The mode of action of peptidylprolyl cis/trans isomerases *in vivo*: binding vs. catalysis. FEBS Lett 426: 17–20.
7. Braaten D, Luban J (2001) Cyclophilin A regulates HIV-1 infectivity, as demonstrated by gene targeting in human T cells. EMBO J 20: 1300–1309.
8. Waldmeier PC, Zimmermann K, Qian T, Tintelnot-Blomley M, Lemasters JJ (2003) Cyclophilin D as a drug target. Curr Med Chem 10: 1485–1506.
9. Hanoulle X, Badillo A, Wieruszeski JM, Verdegem D, Landrieu I, et al. (2009) Hepatitis C virus NS5A protein is a substrate for the peptidyl-prolyl cis/trans isomerase activity of cyclophilins A and B. J Biol Chem 284: 13589–13601.
10. Liu Z, Yang F, Robotham JM, Tang H (2009) Critical role of cyclophilin A and its prolyl-peptidyl isomerase activity in the structure and function of the hepatitis C virus replication complex. J Virol 83: 6554–6565.
11. Watashi K, Ishii N, Hijikata M, Inoue D, Murata T, et al. (2005) Cyclophilin B is a functional regulator of hepatitis C virus RNA polymerase. Mol Cell 19: 111–122.
12. Kuramochi K, Haruyama T, Takeuchi R, Sunoki T, Watanabe M, et al. (2005) Affinity capture of a mammalian DNA polymerase beta by inhibitors immobilized to resins used in solid-phase organic synthesis. Bioconjug Chem 16: 97–104.
13. Aoki S, Morohashi K, Sunoki T, Kuramochi K, Kobayashi S, et al. (2007) Screening of paclitaxel-binding molecules from a library of random peptides displayed on T7 phage particles using paclitaxel-photoimmobilized resin. Bioconjug Chem 18: 1981–1986.
14. Smith GP, Petrenko VA (1997) Phage Display. Chem Rev 97: 391–410.
15. Rodi DJ, Soares AS, Makowski L (2002) Quantitative assessment of peptide sequence diversity in M13 combinatorial peptide phage display libraries. J Mol Biol 322: 1039–1052.
16. Mandava S, Makowski L, Devarapalli S, Uzubell J, Rodi DJ (2004) RELIC--a bioinformatics server for combinatorial peptide analysis and identification of protein-ligand interaction sites. Proteomics 4: 1439–1460.
17. Rodi DJ, Mandava S, Makowski L (2004) DIVAA: analysis of amino acid diversity in multiple aligned protein sequences. Bioinformatics 20: 3481–3489.
18. *Makowski L, Rodi DJ (2003) Genome-wide characterisation of the binding* repertoire of small molecule drugs. Hum Genomics 1: 41–51.
19. Aoki S, Ohta K, Yamazaki T, Sugawara F, Sakaguchi K (2005) Mammalian mitotic centromere-associated kinesin (MCAK): a new molecular target of sulfoquinovosylacylglycerols novel antitumor and immunosuppressive agents. FEBS J 272: 2132–2140.
20. Morohashi K, Yoshino A, Yoshimori A, Saito S, Tanuma S, et al. (2005) Identification of a drug target motif: an anti-tumor drug NK109 interacts with a PNxxxxP. Biochem Pharmacol 70: 37–46.
21. Kanoh N, Honda K, Simizu S, Muroi M, Osada H (2005) Photo-cross-linked small-molecule affinity matrix for facilitating forward and reverse chemical genetics. Angew Chem Int Ed Engl 44: 3559–3562.
22. Loor F, Tiberghien F, Wenandy T, Didier A, Traber R (2002) Cyclosporin: structure-activity relationships for the inhibition of the human FPR1 formyl peptide receptor. J Med Chem 45: 4613–4628.
23. Yang F, Robotham JM, Nelson HB, Irsigler A, Kenworthy R, et al. (2008) Cyclophilin A is an essential cofactor for hepatitis C virus infection and the principal mediator of cyclosporine resistance in vitro. J Virol 82: 5269–5278.
24. Chatterji U, Bobardt M, Selvarajah S, Yang F, Tang H, et al. (2009) The isomerase active site of cyclophilin A is critical for hepatitis C virus replication. J Biol Chem 284: 16998–17005.
25. Fernandes F, Poole DS, Hoover S, Middleton R, Andrei AC, et al. (2007) Sensitivity of hepatitis C virus to cyclosporine A depends on nonstructural proteins NS5A and NS5B. Hepatology 46: 1026–1033.
26. Robida JM, Nelson HB, Liu Z, Tang H (2007) Characterization of hepatitis C virus subgenomic replicon resistance to cyclosporine in vitro. J Virol 81: 5829–5840.
27. Bouchard R, Bailly A, Blakeslee JJ, Oehring SC, Vincenzetti V, et al. (2006) Immunophilin-like TWISTED DWARF1 modulates auxin efflux activities of Arabidopsis P-glycoproteins. J Biol Chem 281: 30603–30612.
28. Flisiak R, Feinman SV, Jablkowski M, Horban A, Kryczka W, et al. (2009) The cyclophilin inhibitor Debio 025 combined with PEG IFNalpha2a significantly reduces viral load in treatment-naive hepatitis C patients. Hepatology 49: 1460–1468.
29. Ariumi Y, Kuroki M, Abe K, Dansako H, Ikeda M, et al. (2007) DDX3 DEAD-box RNA helicase is required for hepatitis C virus RNA replication. J Virol 81: 13922–13926.
30. Jangra RK, Yi M, Lemon SM (2010) Regulation of hepatitis C virus translation and infectious virus production by the microRNA miR-122. J Virol 84: 6615–6625.
31. Goh PY, Tan YJ, Lim SP, Tan YH, Lim SG, et al. (2004) Cellular RNA helicase p68 relocalization and interaction with the hepatitis C virus (HCV) NS5B protein and the potential role of p68 in HCV RNA replication. J Virol 78: 5288–5298.
32. Larrea E, Garcia N, Qian C, Civera MP, Prieto J (1996) Tumor necrosis factor a gene expression and the response to interferon in chronic hepatitis C. *Hepatology* 23: 210–217.
33. Okanami M, Meshi T, Iwabuchi M (1998) Characterization of a DEAD box ATPase/RNA helicase protein of *Arabidopsis thaliana*. Nucleic Acids Res 26: 2638–2643.
34. Watashi K, Hijikata M, Hosaka M, Yamaji M, Shimotohno K (2003) Cyclosporin A suppresses replication of hepatitis C virus genome in cultured hepatocytes. Hepatology 38: 1282–1288.
35. Imai A, Sahara H, Tamura Y, Jimbow K, Saito T, et al. (2007) Inhibition of endogenous MHC class II-restricted antigen presentation by tacrolimus (FK506) via FKBP51. Eur J Immunol 37: 1730–1738.
36. Watashi K, Hijikata M, Tagawa A, Doi T, Marusawa H, et al. (2003) Modulation of retinoid signaling by a cytoplasmic viral protein via sequestration of Sp110b, a potent transcriptional corepressor of retinoic acid receptor, from the nucleus. Mol Cell Biol 23: 7498–7509.

Available online at www.sciencedirect.com
ScienceDirect
Current Opinion in Virology

Lipoprotein component associated with hepatitis C virus is essential for virus infectivity

Yuko Shimizu[1,3], Takayuki Hishiki[1,3], Saneyuki Ujino[1], Kazuo Sugiyama[2], Kenji Funami[1] and Kunitada Shimotohno[1]

Many chronic hepatitis patients with hepatitis C virus (HCV) are observed to have a degree of steatosis which is a factor in the progression of liver diseases. Transgenic mice expressing HCV core protein develop liver steatosis before the onset of hepatocellular carcinoma, suggesting active involvement of HCV in the de-regulation of lipid metabolism in host cells. However, the role of lipid metabolism in HCV life cycle has not been fully understood until the establishment of *in vitro* HCV infection and replication system.In this review we focus on HCV production with regard to modification of lipid metabolism observed in an *in vitro* HCV infection and replication system. The importance of lipid droplet to HCV production has been recognized, possibly at the stage of virus assembly, although the precise mechanism of lipid droplet for virus production remains elusive. Association of lipoprotein with HCV in circulating blood in chronic hepatitis C patients is observed. In fact, HCV released from culture medium is also associated with lipoprotein. The fact that treatment of HCV fraction with lipoprotein lipase (LPL) abolished infectivity indicates the essential role of lipoprotein's association with virus particle in the virus life cycle. In particular, apolipoprotein E (ApoE), a component of lipoprotein associated with HCV plays a pivotal role in HCV infectivity by functioning as a virus ligand to lipoprotein receptor that also functions as HCV receptor. These results strongly suggest the direct involvement of lipid metabolism in the regulation of the HCV life cycle.

Addresses
[1] Research Institute, Chiba Institute of Technology, Tsudanuma, Narashino, Chiba 275-0016, Japan
[2] Center for Integrated Medical Research, Keio University, Shinjuku-ku, Shinanomachi 35, Tokyo 160-8582, Japan

Corresponding author: Shimotohno, Kunitada (kunitada.shimotono@it-chiba.ac.jp)
[3] These authors contributed equally.

Current Opinion in Virology 2011, 1:19–26

This review comes from a themed issue on
Virus Entry
Edited by François-Loïc Cosset and Urs Greber

Available online 12th June 2011

1879-6257/$ – see front matter

DOI 10.1016/j.coviro.2011.05.017

Introduction

Infection with hepatitis C virus (HCV), which persists with a rate of up to 80% and is difficult to eliminate, is estimated to occur in about 3% of the world population [1]. HCV infection frequently causes chronic hepatitis, which often leads to the development of liver cirrhosis and hepatocellular carcinoma after a long latency period [2]. The combined therapy of ribavirin and interferon is currently a major treatment to infected patients, although half of them have experienced the benefit of this treatment along with a severe side effect. Therefore, clarification of the underlying molecular mechanism of HCV life cycle is necessary for the development of a new effective therapy.

The progression of liver disease in patients with HCV is thought to result from a persistent inflammation accompanied by periportal necrosis and fibrosis [3]. Many chronic hepatitis patients with HCV, but not with HBV, are also noted to have a degree of steatosis by the examination of their liver biopsies [4]. Hepatic steatosis is defined as excessive lipid accumulation/infiltration within the hepatocyte, and has recently been recognized as an important cause for cirrhosis [5]. It seems likely that hepatic steatosis in chronic hepatitis C patients is somehow related to HCV infection and its replication. Furthermore, the combination of steatosis and the presence of HCV has been associated with a more rapid progression of fibrosis. Although the precise mechanism of how HCV infection results in the accumulation of excessive lipid levels and causes hepatocyte steatosis remains elusive, increasing evidence strongly suggests that HCV-encoded protein(s) plays some roles in this process.

HCV, which belongs to the family *Flaviviridae*, has a 9.6-kb positive single strand of RNA as a genome. The HCV RNA is translated into a precursor polyprotein that is processed concertedly with translation, or after the translation by cleavage with cellular and viral proteases to produce about 10 viral proteins, structural proteins (core, E1, and E2), and nonstructural proteins (p7, NS2, NS3, NS4A, NS4B, NS5A, and NS5B). With the help of nonstructural proteins, viral replication occurs in the endoplasmic reticulum (ER) membranous structure. In this review, we discuss the effect of HCV infection on host lipid metabolism and transfer, as well as the early event of virus entry required for HCV life cycle.

Regulation of lipid metabolism by HCV proteins

Expression of HCV core as well as the complete HCV genome in some transgenic mice induces steatosis [6,7]. It is notable to observe the association of HCV core with the surface of lipid droplet as well as apolipoprotein AII *in vitro* [8,9]. Interaction of core with lipid droplet was molecularly dissected using core mutants, and as a result the responsive region as well as structure of core was revealed [10,11••,12•]. Moreover, it has been shown that the core has a negative effect on the microsomal triglyceride transfer protein (MTP) activity [13]. Besides the HCV core, the presence of subgenomic replicon that lacks core expression has also been found to disturb MTP activity in the hepatocytes [14]. In this case, NS5A has been observed to interfere with MTP function [14]. As MTP is an essential chaperone for the assembly of very low-density lipoproteins (VLDL), which transfers triglyceride, phospholipids, and cholesterol from the hepatocytes, regulation of MTP is closely related to the accumulation of lipids in the hepatocytes. In fact, MTP deficiency results in large fat droplets in the hepatocytes and scattered accumulation of inflammatory cells [15]. HCV type-3 infected patients show reduced MTP activity and mRNA levels as well as high degree of steatosis [16]. So far, it is not clear whether MTP activity is directly regulated by HCV. Rather, MTP is likely to be controlled by activators (HNF1α, LRH-1, and HNF4α) and repressors (insulin and SREBP), some of which are modulated by HCV [14,17]. Reduced activity of MTP results in decreased secretion of VLDL, which seemingly leads to lipid accumulation. However, it is noteworthy that MTP activity is not completely suppressed by HCV. As will be described later, MTP activity is required for virus egress from infected cells. Collectively, these results suggest that HCV proteins alter lipid metabolism by activating lipid synthesis and modulating secretion of lipoprotein through interaction with cellular proteins, which results in accumulation and storage of lipids in cells expressing those viral proteins. However, the role of these viral proteins in modulating lipid metabolism related to HCV proliferation remains unknown until an *in vitro* HCV infection system was established.

Association of HCV with lipoproteins in the blood of HCV-infected individuals

HCV particles present in circulating serum show properties of heterogenous and lower density than those expected from its putative viral structure and can be captured by antilipoprotein antibody, which partly reflects the binding of a fraction of the virions to VLDL or low-density lipoproteins (LDLs) [18–22]. These low-density HCV-RNA-containing particles (called as lipo-viro-particle: LVP) contain core and apolipoprotein B (ApoB), and are rich in triglyceride with a diameter of >100 nm [19].

Although the physiological meaning of HCV-containing LVP in the circulating blood is not clear, it seems that HCV has either a high affinity to lipoproteins or is assembled with lipoproteins through the mechanism of lipoprotein synthesis. LVP-like structure may self-protect from the host immunological surveillance and/or increase interaction with lipoprotein receptor(s) which may act as a HCV receptor [20].

Importance of the lipid droplet in establishing a microenvironment for HCV assembly

The roles of modulation of lipid metabolism and association of HCV proteins with host factors involved in lipid metabolism for life cycle of HCV were not clear until an infectious *in vitro* HCV replication system was established [23–25].

Subcellular localization of HCV proteins in cells with replication of the infectious HCV RNA revealed association of core with ER membrane as well as lipid droplet. This finding is consistent with the previous reports that analyzed cells expressing on the core complex [11]. NS proteins, such as NS5A and NS5B, were found to be distributed around the core-coated lipid droplet as well as ER membrane. HCV envelope protein, E2, was detectable in the lipid droplet-enriched fraction isolated by density gradient centrifugation. Importantly, the lipid droplet present in the cytoplasm, detected by BODIPY 493/503 staining, was observed to be enriched in HCV genome replicating cells in a core-dependent manner. Furthermore, it was noted that the cells harboring HCV genome, which lacked core-coding region, did not accumulate the lipid droplet, indicating the importance of core function to activate cellular lipid metabolism, as suggested previously [17]. Moreover, the HCV genome encoding a mutant core, unable to associate with the lipid droplet, failed to produce virus. This suggests the importance of the association of core with the lipid droplet for virus assembly and release. The core-coated lipid droplet is surrounded by membranous components that are rich in nonstructural HCV proteins that constitute HCV replication complex. This spatial microenvironment seems to be important not only for virus assembly, but also for infectious virus production, because the HCV genomes carrying NS5A point mutations, which are not associated with the core-coated lipid droplet, reduce or inhibit the production of infectious virus despite minimal interference with the replication of the genome [11,26•]. Moreover, other NS proteins do not associate with the lipid droplet in cells bearing the NS5A-mutated HCV replicon. Thus, NS5A may have a crucial role in recruiting other NS proteins around the core-coated lipid droplet. However, how the HCV assembly takes place from such a microenvironment is still unclear.

Recent data have shown the importance of NS2 for viral morphogenesis. Molecular interactions between NS2 and other HCV proteins, such as envelope proteins (E1/E2), p7 and NS3 have been demonstrated, which suggest bridging between structural and nonstructural viral proteins and involvement in the assembly process [27–29]. NS2 accumulates in the ER-derived membranous

structures and co-localizes with the viral envelope glycoproteins and viral components of the replication complex at close proximity to the HCV core protein and lipid droplets.

Using HCV subgenome replicon cells, we have previously shown that very few HCV nonstructural protein complexes embedded in the membranous structure (referred as 'replication complex'; areas stained with dark blue color (Figure 2) are sufficient to synthesize HCV RNA present in the HCV replicon cells [30]. The level of the HCV proteins in the 'replication complex,' estimated by western blot analysis, has been found to be lower than one-tenth of the total viral proteins in the cells. The majority of the other HCV nonstructural proteins have been observed to remain associated with the ER membrane, possibly as a complex that is not protected by membranous components. As NS2 is dispensable for HCV RNA synthesis, it is likely that NS2 is not necessarily associated with the 'replication complex.' However, NS2 that is associated with envelopes and p7 has also been found to be associated with NS3 in the nonstructural protein complex that is not protected by the membrane. In this study, we refer to this complex as the 'HCV protein complex.'

Involvement of lipoproteins in HCV assembly and its infectivity

Lipoprotein is a biochemical particle consisting of apolipoproteins, triglyceride, cholesterol, and phospholipids, and transfers lipids through the bloodstream to the tissues. Liver, an endogenous source of lipoproteins, synthesizes VLDL using MTP. Lipoprotein lipase (LPL) hydrolyzes VLDL to supply lipids to the tissues, and converts VLDL into intermediate density lipoprotein (IDL). Hepatic triglyceride lipase (HTGL) hydrolyzes IDL to LDL.

ApoB is a main component of VLDL produced in the hepatocytes. Several groups have asserted the requirement of ApoB for HCV production [31•,32•,33•]. Huang *et al.* [31•] demonstrated that ApoB reduction by MTP inhibitor or a siRNA against ApoB led to decreased infectious HCV production. Gastaminza *et al.* [32•] reported similar results. Icard *et al.* [33•] showed that the release of HCV envelopes depended on the secretion of ApoB. Another study [34•] showed negative data for the requirement of ApoB, in which the authors described that apolipoprotein E (ApoE) rather than ApoB is important for HCV production and infectivity. Thus, ApoB requirement for virus production is still unclear.

ApoE, a component of lipoproteins, has attracted much attention as an important factor for HCV infectivity, because it has been shown that knockdown of ApoE could reduce HCV infectivity at a higher degree than the knockdown of ApoB, apolipoprotein A1 (ApoA1), and ApoC1 ([35••,36••], and data not shown). ApoE has three major isoforms (ApoE2, ApoE3, and ApoE4) differing by amino acid substitution at one or two sites (residues 130 and 176), which have different effects on lipid and neuronal homeostasis. ApoE3 is the most common isoform with no report of association with disease. ApoE2 has lower affinity for the low-density lipoprotein receptor (LDLR) and is a major risk factor for type III hyperlipoproteinemia, while ApoE4 is the major risk factor for Alzheimer's disease. Since ApoE not only functions as a ligand for LDLR and scavenger receptor class B type 1 (SR-B1), but also is associated with HCV, the effect of ApoE associated with HCV on the interaction of these lipoprotein receptors was examined by measuring the infectivity in naïve cells. Rescue of ApoE with ApoE3 ectopic expression in ApoE-knockdown cells recovered HCV infectivity, whereas ectopic ApoE2 expression did not. This result strongly indicates that ApoE, in particular some isoforms of ApoE, is necessary for HCV infectivity. ApoA1, a component of chylomicron, LDL, and high-density lipoprotein (HDL), is also important for HCV production, but is found to be less effective than ApoE ([37] and unpublished data). Taken together, HCV is seemingly produced as a hybrid of HCV and lipoproteins. While VLDL is a main lipoprotein secreted from normal hepatocytes, HCV may modulate the production of lipoproteins in the host cells to make the original lipoproteins more effective/appropriate for viral replication and persistence.

To further strengthen the involvement of lipoproteins in HCV infectivity, we evaluated HCV as a substrate of LPL [38•]. LPL treatment significantly suppressed HCV infectivity and increased the buoyant density of HCV (Figure 1a; modified from Ref. [38•]). This indicates that LPL hydrolyzes lipoproteins fused with HCV to result in decreased HCV infectivity. In accordance with the change in the buoyant density, the amount of ApoE associated with HCV decreased. As the HCV-bearing supernatant used in this study contained endogenous HTGL from the hepatocytes, these effects might result from HTGL in addition to LPL. Thus, we consider that detachment of ApoE from the HCV particle led to reduced HCV entry.

Relation between HCV particle size and infectivity

Ultracentrifugation of HCV in a gradient of iodixanol has revealed the discrepancy in buoyant density between the major virus peak and the virus with infectivity; the latter showed lower buoyant density than the former. However, the underlying physicochemical differences between noninfectious and infectious viruses still remain elusive. Thus, we tried to characterize the infectious virus from a different perspective. To evaluate the relationship between virus size and infectivity, the virus was analyzed by gel filtration chromatography (Shimizu *et al.*, unpublished data). HCV released from infected HuH7.5 cells was applied to in-tandem-connected columns (300 mm × 7.8 mm) of TSKgel LipopropakXL resin (Tosoh, Tokyo). The eluent from the column was continuously separated into a total of 50 fractions. Then, each fraction was analyzed for core, HCV RNA, infectivity, ApoE, and E2. The major peak of the core was in fraction (frac.) 11 (Figure 1b). The HCV RNA peak corresponded to the core peak. E2 associated with the viral particle, analyzed by immunoprecipitation (IP) using anti-E2 antibody followed by RT-PCR for HCV RNA, was also in this fraction. This suggests that HCV eluted to frac. 11 retained the virus-like structure. However, importantly, HCV in frac. 11 did not have infectivity. The HCV fraction associated with infectivity showed multiple peaks ranging from frac. 15 to 22. Furthermore, frac. 15 demonstrated highest infectivity among all the fractions, and there was no linear correlation between the virus size and infectivity.

Figure 1

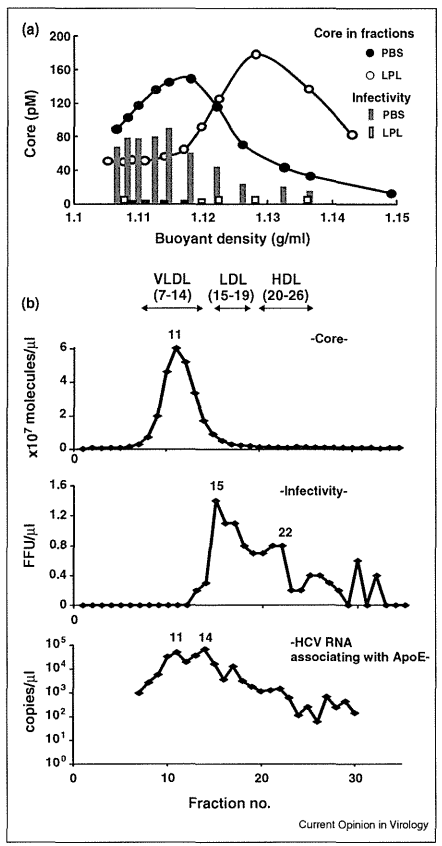

Relationship between physicochemical properties and infectivity of HCV. **(a)** LPL treatment shifts HCV to higher buoyant density and reduces HCV infectivity. The HCV (JFH1)-bearing culture medium was treated with PBS or LPL (500 μg/ml) for 1 hour at 37 °C and ultracentrifuged through iodixanol gradients. Thirty fractions were collected for analyzing the amount of core by ELISA. Culture medium from HuH7.5 cells inoculated with aliquots of each fraction was subjected to Core ELISA for infectivity. **(b)** Size distribution of HCV, infectious HCV, and HCV associated with ApoE. The HCV (JFH1)-bearing culture medium was subjected to gel filtration chromatography. The sample was eluted with 0.05 mol/l Tris-buffered acetate (pH 8.0) containing 0.3 mol/l sodium acetate, 0.05% sodium azide, and 0.005% Brij-35. A total of 50 fractions collected were analyzed for core, infectivity, and HCV RNA associated with ApoE. The representative fractions from 1 to 35 (core and infectivity) and from 7 to 30 (HCV RNA associated with ApoE) are shown. Elution of VLDL, LDL, and HDL was found in fractions 7–14, 15–19, and 20–26, respectively.

To determine whether the lack of ApoE is implicated in undetectable infectivity of HCV in frac. 11, we quantified HCV RNA associated with ApoE in each fraction by IP using anti-ApoE antibody, followed by RT-PCR. The HCV RNA associated with ApoE was detected from fractions irrespective of HCV infectivity (Figure 1b). This indicates that the association with ApoE is a necessary factor, but not sufficient for HCV infectivity.

Model of HCV budding into ER lumen

By taking these observations on HCV assembly into consideration, we drew the model of HCV assembly process and virus egress to ER lumen (Figure 2). The microenvironment of membranous structure of the core-coated lipid droplet has been found to play important roles in virus assembly [11••]. However, there is no proof to show a direct interaction of the core-coated lipid droplet with other HCV proteins. We presume that the core-coated lipid droplet may be localized at the vicinity of the 'HCV protein complex' enriched ER membrane, and that the triglyceride and cholesterol of the lipid droplet are reversely transferred to the inside of the bilayer of the ER membrane to where the core gets accumulated (Figure 2, stage a) [11••]. Core protein is not only enriched on the lipid droplet, but also visible on the ER by confocal microscopy [11••]. The presence of membranous web structure in the HCV genome replicating cells suggests dynamic alteration of the ER membrane structure [39]. Formation of the membranous web may include production of the 'replication complex' as well as dynamic alteration of ER membranous structure surrounding the core-coated lipid droplet, to make close association of 'replication complex' with core-enriched putative budding site of the viral particle (Figure 2, stage b). HCV protein complexes may gather each other to establish a compartment to constitute the 'replication complex' and putative virus precursor, so that the HCV

Figure 2

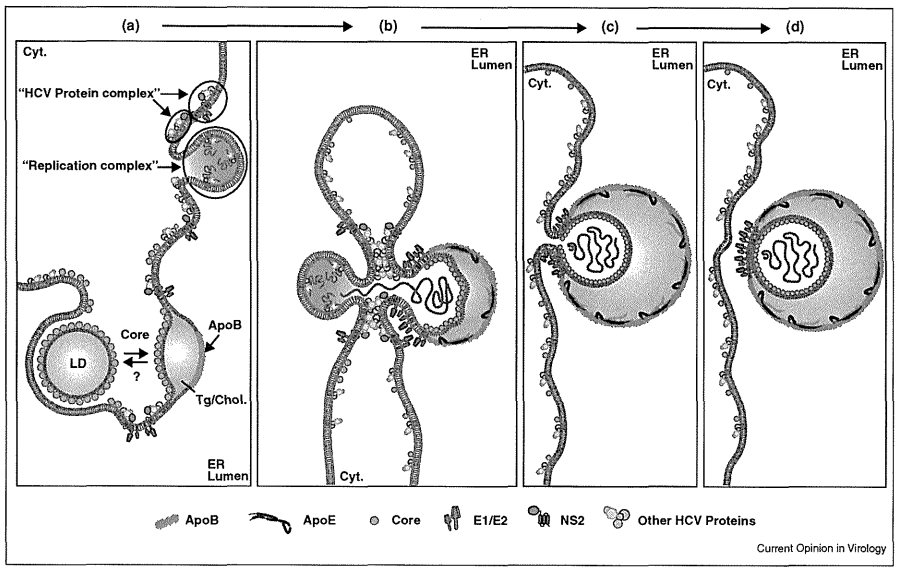

A model of virus egress to ER lumen. Stage **(a)**: Accumulation of triglyceride and cholesterol in the inside of the ER bilayer membrane enhances core association with the cytoplasmic monolayer membrane. These lipids may be reversely transferred from the core-coated lipid droplet or may be present in the inside of the ER bilayer membrane *ab origine*. On the membrane of ER, 'replication complex' as well as 'HCV protein complex' exists. Stage **(b)**: Distortion of the ER membrane, which seems to be driven by HCV protein complexes, makes the "Replication complex" location in the vicinity of the core-coated lipid-rich ER membrane, where HCV RNA secreted from the "replication complex" is exported to the putative virus budding site to establish a nascent HCV nucleocapsid. Simultaneously, ApoB and MTP function to synthesize lipoprotein-like structure surrounding the viral particle. Stages **(c)** and **(d)**: Progressing images of Stage B until egress of the virus/lipoprotein complex into ER lumen.

genome synthesized in the 'replication complex' is exported to the putative precursor of the viral particle to make a nascent HCV nucleocapsid. Simultaneously, lipoprotein formation proceeds with the help of MTP and ApoB, and buds into the ER lumen (Figure 2, stages c and d). It is still not clear at which stage of the virus assembly, other apolipoproteins, such as ApoA1 and ApoE, are incorporated into the virus/lipoprotein complex. However, NS5A may play some roles in incorporating ApoE into virus/lipoprotein complex during the process of virus assembly, because ApoE associates with NS5A [40].

Both LDLR and SR-B1 are likely to be recognized by HCV for adsorption into naïve cells for entry

Several cell-surface molecules, such as CD81, Claudin, Occludin, SR-B1, LDLR, and glycosaminoglycan heparan sulfate (HS) function as receptors for HCV infection [41,42,43•,44••,45]. Suppressed expression of any of these molecules in naïve HuH7.5 cells reduces or inhibits HCV infection [44••,46], indicating the necessity of concerted action by these molecules for entry and full establishment of HCV infection. However, hierarchical order of actions by these molecules in the process of HCV entry remains elusive.

SR-B1 is expressed in many cells, but is mainly expressed in the liver and steroidogenic tissues. SR-B1 recognizes various types of lipoproteins that include HDL, LDL, and VLDL, as well as modified lipoproteins, such as oxidized and acetylated LDL. In addition, SR-B1 is shown to be associated with the soluble recombinant HCV E2 glycoprotein [47]. LDLR, expressed in many tissues including liver, is a cell-surface receptor that recognizes ApoB in LDL and ApoE in IDL and VLDL.

It is still controversial whether LDLR or SR-B1 is used as an entry receptor by HCV [42,44••]. To address this problem, infectivity was analyzed on HCV bearing a different ApoE isoform [36••]. As described earlier,

Figure 3

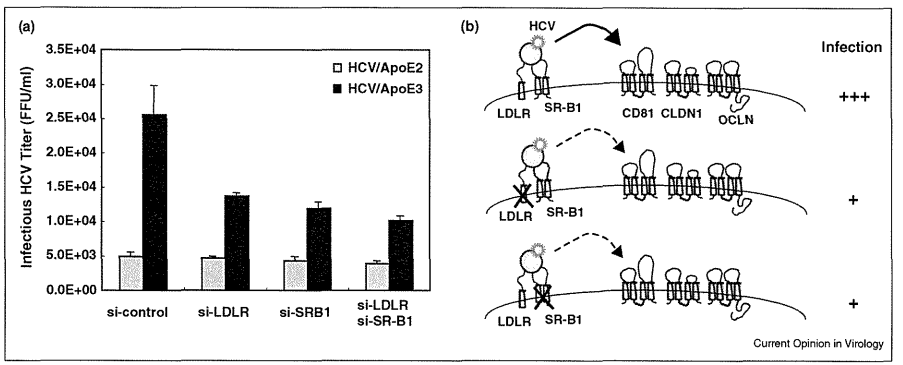

Both LDLR and SR-B1 are required for HCV entry. **(a)** HCV produced from cells bearing ApoE2 (white) or ApoE3 (black) expression was used to infect HuH7.5 cells, whose LDLR and/or SR-B1 were knocked down. Forty-eight hours after inoculation, HCV infection was analyzed by fluorescence microscopy after staining with anti-NS5A antibodies. Infectious HCV titer was quantified by focus-forming unit assay. HCV/ApoE2: HCV-bearing ApoE2; HCV/ApoE3: HCV-bearing ApoE3. The data represent the means of three independent experiments. **(b)** A model for HCV entry. Both LDLR and SR-B1 are required for HCV to gain high infectivity. On the other hand, HCV infectivity of cells is found to be reduced if only one of them is expressed.

HCV-bearing ApoE2 showed reduced infectivity in HuH7.5 cells, which indicates that LDLR is a necessary receptor for HCV infection [36••]. Further, infectivity of HCV to LDLR or SR-B1 knockdown cells was examined. Infectivity of HCV-bearing ApoE3 was reduced almost to the same level in LDLR or SR-B1 knockdown cells. With the expectation of additive reduction in infectivity in the cells with double knockdown of LDLR and SR-B1, infection in the double knockdown cells was analyzed [36••]. Unexpectedly, cells with suppressed expression of both the receptors did not show additive reduction in infectivity (Figure 3a). The level of infection of HCV-bearing ApoE2 to cells with suppressed expression of LDLR, SR-B1, or LDLR/SR-B1 was almost the same as that of the si-control transduced HuH7.5 cells (Figure 3a).

With regard to LDLR knockdown cells, the result was as expected, because ApoE2 has been found to have low affinity to LDLR. However, with regard to SR-B1 knockdown cells, we expected further reduction in HCV infection than that observed in si-control cells, because there was no significant difference in the association of ApoE2 and ApoE3 with SR-B1 [48]. Infectivity analysis using antibodies against LDLR/SR-B1 showed similar result as that observed in infectivity to LDLR or SR-B1 knockdown cells. From these results, we presume that HCV requires both LDLR and SR-B1 for infection and lack of either of the proteins suppresses HCV infectivity, as shown in Figure 3b. However, it is not known why the interaction of HCV with these two molecules results in high infectivity.

It is unlikely that in cells with suppressed expression of LDLR or SR-B1, the presence of residual amount of these proteins could establish infectivity of HCV-bearing ApoE3, because >90% reduction of these proteins in the knockdown cells has been confirmed [36]. However, this suggests the presence of another receptor through which ApoE-associated HCV could interact. To isolate a new candidate for HCV receptor(s), we focused our attention on lipoprotein receptor(s) in HuH7.5 cells. High expression of LRP1 and LRP8 was observed in this cell line among the candidates. However, knockdown of these genes in the cells did not reduce their susceptibility to HCV infection. Thus, it is likely that an unidentified protein in the HuH7.5 cells could play a role.

Conclusion

Patients with chronic hepatitis C often develop steatohepatitis. However, the reason why HCV-infected individuals cause abnormal lipid metabolism remains elusive. Recently it is suggested that HCV diverts lipid metabolism of host cells to establish its own proliferative machinery. This includes accumulation of lipid droplets to establish the microenvironment for virus assembly as modeled in this paper, and modification of lipid transfer for virus egress. Association of lipoprotein with HCV was biochemically demonstrated. Moreover, lipoprotein component(s) such as ApoE associated with virus is required for viral entry and may determine cell tropism. Further elucidation of the entire mechanism of HCV infection as well as identification of the host factors involved in this

process may contribute to more effective therapies for liver diseases caused by HCV infection.

Acknowledgements

We are grateful to Drs C. Rice and T. Wakita for HuH7.5 and JFH1 cells, respectively, and Dr J. McCubrey, East Carolina University, for comments on this manuscript. This work was supported by Grants-in-Aid for Scientific Research from the Ministry of Health, Labor, and Welfare of Japan and from the Ministry of Education, Culture, Sports, Science, and Technology.

References and recommended reading

Papers of particular interest, published within the period of review, have been highlighted as:

- • of special interest
- •• of outstanding interest

1. World Health Organization: **Hepatitis C: global prevalence**. *Wkly Epidemiol Rec* 2000, **75**:18-19.
2. Liang TJ, Jeffers LJ, Reddy KR, de Medina M, Parker IT, Cheinquer H, Idrovo V, Rabassa A, Schiff ER: **Viral pathogenesis of hepatocellular carcinoma in the United States**. *Hepatology* 1993, **18**:1326-1333.
3. Yoon EJ, Hu K-Q: **Hepatitis C virus infection and hepatic steatosis**. *Int J Med Sci* 2006, **3**:53-56.
4. Goodman ZD, Ishak KG: **Histopathology of hepatitis C virus infection**. *Semin Liver Dis* 1995, **15**:70-91.
5. Brunt EM: **Nonalcoholic steatohepatitis: definition and pathology**. *Semin Liver Dis* 2001, **21**:3-16.
6. Moriya K, Fujie H, Shintani Y, Yotsuyanagi H, Tsutsumi T, Ishibashi K, Matsuura Y, Kimura S, Miyamura T, Koike K: **The core protein of hepatitis C virus induces hepatocellular carcinoma in transgenic mice**. *Nat Med* 1998, **4**:1065-1070.
7. Lerat H, Honda M, Beard MR, Loesch K, Sun J, Yang Y, Okuda M, Gosert R, Xiao SY, Weinman SA *et al.*: **Steatosis and liver cancer in transgenic mice expressing the structural and nonstructural proteins of hepatitis C virus**. *Gastroenterology* 2002, **122**:352-365.
8. Barba G, Harper F, Harada T, Kohara M, Goulinet S, Matsuura Y, Eder G, Schaff Z, Chapman M, Miyamura T *et al.*: **Hepatitis C virus core protein shows a cytoplasmic localization and associates to cellular lipid storage droplets**. *Proc Natl Acad Sci U S A* 1997, **94**:1200-1205.
9. Sabile A, Perlemuter G, Bonbo F, Kohara K, Demaugre F, Matsuura Y, Brechot C, Barba G: **Hepatitis C virus core protein binds to apolipoprotein A11 and its secretion is modulated by fibrates**. *Hepatology* 1999, **4**:1064-1076.
10. Targett-Adams P, Hope G, Boulant S, McLauchlan J: **Maturation of hepatitis C virus core protein by signal peptide peptidase is required for virus production**. *J Biol Chem* 2008, **283**:16850-16859.
11. •• Miyanari Y, Atsuzawa K, Usuda N, Watashi K, Hishiki T, Zayas M, Bartenschlager R, Wakita T, Hijikata M, Shimotohno K: **The lipid droplet is an important organelle for hepatitis C virus production**. *Nat Cell Biol* 2007, **9**:1089-1097.

Increased lipid droplet by HCV infection was shown to be important for virus production.

12. • Shavinskaya A, Boulant S, Penin F, McLauchlan J, Bartenschlager R: **The lipid droplet binding domain of hepatitis C virus core protein is a major determinant for efficient virus assembly**. *J Biol Chem* 2007, **282**:37158-37169.

Association of HCV core with the lipid droplet requires HCV production.

13. Perlemuter G, Sabile A, Letteron P, Vona G, Topilco A, Chrétien Y, Koike K, Pessayre D, Chapman J, Barba G *et al.*: **Hepatitis C virus core protein inhibits microsomal triglyceride transfer protein activity and very low density lipoprotein secretion: a model of viral-related steatosis**. *FASEB J* 2002, **16**:185-194.
14. Domitrovich AM, Femlee DJ, Siddiqui A: **Hepatitis C virus nonstructural proteins inhibit apolipoprotein B100 secretion**. *J Biol Chem* 2005, **280**:39802-39808.
15. Partin JS, Partin JC, Schubert WK, McAdams AJ: **Liver ultrastructure in abetalipoproteinemia: evolution of micronodular cirrhosis**. *Gastroenterology* 1974, **67**:107-118.
16. Mirandola S, Realdon S, Iqbal J, Gerotto M, Dal Pero F, Bortoletto G, Marcolongo M, Vario A, Datz MM, Hussain MM *et al.*: **Liver microsomal trigriceride transfer protein is involved in hepatitis C liver steatosis**. *Gastroenterology* 2006, **130**:1661-1669.
17. Moriishi K, Mochizuki R, Moriya K, Miyamoto H, Mori Y, Abe T, Murata S, Tanaka K, Miyamura T, Suzuki T *et al.*: **Critical role of PA28gannma in hepatitis C virus-associated steatogenesis and hepatocellular carcinoma**. *Proc Natl Acad Sci U S A* 2007, **104**:1661-1666.
18. Thomssen R, Bonk S, Thiele A: **Density heterogeneities of hepatitis C virus in human sera due to the binding of β-lipoproteins and immunoglobulins**. *Med Microbiol Immunol* 1993, **182**:329-334.
19. André P, Komurian-Pradel F, Deforges S, Perret M, Berland JL, Sodoyer M, Pol S, Bréchot C, Paranhos-Baccalà G, Lotteau V: **Characterization of low- and very-low-density hepatitis C virus RNA-containing particles**. *J Virol* 2002, **76**:6919-6928.
20. *Agnello V, Abel G, Elfahal M, Knight GB, Zhang QX*: **Hepatitis C virus and other flaviviridae viruses enter cells via low density lipoprotein receptor**. *Proc Natl Acad Sci U S A* 1999, **96**:12766-12771.
21. Molina S, Castet V, Fournier-Wirth C, Pichard-Garcia L, Avner R, Harats D, Roitelman J, Barbaras R, Graber P, Ghersa P *et al.*: **The low-density lipoprotein receptor plays a role in the infection of primary human hepatocytes by hepatitis C virus**. *J Hepatol* 2007, **46**:411-419.
22. Thomssen R, Bonk S, Propfe C, Heermann K-H, Köchel HG, Uy A: **Association of hepatitis C virus in human sera with β-lipoprotein**. *Med Microbiol Immunol* 1992, **181**:293-300.
23. Lindenbach BD, Evans MJ, Syder AJ, Wolk B, Tellinghuisen TL, Liu CC, Maruyama T, Hynes RO, Burton DR, McKeating JA *et al.*: **Complete replication of hepatitis C virus in cell culture**. *Science* 2005, **309**:623-626.
24. *Wakita T, Pietschmann T, Kato T, Date T, Miyamoto M, Zhao Z, Murthy K, Habermann A, Krausslich HG, Mizokami M et al.*: **Production of infectious hepatitis C virus in tissue culture from a cloned viral genome**. *Nat Med* 2005, **11**:791-796.
25. Zhong J, Gastaminza P, Cheng G, Kapadia S, Kato T, Burton DR, Wieland SF, Uprichard SL, Wakita T, Chisari FV: **Robust hepatitis C virus infection in vitro**. *Proc Natl Acad Sci U S A* 2005, **102**:9294-9299.
26. • Masaki T, Suzuki R, Murakami K, Aizaki H, Ishii K, Murayama A, Date T, Matsuura Y, Miyamura T, Wakita T *et al.*: **Interaction of hepatitis C virus nonstructural protein 5A with core protein is critical for the production of infectious virus particles**. *J Virol* 2008, **82**:7964-7976.

Point mutation in the domain 3 of HCV NS5A protein abrogates production of virus particle.

27. Yi M, Ma Y, Yates J, Lemon SM: **Trans-complementation of an NS2 defect in a late step in hepatitis C virus (HCV) particle assembly and maturation**. *PLoS Pathog* 2009, **5**:e1000403.
28. Jirasko V, Montserret R, Lee JY, Gouttenoire J, Moradpour D, Penin F, Bartenschlager R: **Structural and functional studies of nonstructural protein 2 of the hepatitis C virus reveal its key role as organizer of virion assembly**. *PLoS Pathog* 2010, **6**:e1001233.
29. Ma Y, Anantpadma M, Timpe JM, Shanmugam S, Singh SM, Lemon SM, Yi M: **Hepatitis C virus NS2 protein serves as a scaffold for virus assembly by interacting with both structural and nonstructural proteins**. *J Virol* 2011, **85**:1706-1717.
30. Miyanari Y, Hijikata M, Yamaji M, Hosaka M, Takahashi H, Shimotohno K: **Hepatitis C virus non-structural proteins in the probable membranous compartment function in viral genome replication**. *J Biol Chem* 2003, **278**:50301-50308.
31. • Huang H, Sun F, Owen DM, Li W, Chen Y, Gale M Jr, Ye J: **Hepatitis C virus production by human hepatocytes dependent on assembly and secretion of very low-density lipoproteins**. *Proc Natl Acad Sci U S A* 2007, **104**:5848-5853.

Functional association of HCV egress and VLDL has been shown.

32. • Gastaminza P, Cheng G, Wieland S, Zhong J, Liao W, Chisari FV: **Cellular determinants of hepatitis C virus assembly, maturation, degradation, and secretion**. *J Virol* 2008, **82**:2120-2129.

See annotation to [31•].

33. • Icard V, Diaz O, Scholtes C, -Cocon P, Ramière L, Bartenschlager C, Penin R, Lotteau F, André VP: **Secretion of hepatitis C virus envelope glycoproteins depends on assembly of apolipoprotein B positive lipoproteins**. *PLos ONE* 2009, **4**:e4223.

Association of HCV envelope protein and lipoprotein is disclosed.

34. • Jing J, Luo G: **Apolipoprotein E but not B is required for the formation of infectious hepatitis C virus particles**. *J Virol* 2009, **83**:12680-12691.

Importance of apolipoprotein E rather than apolipoprotein B in infectious HCV production is described.

35. •• Chang K-S, Jiang J, Cai Z, Luo G: **Human apolipoprotein E is required for infectivity and production of hepatitis C virus in cell culture**. *J Virol* 2007, **81**:13783-13793.

Apolipoprotein E plays important role in HCV infectivity.

36. •• Hishiki T, Shimizu Y, Tobita R, Sugiyama K, Ogawa K, Funami K, Ohsaki Y, Fujimoto T, Takaku H, Wakita T *et al.*: **Infectivity of hepatitis C virus is influenced by association with apolipoprotein E isoforms**. *J Virol* 2010, **84**:12048-12057.

HCV infectivity is influenced by apolipoprotein E isoforms.

37. Mancone C, Steindler C, Santangelo L, Simonte G, Vlassi C, Longo MA, D'Offizi G, Di Giacomo C, Pucillo LP, Amicone L *et al.*: **Hepatitis C virus production requires apolipoprotein A-I and affects its association with nascent low-density lipoproteins**. *Gut* 2011, **60**:378-386.
38. • Shimizu Y, Hishiki T, Sugiyama K, Ogawa K, Funami K, Kato A, Ohsaki Y, Fujimoto T, Takaku H, Shimotohno K: **Lipoprotein lipase and hepatic triglyceride lipase reduce the infectivity of hepatitis C virus (HCV) through their catalytic activities on HCV-associated lipoproteins**. *Virology* 2010, **407**:152-159.

Association of HCV with lipoprotein is shown by biochemical analysis.

39. Gosert R, Egger D, Lohmann V, Bartenschlager R, Blum HE, Bienz K, Moradpour D: **Identification of the hepatitis C virus RNA replication complex in Huh-7 cells harboring subgenomic replicons**. *J Virol* 2003, **77**:5487-5492.
40. Benga WJ, Krieger SE, Dimitrova M, Zeisel MB, Parnot M, Lupberger J, Hildt E, Luo G, McLauchlan J, Baumert TF *et al.*: **Apolipoprotein E interacts with hepatitis C virus nonstructural protein 5A and determines assembly of infectious particles**. *Hepatology* 2010, **51**:43-53.
41. Pileri P, Uematsu Y, Campagnoli S, Galli G, Falugi F, Petracca R, Weiner AJ, Houghton M, Rosa D, Grandi G *et al.*: **Binding of hepatitis C virus to CD81**. *Science* 1998, **282**:938-941.
42. Bartosch B, Vitelli A, Granier C, Goujon C, Dubuisson J, Pascale S, Scarselli E, Cortese R, Nicosia A, Cosset F-L: **Cell entry of hepatitis C virus requires a set of co-receptors that include the CD81 tetraspanin and the SR-B1 scavenger receptor**. *J Biol Chem* 2003, **278**:41624-41630.
43. • Evans MJ, von Hahn T, Tscherne DM, Syder AJ, Panis M, Wolk B, Hatziioannou T, McKeating JA, Bieniasz PD, Rice CM: **Claudin-1 is a hepatitis C virus co-receptor required for a late step in entry**. *Nature* 2007, **446**:801-805.

Claudin-1 has been shown to be a receptor for HCV.

44. •• Owen DM, Huang H, Ye J, Gale M Jr: **Apolipoprotein E on hepatitis C virion facilitates infection through interaction with low-density lipoprotein receptor**. *Virology* 2009, **394**:99-108.

LDLR is shown to be a receptor for HCV.

45. Barth H, Schafer C, Adah MI, Zhang F, Linhardt RJ, Toyoda H, K-Toyoda A, Toida T, van Kuppevelt TH, Depla E *et al.*: **Cellular binding of hepatitis C virus envelope glycoprotein E2 requires cell surface heparan sulfate**. *J Biol Chem* 2003, **278**:41003-41012.
46. Zeisel MB, Koutsoudakis G, Schnober EK, Haberstroh A, Blum HE, Cosset FL, Wakita T, Jaeck D, Doffoel M, Royer C *et al.*: **Scavenger receptor class B type I is a key host factor for hepatitis C virus infection required for an entry step closely linked to CD81**. *Hepatology* 2007, **46**:1722-1731.
47. Scarselli E, Ansuini H, Cerino R, Roccasecca RM, Acali S, Filocamo G, Traboni C, Nicosia A, Cortese R, Vitell A: **The human scavenger receptor class B type I is a novel candidate receptor for the hepatitis C virus**. *EMBO J* 2002, **21**:5017-5025.
48. *Li X, Kan HY, Lavrentiadou S, Krieger M, Zannis V*: **Reconstituted discoidal ApoE-phospholipid particles are ligands for the scavenger receptor BI**. *J Biol Chem* 2002, **277**:21149-21157.

Virus Research 163 (2012) 390–395

Contents lists available at SciVerse ScienceDirect

Virus Research

journal homepage: www.elsevier.com/locate/virusres

Short communication

The interaction between human initiation factor eIF3 subunit c and heat-shock protein 90: A necessary factor for translation mediated by the hepatitis C virus internal ribosome entry site

Saneyuki Ujino[a], Hironori Nishitsuji[a], Ryuichi Sugiyama[a], Hitoshi Suzuki[a], Takayuki Hishiki[b], Kazuo Sugiyama[c], Kunitada Shimotohno[b], Hiroshi Takaku[a,*]

[a] Department of Life and Environmental Sciences, Chiba Institute of Technology, 2-17-1 Tsudanuma, Narashino-shi, Chiba 275-0016, Japan
[b] Research Institute, Chiba Institute of Technology, 2-17-1 Tsudanuma, Narashino, Chiba 275-0016, Japan
[c] Center for Integrated Medical Research, School of Medicine, Keio University, 35 Shinanomachi, Shinjyuku-ku Tokyo 160-8582, Japan

ARTICLE INFO

Article history:
Received 10 June 2011
Received in revised form 4 October 2011
Accepted 6 October 2011
Available online 14 October 2011

Keywords:
eIF3c
Hsp90
HCV IRES
17-AAG
Translation initiation

ABSTRACT

Heat-shock protein 90 (Hsp90) is a molecular chaperone that plays a key role in the conformational maturation of various transcription factors and protein kinases in signal transduction. The hepatitis C virus (HCV) internal ribosome entry site (IRES) RNA drives translation by directly recruiting the 40S ribosomal subunits that bind to eukaryotic initiation factor 3 (eIF3). Our data indicate that Hsp90 binds indirectly to eIF3 subunit *c* by interacting with it through the HCV IRES RNA, and the functional consequence of this Hsp90–eIF3c–HCV-IRES RNA interaction is the prevention of ubiquitination and the proteasome-dependent degradation of eIF3c. Hsp90 activity interference by Hsp90 inhibitors appears to be the result of the dissociation of eIF3c from Hsp90 in the presence of HCV IRES RNA and the resultant induction of the degradation of the free forms of eIF3c. Moreover, the interaction between Hsp90 and eIF3c is dependent on HCV IRES RNA binding. Furthermore, we demonstrate, by knockdown of eIF3c, that the silencing of eIF3c results in inhibitory effects on translation of HCV-derived RNA but does not affect cap-dependent translation. These results indicate that the interaction between Hsp90 and eIF3c may play an important role in HCV IRES-mediated translation.

The hepatitis C virus (HCV), a member of the *Flaviviridae* family, has a positive-strand RNA genome (Taylor et al., 1999; Bartenschlager and Lohmann, 2001) encoding a large precursor polyprotein that is cleaved by host and viral proteases to generate at least 10 functional viral proteins: core, envelope 1 (E1), E2, p7, nonstructural protein (NS2), NS3, NS4A, NS4B, NS5A, and NS5B (Grakoui et al., 1993; Hijikata et al., 1993). Ishii et al. identified an HCV replicon system in which the full HCV genomic RNA autonomously replicates in the Huh-7 human hepatoma cell line (Fig. 1A) (Ishii et al., 2006). This HCV replicon system allows researchers to study HCV genome replication in cell culture. HCV protein synthesis is initiated by the HCV RNA genome. This genome contains a conserved structure in its 5′-untranslated region (5′-UTR) that acts as an internal ribosome entry site (IRES) (Lukavsky, 2008). Briefly, the small ribosomal subunit (40S) and the eukaryotic initiation factor eIF3 bind specifically to the HCV IRES RNA, allowing for direct recognition of the start codon present in the 5′-UTR of the viral mRNA (Spahn et al., 2001; Collier et al., 2002; Kieft et al., 2002; Fraser and Doudna, 2007; Julien et al., 2009). Consistent with its diverse functions, eIF3 is the largest and most complex initiation factor. The mammalian version, for example, contains 13 nonidentical subunits designated eIF3a to eIF3m. The eIF3 core subunit (eIF3a–c, g, and i) is essential for translation (Kieft et al., 2002; Hinnebusch, 2006; Masutani et al., 2007; Zhou et al., 2008), and eIF3 specifically associates with the apical half of domain III of the HCV IRES (Kieft et al., 2001, 2002; Siridechadilok et al., 2005; Fraser and Doudna, 2007).

Hsp90 is a heat-shock protein that is abundant in the cytosol of eukaryotes and prokaryotes. In contrast to other chaperones, a number of substrates are known to contain Hsp90 (Schulte et al., 1995). Studies of eukaryotes have revealed that these Hsp90 client proteins include a variety of transcription factors (Coumailleau et al., 1995; Garcia-Cardena et al., 1998; Nagata et al., 1999; Sato et al., 2000; Richter and Buchner, 2001; Xu et al., 2001; Waza et al., 2005). Recently, many studies have reported that Hsp90 is involved with not only HCV RNA replication and viral protein but also HCV IRES-mediated translation (Waxman et al., 2001; Kim et al., 2006; Okamoto et al., 2006; Nakagawa et al., 2007; Ujino et al., 2009). In the present study, we demonstrate that eIF3 forms a complex with Hsp90 that is critical for HCV IRES-mediated translation.

* Corresponding author. Tel.: +81 47 478 0407; fax: +81 47 478 0407.
E-mail address: hiroshi.takaku@it-chiba.ac.jp (H. Takaku).

0168-1702/$ – see front matter © 2011 Elsevier B.V. All rights reserved.
doi:10.1016/j.virusres.2011.10.003

Author's personal copy

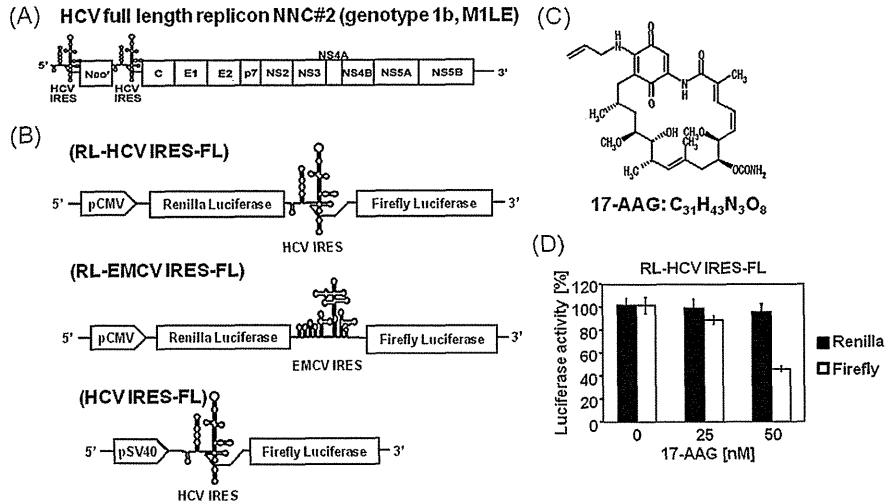

Fig. 1. Inhibition of IRES-mediated translation by an Hsp90 inhibitor. (A) The structure of the HCV replicon RNA molecules comprising the HCV 5′-UTR, including the HCV IRES, the neomycin phosphotransferase gene (Neo^r), and the coding region for the HCV proteins core to NS5B (in the HCV full-length replicon). (B) A schematic representation of the bicistronic HCV IRES or EMCV IRES reporter construct pRenilla-HCV IRES-firefly luciferase (RL-HCV IRES-FL) or pRenilla-EMCV IRES-firefly luciferase (RL-EMCV IRES-FL) driven by the CMV promoter to direct cap-dependent translation of renilla luciferase (RL) and HCV IRES or EMCV IRES-dependent translation of firefly luciferase (FL). The vector construct for HCV IRES-mediated translation of firefly luciferase, pHCV IRES-firefly luciferase (HCV IRES-FL) (Ujino et al., 2010). (C) The structure of the Hsp90 inhibitor 17-AAG (17-allylamino-17-demethoxygeldanamycin, Sigma–Aldrich Chemical Co.). (D) Inhibition of IRES-mediated translation by 17-AAG. Huh-7 cells (1×10^5 cells/well on 12-well plates) treated with 17-AAG (25 and 50 nM) and DMSO as a control for 24 h, and were then transfected with pRenilla-HCV IRES-firefly luciferase (RL-HCV IRES-FL) using Lipofectamine 2000 (Invitrogen). At 24 h post-transfection, Renilla luciferase (cap-dependent translation) and firefly luciferase (HCV IRES-dependent translation) activities were measured with a Dual-Luciferase Reporter Assay System (Promega). The data represent the mean ± standard deviations (SDs) from the experiments performed in triplicate.

To investigate the effects of the *Hsp90* inhibitor 17-AAG on HCV IRES translation, a bicistronic reporter system was used that consisted of an upstream reporter, Renilla luciferase (RL), expressed by cap-dependent translation and a downstream reporter, firefly luciferase (FL), which is under the translational control of the HCV IRES. To construct pcDNA-HCV IRES-firefly Luc, pHCV IRES-firefly Luc (HCV IRES-FL) (Ujino et al., 2010) (Fig. 1B) was digested with BamHI and SalI. The IRES-firefly Luc fragments were inserted into the BamHI-XhoI site of pcDNA3.1 (Invitrogen, Carlsbad, CA). To construct pRenilla-HCV IRES-firefly luciferase (RL-HCV IRES-FL), Renilla luciferase fragments were amplified by PCR from a pFN11A Flexi vector (Promega, Madison, WI), and the PCR products were inserted into the BamHI site of pcDNA-HCV IRES-firefly Luc. The human hepatoma cell line Huh-7 was maintained in Dulbecco's modified Eagle's medium (DMEM; Invitrogen) containing 10% fetal bovine serum (FBS). The benzoquinone ansamycin, the antibiotic geldanamycin (GA) and its less toxic analogue 17-allylamino-17-demethoxygeldanamycin (17-AAG) (Fig. 1C) (Sigma–Aldrich Chemical Co., St Louis, MO) directly bind to the ATP/ADP binding pocket of Hsp90, thus preventing ATP binding and the completion of client protein refolding (Neckers, 2003). The client proteins of Hsp90 appear to shift the role of the primary chaperone from Hsp90 to Hsp70 in cells treated with Hsp90 inhibitors (Doong et al., 2003). It is also well known that 17-AAG causes a modest increase in Hsp70 levels (Morimoto, 1998; Bagatell et al., 2000; Guo et al., 2005). In our previous report, a significant induction of Hsp70 was detected (Ujino et al., 2009).

For the reporter gene assay, Huh-7 cells were treated with different concentrations of the Hsp90 inhibitor, 17-AAG, or DMSO as a control for 24 h. They were then transfected with the bicistronic reporter construct RL-HCV IRES-FL using Lipofectamine 2000 (Invitrogen), which directs cap-dependent translation of the RL gene and HCV IRES-dependent translation of FL genes (Invitrogen). At 24 h post-transfection, the Renilla luciferase (cap-dependent translation) and firefly luciferase (HCV IRES-dependent translation) activities were measured with a Dual-Luciferase Reporter Assay System (Promega, Madison, WI). In cells treated with 50 nM 17-AAG, firefly luciferase activity was reduced by 55% with RL-HCV IRES-FL, whereas Renilla luciferase activity was mostly maintained (Fig. 1D). The inhibition of HCV IRES-mediated translation occurred in a dose-dependent manner. Recently, Kim et al. (2006) demonstrated that Hsp90 regulates ribosomal function by maintaining the stability of 40S ribosomal proteins such as rpS3 and rpS6. The interaction between the 40S ribosomal proteins and Hsp90 has also been associated with ribosomal activities such as protein synthesis. We also found that the Hsp90 inhibitor 17-AAG influences HCV IRES-mediated luciferase activity, suggesting that 17-AAG inhibited HCV RNA replication and HCV IRES-mediated translation.

The HCV IRES is recognized specifically by the small ribosomal subunit and eIF3 before the initiation of viral translation. Although the degradation of rpS3, a component of the small ribosomal subunit, has been shown to occur in the presence of the Hsp90 inhibitor (Kim et al., 2006), the influence of Hsp90 inhibition on eIF3 is not understood. To determine whether 17-AAG affects the expression of the eIF3 subunit, we analyzed eIF3a, eIF3b, eIF3c, eIF3g and eIF3i protein expression by western blot analysis. The HCV replicon cell line NNC#2 (NN/1b/FL), which carries a full genome replicon, was cultured in DMEM with 10% FBS, nonessential amino acids,

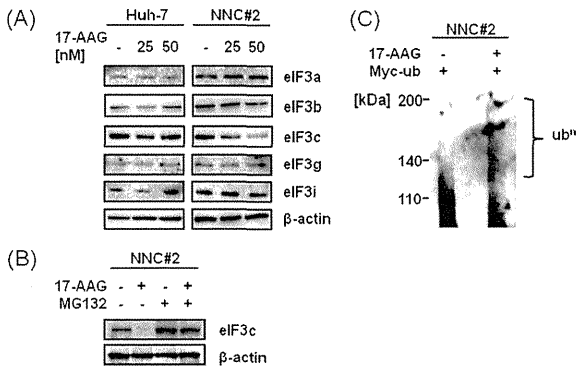

Fig. 2. Effect of 17-AAG treatment on eIF3 expression. (A) Western blot analysis of eIF3 protein expression in Huh-7 or NNC#2 cells treated with 17-AAG (25 nM and 50 nM). The cell lysates were analyzed by western blot 48 h after treatment. The primary antibodies used were monoclonal or polyclonal antibodies against eIF3a, eIF3b, eIF3c, eIF3g, and eIF3i (Santa Cruz Biotechnology). Horseradish peroxidase-conjugated anti-rabbit antibody (Sigma–Aldrich Chemical Co.) was used as the secondary antibody. (B) The reduction of eIF3c expression was prevented by proteasome inhibitor treatment. NNC#2 cells treated with 17-AAG (50 nM) or DMSO as a control. After 8 h treatment, the cells were treated with the proteasome inhibitor MG-132 (5 μM) or DMSO as a control. The cell lysates were analyzed by western blot 40 h after treatment. The primary antibody used was the eIF3c or β-actin (Santa Cruz Biotechnology). Horseradish peroxidase-conjugated anti-rabbit antibody (Sigma–Aldrich Chemical Co.) was used as the secondary antibody. (C) eIF3c degradation is mediated by the ubiquitin-dependent protease pathway. NNC#2 cells were transfected with pCMV-Myc-Ubi using Lipofectamine 2000 (Invitrogen). At 24 h post-transfection, the cells were treated with 17-AAG (50 nM) or DMSO as a control for 8 h and were then treated with the proteasome inhibitor MG-132 (5 μM) for 16 h. The cell lysates were subjected to an immunoprecipitation assay using an anti-αMyc antibody (Cell Signaling) followed by an immunoblot analysis using anti-eIF3c antibody.

L-glutamine, penicillin/streptomycin, and 1 mg/mL G418 (Invitrogen) at 37 °C in 5% CO_2 (Ishii et al., 2006). For western blot analysis, NNC#2 cells and Huh-7 cells were lysed in 1× chloramphenicol acetyltransferase (CAT) enzyme-linked immunosorbent assay buffer (Roche, Basel, Switzerland). The cell lysates were separated by 10% sodium dodecyl sulfate–polyacrylamide gel electrophoresis, transferred to nitrocellulose membranes, and blocked with 5% skimmed milk. The primary antibodies used were monoclonal or polyclonal antibodies against FLAG-M2 (Sigma–Aldrich Chemical Co.), Hsp90 (Cell Signaling Tech., Beverly, MA), eIF3a, eIF3b, eIF3c, eIF3g, and eIF3i (Santa Cruz Biotechnology, Santa Cruz, CA). Horseradish peroxidase-conjugated anti-rabbit antibody (Sigma–Aldrich Chemical Co.) was used as the secondary antibody. When the HCV replicon cell line NNC#2 (NN/1b/FL) and Huh-7 cells were treated with increasing doses of 17-AAG, the expression of the eIF3c subunit was markedly reduced in NNC#2 cells, but the expression in Huh-7 cells was unaffected (Fig. 2A). These results suggest that Hsp90 is involved in eIF3c stability through a physical interaction in the presence of HCV IRES RNA.

Protein degradation in cells is mediated by several protease systems; however, the stability of most proteins is regulated by Hsp90, and they appear to be degraded by proteasomes. To investigate whether the reduction of eIF3c was due to proteasomal degradation, we treated NNC#2 cells with a proteasome inhibitor, MG132, to prevent the 17-AAG-induced degradation of eIF3c. Our results indicated that 17-AAG-induced eIF3c degradation can be blocked by proteasome inhibitors (Fig. 2B). Proteasome inhibitors substantially prevented the degradation of eIF3c in cells treated with 17-AAG. This is most likely because the disruption of Hsp90 by the Hsp90 inhibitor treatment destabilized the eIF3c protein. Therefore, it is clear that proteasome-dependent degradation results in the decreased level of eIF3c protein. This indicates that the stability of eIF3c was supported by Hsp90, and unstable eIF3c was removed by proteasomes. Furthermore, we investigated whether the ubiquitination of eIF3c was affected by the Hsp90 inhibitor, 17-AAG. We transfected pCMV-Myc-Ubi (provided by Dr. A. Ryo) using Lipofectamine 2000 (Invitrogen) into NNC#2 cells, which were then treated with 17-AAG (50 μM). After treatment, the cells were then treated with 5 μM MG132 and subjected to immunoprecipitation with an anti-αMyc antibody (Cell Signaling) followed by an immunoblot analysis using an anti-eIF3c antibody. Notably, polyubiquitinated forms of eiF3c was detected in cells treated with 17-AAG (Fig. 2C). These results suggest that the destabilized eIF3c protein is degraded by proteasome-dependent proteolysis mediated by ubiquitin conjugation, and Hsp90 plays an important role in maintaining the stable form of the eIF3c protein in vivo.

To investigate the influence of eIF3c silencing on HCV IRES-mediated translation, Huh-7 cells were transfected with siRNA targeted to eIF3c at a concentration of 50 nM using Lipofectamine 2000 (Invitrogen), and they were then transfected with RL-HCV IRES-FL. Control small interference RNA (siRNA) and eIF3 p110 (eukaryotic translation initiation factor 3, subunit 8, 110 kDa) siRNA were purchased from Santa Cruz Biotechnology. The protein levels of eIF3c were examined by western blot analysis, and HCV IRES-mediated translation was analyzed with a Dual-Luciferase Assay. As demonstrated in Fig. 3A, when compared to Huh-7 cells treated with control siRNA, the eIF3c protein level was markedly reduced in Huh-7 cells transfected with eIF3 p110 siRNA targeting eIF3c. Furthermore, firefly luciferase activity in RL-HCV IRES-FL was also reduced by approximately 63% in the cells treated with siRNA targeted to eIF3c, whereas Renilla luciferase activity was mostly maintained (Fig. 3B). The inhibition of HCV IRES-mediated translation by siRNA against eIF3c indicates that the suppression of HCV IRES-mediated translation by Hsp90 inhibition leads to a reduction in eIF3c. To further characterize the HCV IRES inhibitory effect of siRNA targeting eIF3c, we used additional bicistronic reporter plasmids for transient transfection assays with Huh-7 cells. Since we were mainly interested in viral IRESs, we chose to investigate the effect of the luciferase activities on translation derived from the IRES of EMCV in place of the HCV IRES (Fig. 1B). To generate pcDNA-EMCV IRES-firefly Luc, EMCV IRES fragments were created by PCR using the following primers: 5′-GAC TGG ATC CCC CCC CCC CCT AAC-3′ and 5′-CAG TGG GCC CTA TTA TCG TGT TTT TCA AAG GAA AAC C-3′. The PCR products were inserted into the BamHI and

Author's personal copy

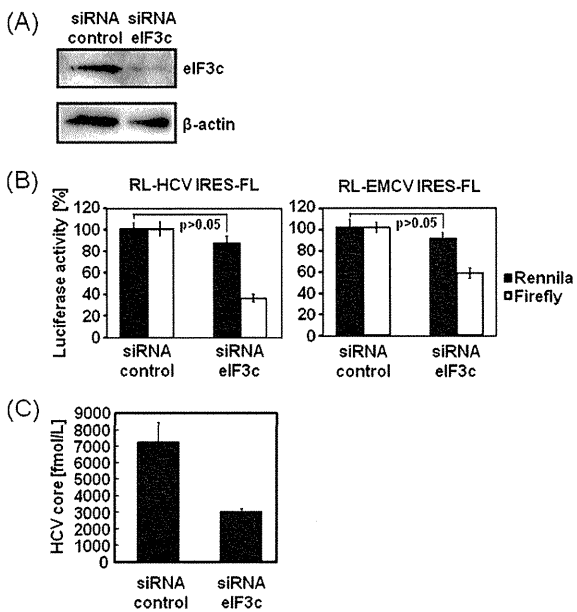

Fig. 3. Knockdown of eIF3c expression inhibits HCV IRES-mediated translation. (A) eIF3c protein expression in Huh-7 cells transfected with control siRNA or eIF3c siRNA at a concentration of 50 nM using Lipofectamine 2000 (Invitrogen). Cell lysates were analyzed by western blot 24 h post-treatment. eIF3c or β-actin antibodies were used as the primary antibodies (Santa Cruz Biotechnology). Horseradish peroxidase-conjugated anti-rabbit antibody (Sigma–Aldrich Chemical Co.) was used as the secondary antibody. (B) Huh-7 cells were transfected with siRNA targeted to eIF3c (50 nM) or nontarget control siRNA (50 nM) using Lipofectamine 2000 (Invitrogen). At 24 h post-transfection, the cells were then transfected with RL-HCV IRES-FL or RL-EMCV IRES-FL using Lipofectamine 2000 (Invitrogen). At 24 h post-transfection, the Renilla luciferase (cap-dependent translation) and firefly luciferase (HCV IRES or EMCV IRES-dependent translation) activities were measured with a Dual-Luciferase Reporter Assay System (Promega). Results are representative of three independent experiments, and error bars indicate the ± standard deviations (SDs) of the means. $P > 0.05$ (Student's t-test). (C) HCV IRES-mediated translational inhibition with eIF3 p110 siRNA by HCV full-genome RNA (NN/1b/FL). Huh-7 cells were transfected with eIF3 p110 siRNA or control siRNA at a concentration of 50 nM using Lipofectamine 2000 (Invitrogen). At 24 h post-transfection, the cells were transfected with 2 μg of HCV full-genome RNA (NN/1b/FL) using Lipofectamine 2000 (Invitrogen). After 24 h, intracellular HCV core-protein levels were measured using a fully automated HCV core-protein antigen chemiluminescent enzyme immunoassay (CLEIA) according to the manufacturer's instructions (Aoyagi et al., 1999). The relative chemiluminescence units were measured and used to determine the concentration of the HCV core antigen according to a standard curve generated using recombinant HCV core antigen. The concentration was expressed in units of femtomole/L (fmol/L). The data represent the mean ± standard deviations (SDs) from the experiments performed in triplicate.

ApaI sites of pcDNA3.1, and firefly Luc fragments were cloned into the ApaI site of the resulting plasmid. To construct pcDNA-Renilla-EMCV IRES-firefly Luc (RL-EMCV IRES-FL), pcDNA-Renilla-EMCV IRES-firefly Luc was digested with BamHI, and the renilla Luc fragments were inserted into BamHI site of pcDNA-EMCV IRES-firefly Luc (Fig. 1B). Huh-7 cells were transfected with control small interference RNA (siRNA) or eIF3 p110 siRNA at a concentration of 50 nM using Lipofectamine 2000 (Invitrogen) and then transfected with RL-EMCV IRES-FL. Following transient transfection in Huh-7 cells, firefly luciferase activity in RL-EMCV IRES-FL was also reduced by approximately 43% in cells treated with siRNA targeting eIF3c, but Renilla luciferase activity was mostly maintained (Fig. 3B). The knockdown of eIF3c expression also resulted in inhibitory effects on translation derived from HCV and EMCV (Fig. 3B) but did not affect cap-dependent translation. These results indicate that eIF3c may play a more important initiation factor in IRES-mediated translation than cap-dependent translation. However, it remains the subject of future investigation to determine whether only eIF3c proteins are subject to the IRES-mediated translation.

We also examined the HCV IRES-mediated translational inhibition with eIF3 p110 siRNA by HCV full-genome RNA ((NN/1b/FL) (Ishii et al., 2006). Huh-7 cells were transfected with eIF3 p110 siRNA or control siRNA at a concentration of 50 nM using Lipofectamine 2000 (Invitrogen). At 24 h post-transfection, the cells were transfected with HCV full-genome RNA (NN/1b/FL). After 24 h, the intracellular HCV core-protein levels were measured using a fully automated HCV core-protein antigen chemiluminescent enzyme immunoassay (CLEIA) according to the manufacturer's instructions (Aoyagi et al., 1999). The core-protein expression in cells treated with eIF3 p110 siRNA was reduced by approximately 61% when compared to cells treated with control siRNA (Fig. 3C). These findings further confirmed that HCV IRES-mediated translational inhibition occurs through a reduction of eIF3c expression caused by the Hsp90 inhibitor-mediated disruption of the interaction between eIF3c and Hsp90 with HCV IRES RNA.

To investigate the role of Hsp90 in HCV IRES-mediated translation further, we confirmed the interaction of eIF3c and Hsp90 by immunoprecipitation. The pFLAG-eIF3c vector was constructed by subcloning a DNA fragment encoding full-length human eiF3c into the EcoRI and XbaI sites of the pFLAG CMV™-2 expression vector (Sigma–Aldrich Chemical Co.) so that the amino-terminal FLAG epitope was fused in-frame with eIF3c. The pFLAG-eIF3c expression vector or the control vector pFLAG-CMV2 was transfected into NNC#2 cells or Huh-7 cells. After 48 h, the immunoprecipitates

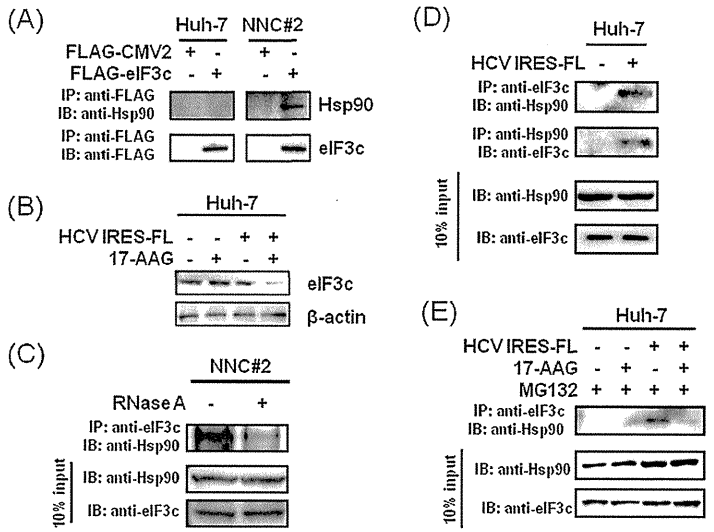

Fig. 4. An interaction between eIF3c and Hsp90 was induced by HCV IRES. (A) The pFLAG-eIF3c vector was constructed by subcloning a DNA fragment encoding full-length human eiF3c into the EcoRI and XbaI sites of the pFLAG CMV™-2 expression vector (Sigma–Aldrich Chemical Co.) such that the amino-terminal FLAG epitope was fused in-frame with eIF3c. Huh-7 and NNC#2 cells were transfected with pFLAG-eIF3c or pFLAG-CMV2 control plasmids using Lipofectamine 2000 (Invitrogen). Cell lysates were immunoprecipitated by the anti-FLAG M2 antibody 48 h after transfection. The precipitates were analyzed by western blot using the anti-Hsp90 antibody. (B) The Huh-7 cells were transfected with or without pHCV IRES-firefly luciferase (HCV IRES-FL) (Fig. 1B) and then treated with or without 17-AAG (50 nM). Cell lysates were analyzed by western blot 48 h post-treatment with an eIF3c primary antibody (Santa Cruz Biotechnology). Horseradish peroxidase-conjugated anti-rabbit antibody (Sigma-Aldrich Chemical Co.) was used as the secondary antibody. β-Actin was used as an internal control. (C) The interruption of Hsp90–eIF3c interaction by RNase A treatment. NNC#2 cell lysates were treated with RNase A (5 U/μL) (Sigma–Aldrich Chemical Co.). After 4 h, the cell lysates were subjected to immunoprecipitation using an anti-eIF3c antibody, followed by immunoblot analysis using an anti-Hsp90 antibody. (D) eIF3c or Hsp90 co-immunoprecipitates with Hsp90 or eIF3c from cells transfected or untransfected with pHCV IRES-FL. Huh-7 cells were transfected with pHCV IRES-FL using Lipofectamine 2000 (Invitrogen) and subject to immunoprecipitation using the indicated antibodies at 24 h post-transfection. The precipitates were analyzed by western blot using the indicated antibodies. (E) The inhibitor 17-AAG dissociates Hsp90 and eIF3c from the HCV IRES complex. Huh-7 cells were transfected with pHCV IRES-FL using Lipofectamine 2000 (Invitrogen). At 24 h post-transfection, cells were treated with 17-AAG (50 nM) or DMSO as a control for 8 h and were then treated with MG132 (5 μM) for 16 h. Cell lysates were subjected to immunoprecipitation using an anti-eIF3c antibody, and the precipitates were analyzed by western blot using the anti-Hsp90 antibody.

(anti-FLAG antibody) were determined by western blot analysis (Fig. 4A). The western blot analysis clearly indicated that eIF3c and Hsp90 coprecipitated in NNC#2 cells, whereas they did not coprecipitate in Huh-7 cells, suggesting that eIF3c was bound to the chaperone complex that formed with Hsp90 in NNC#2 cells (Fig. 4A). This interaction between Hsp90 and eIF3c in NNC#2 cells suggests that HCV translation is due to the interaction between eIF3c and Hsp90. Given the observed binding of eIF3 with the HCV IRES RNA, this Hsp90-eIF3c interaction occurring in HCV replicon cells was likely mediated by HCV IRES RNA. To address this question, Huh-7 cells were transfected with pHCV IRES-firefly luciferase (HCV IRES-FL) (Fig. 1B) using Lipofectamine 2000 (Invitrogen) and then treated with 17-AAG (50 nM) or DMSO as a control. After treatment, the cell lysates were analyzed by western blot (Fig. 4B). The level of eIF3c was reduced by the 17-AAG treatment in cells transfected with pHCV IRES-FL compared to control DMSO, but eIF3c was not reduced in cells transfected with pHCV IRES-FL. The disruption of Hsp90 activity by the Hsp90 inhibitor, 17-AAG, appears to dissociate eIF3c from the Hsp90-eIF3c-HCV IRES complex and induce the degradation of the free forms of eIF3c. To verify this result, NNC#2 cell lysates were further treated with RNase A (5 U/μL) (Sigma–Aldrich Chemical Co.). After treatment, anti-eIF3c antibody immunoprecipitates were determined by western blot analysis (Fig. 4C). The analysis clearly indicated that eIF3c and Hsp90 coprecipitated in NNC#2 cell lysates, whereas they did not coprecipitate in NNC#2 cells lysates treated with RNase A. The interaction between Hsp90 and eIF3c was interrupted by RNase A treatment. These results suggest that the interaction of eIF3c and Hsp90 is dependent on HCV IRES binding. Next, to further demonstrate whether HCV IRES is required for the interaction between eIF3c and Hsp90, we performed a co-immunoprecipitation assay using the extracts of cells transfected with pHCV IRES-FL. eIF3c co-immunoprecipitated with anti-Hsp90 (Fig. 4D). The interaction of eIF3c and Hsp90 was further confirmed by reverse co-immunoprecipitation of Hsp90 and eIF3c (Fig. 4D). These results also indicated that the interaction of eIF3c and Hsp90 was supported by the HCV IRES. Furthermore, we performed an immunoprecipitation assay to confirm that eIF3c and Hsp90 interaction was influenced by the treatment with 17-AAG in cells transfected with pHCV IRES-FL. Huh-7 cells were transfected with pHCV IRES-FL using Lipofectamine 2000 (Invitrogen). At 24 h post-transfection, the cells were treated with 17-AAG (50 nM) or DMSO as a control for 8 h and then MG132 (5 μM) for 16 h. An immunoprecipitation assay with the cell lysates was performed using the anti-eIF3c antibody, and the precipitates were analyzed by western blot using the anti-Hsp90 antibody. Although treatment with both 17-AAG and MG132 in cells transfected with pHCV IRES-FL resulted in a reduction in the interaction of Hsp90 and eIF3c, eIF3c expression recovered upon treatment with the proteasome inhibitor MG132 (Fig. 4E), but the interaction between Hsp90 and eIF3c was not restored (Fig. 4E). Furthermore, eIF3c was not detected in cells not treated with MG132 (Fig. 2B), which indicates that eIF3c is a client protein for active Hsp90 (Fig. 2C). In contrast, an interaction between Hsp90 and eIF3c was observed in cells not treated with 17-AAG (Fig. 4E). These results suggest that the interaction between Hsp90 and eIF3c is specific to HCV IRES-expressing cells. However, the interaction of Hsp90 and eIF3c in the presence of 17-AAG, which blocks the association of Hsp90 with eIF3c, may dissociate Hsp90 and eIF3c from the overall HCV IRES complex (Figs. 2B and C, and 4B and E).

In conclusion, our results demonstrate that HCV IRES-mediated translational inhibition occurs through a reduction of eIF3c expression caused by the Hsp90 inhibitor-mediated disruption of the interaction between eIF3c and Hsp90 with HCV IRES RNA. Furthermore, the interaction between Hsp90 and eIF3c requires HCV IRES RNA. Taken together, our results suggest that the interaction between Hsp90 and eIF3c plays an important role in HCV IRES-mediated translation. More experiments are needed to verify the relationship between eukaryotic initiation factor 3 (eIF3) and Hsp90.

Conflict of interest

The authors declare no conflict of interest.

Acknowledgements

We thank Dr. A. Ryo for providing pCMV-Myc-Ubi. We are grateful to S. Yamaguchi, M. Sato, and Y. Katumura for their excellent technical assistance. This work was supported by a Grant-in-Aid for HCV Research from the Ministry of Health, Labor, and Welfare of Japan, by a Grant-in-Aid for High Technology Research (HTR) from the Ministry of Education, Science, Sports, and Culture of Japan, and a Grant from the Strategic Research Foundation Grant-aided Project for Private Universities from the Ministry of Education, Culture, Sport, Science, and Technology, Japan (MEXT).

References

Aoyagi, K., Ohue, C., Iida, K., Kimura, T., Tanaka, E., Kiyosawa, K., Yagi, S., 1999. Development of a simple and highly sensitive enzyme immunoassay for hepatitis C virus core antigen. J. Clin. Microbiol. 37 (6), 1802–1808.
Bagatell, R., Paine-Murrieta, G.D., Taylor, C.W., Pulcini, E.J., Akinaga, S., Benjamin, J., Whitesell, L., 2000. Induction of a heat shock factor 1-dependent stress response alters the cytotoxic activity of hsp90-binding agents. Clin. Cancer Res. 6 (8), 3312–3318.
Bartenschlager, R., Lohmann, V., 2001. Novel cell culture systems for the hepatitis C virus. Antivir. Res. 52 (1), 1–17.
Collier, A.J., Gallego, J., Klinck, R., Cole, P.T., Harris, S.J., Harrison, G.P., Aboul-Ela, F., Varani, G., Walker, S., 2002. A conserved RNA structure within the HCV IRES eIF3-binding site. Nat. Struct. Biol. 9 (5), 375–380.
Coumailleau, P., Poellinger, L., Gustafsson, J.A., Whitelaw, M.L., 1995. Definition of a minimal domain of the dioxin receptor that is associated with Hsp90 and maintains wild type ligand binding affinity and specificity. J. Biol. Chem. 270 (42), 25291–25300.
Doong, H., Rizzo, K., Fang, S., Kulpa, V., Weissman, A.M., Kohn, E.C., 2003. CAIR-1/BAG-3 abrogates heat shock protein-70 chaperone complex-mediated protein degradation: accumulation of poly-ubiquitinated Hsp90 client proteins. J. Biol. Chem. 278 (31), 28490–28500.
Fraser, C.S., Doudna, J.A., 2007. Structural and mechanistic insights into hepatitis C viral translation initiation. Nat. Rev. Microbiol. 5 (1), 29–38.
Garcia-Cardena, G., Fan, R., Shah, V., Sorrentino, R., Cirino, G., Papapetropoulos, A., Sessa, W.C., 1998. Dynamic activation of endothelial nitric oxide synthase by Hsp90. Nature 392, 821–824.
Grakoui, A., Wychowski, C., Lin, C., Feinstone, S.M., Rice, C.M., 1993. Expression and identification of hepatitis C virus polyprotein cleavage products. J. Virol. 67 (3), 1385–1395.
Guo, F., Rocha, K., Bali, P., Pranpat, M., Fiskus, W., Boyapalle, S., Kumaraswamy, S., Balasis, M., Greedy, B., Armitage, E.S., Lawrence, N., Bhalla, K., 2005. Abrogation of heat shock protein 70 induction as a strategy to increase antileukemia activity of heat shock protein 90 inhibitor 17-allylamino-demethoxy geldanamycin. Cancer Res. 65 (22), 10536–10544.
Hijikata, M., Mizushima, H., Shimotohno, K., 1993. Two distinct proteinase activities required for the processing of a putative nonstructural precursor protein of hepatitis C virus. J. Virol. 67 (8), 4665–4675.
Hinnebusch, A.G., 2006. eIF3: a versatile scaffold for translation initiation complexes. Trends Biochem. Sci. 10, 553–562.
Ishii, N., Watashi, K., Hishiki, T., Goto, K., Inoue, D., Hijikata, M., Wakita, T., Kato, N., Shimotohno, K., 2006. Diverse effects of cyclosporine on hepatitis C virus strain replication. J. Virol. 80 (9), 4510–4520.
Julien, P., Rodolfo, R., Jan, M., Isabel, A., Jerome, B., Emmanuel, D., Florence, B., 2009. Human initiation factor eIF3 subunit b interacts with HCV IRES RNA through its N-terminal RNA recognition motif. FEBS Lett. 583 (1), 70–74.
Kieft, J.S., Zhou, K., Jubin, R., Doudna, J.A., 2001. Mechanism of ribosome recruitment by hepatitis C IRES RNA. RNA 7 (2), 194–206.
Kieft, J.S., Zhou, K., Grech, A., Jubin, R., Doudna, J.A., 2002. Crystal structure of an RNA tertiary domain essential to HCV IRES-mediated translation initiation. Nat. Struct. Biol. 9 (5), 370–374.
Kim, T.S., Jang, K., Kim, C.-Y., Lee, H.D., Ahn, J.Y., Kim, B.-Y., 2006. J. Interaction of Hsp90 with ribosomal proteins protects from ubiquitination and proteasome-dependent degradation. Mol. Biol. Cell 17 (2), 824–833.
Lukavsky, P.J., 2008. Structure and function of HCV IRES domains. Virus Res. 139 (2), 166–171.
Masutani, M., Sonenberg, N., Yokoyama, S., Imataka, H., 2007. Reconstitution reveals the functional core of mammalian eIF3. EMBO J. 26 (14), 3373–3383.
Morimoto, R.I., 1998. Regulation of the heat shock transcriptional response: cross talk between a family of heat shock factors, molecular chaperones, and negative regulators. Genes Dev. 12 (24), 3788–3796.
Nagata, Y., Anan, T., Yoshida, T., Mizukami, T., Taya, Y., Fujiwara, T., Kato, H., Saya, H., Nakao, M., 1999. The stabilization mechanism of mutant-type p53 by impaired ubiquitination: the loss of wild-type p53 function and the hsp90 association. Oncogene 18 (44), 6037–6049.
Neckers, L., 2003. Development of small molecule Hsp90 inhibitors: utilizing both forward and reverse chemical genomics for drug identification. Curr. Med. Chem. 10 (9), 733–739.
Nakagawa, S., Umehara, T., Matsuda, C., Kuge, S., Sudoh, M., Kohara, M., 2007. Hsp90 inhibitors suppress HCV replication in replicon cells and humanized liver mice. Biochem. Biophys. Res. Commun. 353 (4), 882–888.
Okamoto, T., Nishimura, Y., Ichimura, T., Suzuki, K., Miyamura, T., Suzuki, T., Moriishi, K., Matsuura, Y., 2006. hepatitis C virus RNA replication is regulated by FKBP8 and Hsp90. EMBO J. 25 (20), 5015–5025.
Richter, K., Buchner, J., 2001. Hsp90, chaperoning signal transduction. J. Cell. Physiol. 188 (3), 281–290.
Sato, S., Fujita, N., Tsuruo, T., 2000. Modulation of Akt kinase activity by binding to Hsp90. Proc. Natl. Acad. Sci. U.S.A. 97 (20), 10832–10837.
Schulte, T.W., Blagosklonny, M.V., Ingui, C., Neckers, L., 1995. Disruption of the Raf-1-Hsp90 molecular complex results in destabilization of Raf-1 and loss of Raf-1-Ras association. J. Biol. Chem. 270 (41), 24585–24588.
Siridechadilok, B., Fraser, C.S., Hall, R.J., Doudna, J.A., Nogales, E., 2005. Structural roles for human translation factor eIF3 in initiation of protein synthesis. Science 310, 1513–1515.
Spahn, C.M., Kieft, J.S., Grassucci, R.A., Penczek, P.A., Zhou, K., Doudna, J.A., Frank, J., 2001. Hepatitis C virus IRES RNA-induced changes in the conformation of the 40s ribosomal subunit. Science 291, 1959–1962.
Taylor, D.R., Shi, S.T., Tomano, P.R., Barber, G.N., Lai, M.M., 1999. Inhibition of the interferon-inducible protein kinase PKR by HCV E2 protein. Science 285, 107–110.
Ujino, S., Yamaguchi, S., Shimotohno, K., Takaku, H., 2009. Heat-shock protein 90 is essential for stabilization of the hepatitis C virus nonstructural protein NS3. J. Biol. Chem. 284 (11), 6841–6846.
Ujino, S., Yamaguchi, S., Shimotohno, K., Takaku, H., 2010. Combination therapy for hepatitis C virus with heat-shock protein 90 inhibitor 17-AAG and proteasome inhibitor MG132. Antivir. Chem. Chemother. 20 (4), 161–167.
Waxman, L., Whitney, M., Pollok, B.A., Kuo, L.C., Darke, P.L., 2001. Host cell factor requirement for hepatitis C virus enzyme maturation. Proc. Natl. Acad. Sci. U.S.A. 98 (24), 13931–13935.
Waza, M., Adachi, H., Katsuno, M., Minamiyama, M., Sang, C., Tanaka, F., Inukai, A., Doyu, M., Sobue, G., 2005. 17-AAG, an Hsp90 inhibitor, ameliorates polyglutamine-mediated motor neuron degeneration. Nat. Med. 11 (10), 1088–1095.
Xu, W., Mimnaugh, E., Rosser, M.F., Nicchitta, C., Marcu, M., Yarden, Y., Neckers, L., 2001. Sensitivity of mature Erbb2 to geldanamycin is conferred by its kinase domain and is mediated by the chaperone protein Hsp90. J. Biol. Chem. 276 (5), 3702–3708.
Zhou, M., Sandercock, A.M., Fraser, C.S., Ridlova, G., Stephens, E., Schenauer, M.R., Yokoi-Fong, T., Barsky, D., Leary, J.A., Hershey, J.W., Doudna, J.A., Robinson, C.V., 2008. Mass spectrometry reveals modularity and a complete subunit interaction map of the eukaryotic translation factor eIF3. Proc. Natl. Acad. Sci. U.S.A. 105 (47), 18139–18144.

Author's personal copy

JOURNAL OF VIROLOGY, Sept. 2011, p. 8556–8568 Vol. 85, No. 17
0022-538X/11/$12.00 doi:10.1128/JVI.00146-11

Hepatitis C Virus Infection Promotes Hepatic Gluconeogenesis through an NS5A-Mediated, FoxO1-Dependent Pathway▽

Lin Deng,[1] Ikuo Shoji,[1] Wataru Ogawa,[2] Shusaku Kaneda,[1] Tomoyoshi Soga,[3] Da-peng Jiang,[1] Yoshi-Hiro Ide,[1] and Hak Hotta[1]*

Division of Microbiology, Center for Infectious Diseases,[1] and Division of Diabetes, Metabolism and Endocrinology,[2] Kobe University Graduate School of Medicine, 7-5-1 Kusunoki-cho, Chuo-ku, Kobe 650-0017, Japan, and Institute for Advanced Biosciences, Keio University, 246-2 Mizukami, Kakuganji, Tsuruoka, Yamagata 997-0052, Japan[3]

Received 21 January 2011/Accepted 7 June 2011

Chronic hepatitis C virus (HCV) infection is often associated with type 2 diabetes. However, the precise mechanism underlying this association is still unclear. Here, using Huh-7.5 cells either harboring HCV-1b RNA replicons or infected with HCV-2a, we showed that HCV transcriptionally upregulated the genes for phosphoenolpyruvate carboxykinase (PEPCK) and glucose 6-phosphatase (G6Pase), the rate-limiting enzymes for hepatic gluconeogenesis. In this way, HCV enhanced the cellular production of glucose 6-phosphate (G6P) and glucose. PEPCK and G6Pase gene expressions are controlled by the transcription factor forkhead box O1 (FoxO1). We observed that although neither the mRNA levels nor the protein levels of FoxO1 expression were affected by HCV, the level of phosphorylation of FoxO1 at Ser319 was markedly diminished in HCV-infected cells compared to the control cells, resulting in an increased nuclear accumulation of FoxO1, which is essential for sustaining its transcriptional activity. It was unlikely that the decreased level of FoxO1 phosphorylation was mediated through Akt inactivation, as we observed an increased phosphorylation of Akt at Ser473 in HCV-infected cells compared to control cells. By using specific inhibitors of c-Jun N-terminal kinase (JNK) and reactive oxygen species (ROS), we demonstrated that HCV infection induced JNK activation via increased mitochondrial ROS production, resulting in decreased FoxO1 phosphorylation, FoxO1 nuclear accumulation, and, eventually, increased glucose production. We also found that HCV NS5A mediated increased ROS production and JNK activation, which is directly linked with the FoxO1-dependent increased gluconeogenesis. Taken together, these observations suggest that HCV promotes hepatic gluconeogenesis through an NS5A-mediated, FoxO1-dependent pathway.

Hepatitis C virus (HCV) is a small, enveloped RNA virus that belongs to the genus *Hepacivirus* of the family *Flaviviridae*, and the molecular mechanisms underlying its viral replication are currently being unraveled (40). The HCV genome encodes a single polyprotein of about 3,000 amino acids, which is cleaved by host and viral proteases to generate at least 10 viral proteins, such as core, envelope 1 (E1), E2, p7, NS2, NS3, NS4A, NS4B, NS5A, and NS5B. HCV can be classified into seven genotypes, with each genotype further classified into a number of subtypes, such as HCV-1a and HCV-1b (18, 24, 59).

HCV infects more than 120 million people worldwide (57). Persistent HCV infection causes not only liver diseases (chronic hepatitis, liver cirrhosis, and hepatocellular carcinoma) but also extrahepatic manifestations, such as type 2 diabetes (2, 11, 20, 23). While it is known that liver cirrhosis impairs the glucose metabolism of the liver, there are some reports showing that HCV-infected patients over 40 years of age have an increased risk of type 2 diabetes compared with individuals without HCV infection (43). In addition, insulin receptor substrate 1 (IRS-1)/phosphatidylinositol 3-kinase (PI3-kinase) signaling was more impaired in HCV-infected patients than in non-HCV-infected controls (3). These studies imply that HCV infection may directly predispose the host toward type 2 diabetes. However, the precise mechanisms are poorly understood.

Hepatocytes play an important role in maintaining plasma glucose homeostasis by adjusting the balance between hepatic glucose production and utilization via the gluconeogenic and glycolytic pathways, respectively. It was proposed previously that increased hepatic glucose production is a major feature of type 2 diabetes (13). It is also known that hyperglycemia and the subsequent development of type 2 diabetes mellitus result, at least in part, from impaired insulin signaling together with elevated glucagon levels (5, 19). Hepatic glucose production and utilization, physiologically opposed cascades, are regulated, at least in part, at the transcriptional level of the glucose 6-phosphatase (G6Pase) and glucokinase (GK) genes, which catalyze the last and the first rate-limiting steps in gluconeogenesis and glycolysis, respectively. A number of studies have shown that fasting/feeding (or hormones) controls the transcription of these two enzymes in the opposite directions. G6Pase transcription is negatively regulated by insulin or feeding and is markedly increased in a fasting state (62). On the other hand, GK transcription is positively regulated by insulin or feeding and markedly decreased in a fasting state (33). It has also been reported that the gene expressions of gluconeogenic and glycolytic enzymes, such as G6Pase, GK, and phosphoenolpyruvate carboxykinase (PEPCK), another rate-limiting enzyme for hepatic gluconeogenesis, are regulated by certain transcription factors, including forkhead box O1 (FoxO1) (26, 50, 54), hepatic nuclear factor 4α (HNF-4α) (26), Krüppel-like factor 15 (KLF15) (64), and cyclic AMP (cAMP) response element binding protein (CREB) (52, 56). The deregulation of the otherwise balanced control of hepatic glucose homeostasis would potentially lead to hyperglycemia and, eventually, type 2 diabetes.

In this study, by using Huh-7.5 cells harboring HCV-1b RNA replicons, i.e., either a subgenomic RNA replicon (SGR) or a full-genomic RNA replicon (FGR) (37), and cells infected with HCV-2a (14, 37, 39), we investigated the possible effects of HCV on glucose metabolism. We report here that HCV promotes hepatic gluconeogenesis, resulting in increased cellular glucose production in hepatocytes via an NS5A-mediated, FoxO1-dependent pathway.

* Corresponding author. Mailing address: Division of Microbiology, Center for Infectious Disease, Kobe University Graduate School of Medicine, 7-5-1 Kusunoki-cho, Chuo-ku, Kobe 650-0017, Japan. Phone: 81-78-382-5500. Fax: 81-78-382-5519. E-mail: hotta@kobe-u.ac.jp.

▽ Published ahead of print on 22 June 2011.

TABLE 1. Sequences and positions of primers used in this study

Gene (GenBank accession no.)	Primer	Positions	PCR product (bp)
GK (M69051)	5′-GCCTCCCAAAGCATCTACCTC-3′	119–139	444
	5′-GCTCCACTGCCCCTCCTCACC-3′	562–542	
G6Pase (U01120)	5′-CCTGGGGCTGGCTCTCAACTC-3′	889–909	309
	5′-AATAGTAGTCCTCCTCAATCC-3′	1197–1177	
PEPCK (BC023978)	5′-CCAGGCAGTGAGGGAGTTTCT-3′	210–230	217
	5′-ACTGTGTCTCTTTGCTCTTGG-3′	426–406	
FoxO1 (NM_002915)	5′-GAGGGTTAGTGAGCAGGTTAC-3′	2352–2372	217
	5′-AGTCCTTATCTACAGCAGCAC-3′	2568–2548	
HCV NS5A (JF343793)	5′-AGACGTATTGAGGTCCATGC-3′	6899–6918	133
	5′-CCGCAGCGACGGTGCTGATAG-3′	7011–7031	
β-Glucuronidase (M15182)	5′-ATCAAAAACGCAGAAAATACG-3′	1747–1767	238
	5′-ACGCAGGTGGTATCAGTCTTG-3′	1984–1964	
GAPDH (NM_002046)	5′-GCCATCAATGACCCCTTCATT-3′	196–216	149
	5′-TCTCGCTCCTGGAAGATGG-3′	326–344	

MATERIALS AND METHODS

Cells, HCV RNA replicons, and virus. The human hepatoma-derived cell line Huh-7.5 (7) was kindly provided by C. M. Rice (Rockefeller University, New York, NY). The SGR and FGR were prepared by using pFK5B/2884Gly (41) (a kind gift from R. Bartenschlager, University of Heidelberg, Heidelberg, Germany) and pON/C-5B (31) (a kind gift from N. Kato, Okayama University, Okayama, Japan), respectively. The SGR and FGR cells are of polyclonal origin to avoid clonal variation. Plasmid pFL-J6/JFH1, which encodes the entire viral genome of a chimeric strain of HCV-2a (J6/JFH1) (39), was kindly provided by C. M. Rice. The HCV RNA genome was transcribed *in vitro* from pFL-J6/JFH1 and transfected into Huh-7.5 cells to yield infectious HCV particles, as described previously (14). A cell culture-adapted P-47 strain (9, 14) was used throughout the experiments. Virus infection was performed at a multiplicity of infection (MOI) of 2.0. Virus infectivity was measured by indirect immunofluorescence analysis, as described below, and expressed as cell-infecting units/ml. In some experiments, SGR and FGR cells, as well as HCV-infected cells at 5 days after virus infection, were treated with 1,000 IU/ml of alpha interferon (IFN) (Sigma Chemical, St. Louis, MO) for 10 days to eliminate HCV replication.

Plasmid construction. Expression plasmids for core, p7, NS2, NS3, NS3/4A, NS4A, NS4B, NS5A, and NS5B were reported elsewhere previously (15, 32).

Real-time quantitative RT-PCR. Total cellular RNA was isolated by using RNAiso reagent (Takara, Kyoto, Japan), and cDNA was generated by using a QuantiTect reverse transcription (RT) system (Qiagen, Valencia, CA). Real-time quantitative PCR was performed by using SYBR Premix Ex *Taq* (Takara) with SYBR green chemistry on an ABI Prism 7000 system (Applied Biosystems, Foster City, CA), as reported previously (37). β-Glucuronidase and GAPDH (glyceraldehyde-3-phosphate dehydrogenase) were used as internal controls. The primers used are shown in Table 1.

G6P production assay. Huh-7.5 cells seeded into a 10-cm dish at a density of 1.0×10^6 cells/dish were infected with HCV or left uninfected. At different time points after infection, the cells were washed twice with 5% mannitol solution and covered with methanol (1 ml) containing 25 μM (each) four internal standards (3-aminopyrolidine, L-methionine sulfone, trimesate, and 2-morpholinoethanesulfonic acid) for enzyme inactivation. The mixtures of methanol and cells were collected and mixed with Milli-Q water and chloroform at ratios of 2:1:2. Both the medium and cell sample solutions were then centrifuged at 20,000 × *g* for 15 min, and the aqueous layers were collected for centrifugal filtration through a 5-kDa-cutoff filter at 9,000 × *g* for 2 h. The extracted metabolites were concentrated with a centrifugal concentrator and stored at −80°C until analysis. Glucose 6-phosphate (G6P) concentrations were measured by capillary electrophoresis time-of-flight mass spectrometry (CE-TOFMS), and the results were normalized to the cell number as described previously (60, 61).

Glucose production assay. Culture medium was replaced with glucose production buffer consisting of glucose-free Dulbecco's modified Eagle's medium (DMEM) (Sigma Chemical), without phenol red, supplemented with a gluconeogenic substrate (2 mM sodium pyruvate and 20 mM sodium lactate). After 24 h of incubation, the medium was collected, and the total glucose concentration was measured by using a commercial kit (Glucose CII Test Wako; Wako Pure Chemical Industries, Osaka, Japan) and normalized to the cellular protein content. As the baseline of glucose production, glucose-free DMEM with neither sodium pyruvate nor sodium lactate was used. Glucose production via gluconeogenesis equals the total glucose production minus the baseline glucose production.

Luciferase reporter assay. The PEPCK gene promoter (position −1263/+225) and a deletion mutant (position −998/+225) were inserted into the pGL3 luciferase reporter plasmid (Promega, Madison, WI). The constructs were designated rPEPCK-P5(−1263)-pGL3basic and rPEPCK-P4(−998)-pGL3basic. pRL-CMV-Renilla (Promega), which expresses *Renilla* luciferase, was used as an internal control. Huh-7.5 cells prepared in a 12-well tissue culture plate at a density of 1.0×10^5 cells/well were transiently transfected with pRL-CMV-Renilla and rPEPCK-P5(−1263)-pGL3basic or rPEPCK-P4(−998)-pGL3basic in the presence of pEF1/NS4A, pEF1/NS5A, or a control vector (32). After 48 h, a luciferase assay was performed by using the Dual-Luciferase reporter assay system (Promega). Firefly and *Renilla* luciferase activities were measured with a Lumat LB 9501 luminometer (Berthold, Bad Wildbad, Germany). Firefly luciferase activity was normalized to *Renilla* luciferase activity for each sample.

Detection of mitochondrial ROS. Mitochondrial reactive oxygen species (ROS) production was analyzed as described previously (14). Briefly, cells seeded onto glass coverslips in a 24-well plate were incubated with 5 μM MitoSOX red (Molecular Probes, Eugene, OR) at 37°C for 10 min and then fixed with 3.7% paraformaldehyde and observed under a confocal laser scanning microscope (Carl Zeiss, Oberkochen, Germany). When needed, the fixed cells

were subjected to indirect immunofluorescence analysis to confirm HCV infection or NS5A expression, as described below.

Indirect immunofluorescence. Huh-7.5 cells seeded onto glass coverslips in a 24-well plate were infected with HCV or transfected with an NS5A expression plasmid. At 5 days postinfection (dpi) or 3 days posttransfection, the cells were fixed with 3.7% paraformaldehyde in phosphate-buffered saline (PBS) for 15 min at room temperature and permeabilized with 0.1% Triton X-100 in PBS for 15 min at room temperature. Mock-infected or empty-vector-transfected cells were similarly treated as controls for comparisons. After being washed with PBS twice, cells were consecutively stained with primary and secondary antibodies. The primary antibodies used were anti-FoxO1 rabbit monoclonal antibody (Cell Signaling Technology, Danvers, MA), anti-NS5A mouse monoclonal antibody (Chemicon International, Temecula, CA), and serum from an HCV-infected patient. Secondary antibodies used were Alexa Fluor 488-conjugated goat anti-rabbit immunoglobulin G (IgG), Alexa Fluor 594-conjugated goat anti-mouse IgG or anti-human IgG (Molecular Probes), and fluorescein isothiocyanate (FITC)-conjugated goat anti-mouse IgG or anti-human IgG (MBL, Nagoya, Japan). The stained cells were observed under a confocal laser scanning microscope (Carl Zeiss).

Cell fractionation and immunoblotting. Nuclear and cytoplasmic extracts from cells were prepared by using an NE-PER nuclear and cytoplasmic extraction reagent kit (Pierce Chemical, Rockford, IL). For immunoblotting, cells were lysed with SDS sample buffer, and equal amounts of protein were subjected to SDS-polyacrylamide gel electrophoresis and transferred onto a polyvinylidene difluoride membrane (Millipore, Bedford, MA), which was then incubated with the respective primary antibodies. The primary antibodies used were mouse monoclonal antibodies against HCV core (clone 2H9; a kind gift from T. Wakita, Department of Virology II, National Institute of Infectious Diseases, Tokyo, Japan), NS3, NS4A, NS5A, GAPDH (Chemicon), FoxO1 (Sigma Chemical), phospho-Akt (Ser473) (Cell Signaling Technology), and c-Myc (9E10; Santa Cruz Biotechnology, Santa Cruz, CA); rabbit polyclonal antibodies against phospho-FoxO1 (Ser139), Oct-1 (Santa Cruz Biotechnology), c-Jun N-terminal kinase (JNK), phospho-JNK (Thr183/Tyr185), c-Jun, phospho-c-Jun (Ser63), and Akt (Cell Signaling Technology); and goat polyclonal antibody against HSP60 (Santa Cruz Biotechnology). Horseradish peroxidase-conjugated goat anti-mouse IgG, goat anti-rabbit IgG (Molecular Probes), and donkey anti-goat IgG (Santa Cruz Biotechnology) were used to visualize the respective proteins by means of an enhanced chemiluminescence detection system (ECL; GE Healthcare, Buckinghamshire, United Kingdom).

Statistical analysis. Results were expressed as means ± standard errors of the means (SEM). Statistical significance was evaluated by analysis of variance (ANOVA) and was defined as a P value of <0.05.

RESULTS

HCV upregulates gene expression of PEPCK and G6Pase and downregulates gene expression of GK. We first examined the expression levels of the genes for the rate-limiting enzymes in hepatic gluconeogenesis, PEPCK and G6Pase, and of those for GK, which catalyzes the first step of glycolysis, by means of real-time quantitative RT-PCR analysis. We observed that the PEPCK and G6Pase genes were transcriptionally activated in SGR- and FGR-harboring cells (Fig. 1A and B, left). Similarly, the PEPCK and G6Pase genes were upregulated in HCV-infected cells in a time-dependent manner, starting from 3 or 5 days postinfection (dpi) up to 14 dpi (Fig. 1A and B, middle). On the other hand, the GK gene was transcriptionally downregulated in SGR- and FGR-harboring cells and HCV-infected cells in a time-dependent manner (Fig. 1C). It is noteworthy that the gene expressions of six glycolytic enzymes (not including GK) were observed to be upregulated in HCV-infected cells at 1 dpi (16).

When IFN treatment eliminated HCV from the cells, the observed upregulation of PEPCK and G6Pase gene expressions as well as the downregulation of GK gene expression in SGR- and FGR-harboring cells and HCV-infected cells were cancelled (Fig. 1A, B, and C, left and right). Thus, our results suggest that there was a trend toward an increase in gluconeogenesis in SGR- and FGR-harboring cells and HCV-infected cells. In subsequent studies we further examined whether or not HCV replication was correlated with gluconeogenesis.

HCV promotes cellular production of glucose and G6P. We then examined the effect of HCV on cellular glucose production. The results showed that SGR- and FGR-harboring cells and HCV-infected cells produced greater amounts of glucose than did the control cells (Fig. 2A, top and middle). IFN treatment cancelled the enhanced glucose production in SGR- and FGR-harboring cells and in HCV-infected cells (Fig. 2A, top and bottom). We also investigated the production of G6P, which is an important precursor molecule that is converted to glucose in the gluconeogenesis pathway, by means of metabolome analysis. As shown in Fig. 2B, a significantly higher level of G6P was accumulated in HCV-infected cells than in control cells. Taken together, these results indicate that HCV indeed promotes hepatic gluconeogenesis to cause hyperglycemia. In the following analyses, we examined the possible mechanisms of HCV-induced increased gluconeogenesis.

HCV suppresses FoxO1 phosphorylation at Ser319, leading to the nuclear accumulation of FoxO1. It was demonstrated previously that FoxO1 in hepatocytes enhances gluconeogenesis through the transcriptional activation of various genes, including G6Pase and PEPCK (25). To investigate the possible effects of FoxO1 on HCV-induced gluconeogenesis, we examined the gene expression levels of FoxO1 by real-time quantitative RT-PCR analysis. As shown in Fig. 3A, there was neither an upregulation nor a downregulation of FoxO1 gene expression in SGR- or FGR-harboring cells or HCV-infected cells. The FoxO1 transcription factor is controlled by various post-translational modifications, which include phosphorylation, ubiquitylation, and acetylation. The phosphorylated form of FoxO1 is exported from the nucleus and thereby loses its transcriptional function (30). We therefore examined the phosphorylation status of FoxO1 at Ser319, which is critical for FoxO1 nuclear exclusion (72). The results showed that FoxO1 phosphorylation at Ser319 was markedly suppressed in HCV-infected cells from 4 dpi up to 8 dpi, compared to that in the HCV-negative control cells (Fig. 3B, first panel), in a time-dependent manner that was roughly the inverse of the pattern observed for PEPCK and G6Pase mRNA upregulations (Fig. 1A and B) and glucose production (Fig. 2A), while the total protein expression levels of FoxO1 were unchanged (Fig. 3B, second panel). Regarding this connection, Banerjee et al. reported previously that FoxO1 phosphorylation at Ser256 was also inhibited in HCV-infected cells (4). Since FoxO1 is known to be phosphorylated by Akt so as to be exported from the nucleus and transcriptionally inactivated (38), we examined whether Akt function was suppressed through its impaired phosphorylation in HCV-infected cells. The result obtained revealed that this was not the case: Akt phosphorylation was enhanced in HCV-infected cells from 4 dpi up to 6 dpi compared with the control cells (Fig. 3B, third panel), while the total protein expression levels of Akt were comparable (Fig. 3B, fourth panel). This result is consistent with a recent observation by Burdette et al. (10) showing that the Akt phosphorylation level was elevated in HCV-infected cells. These data suggest that the observed decrease in FoxO1 phosphorylation in HCV-infected cells is caused by a mechanism independent of Akt.

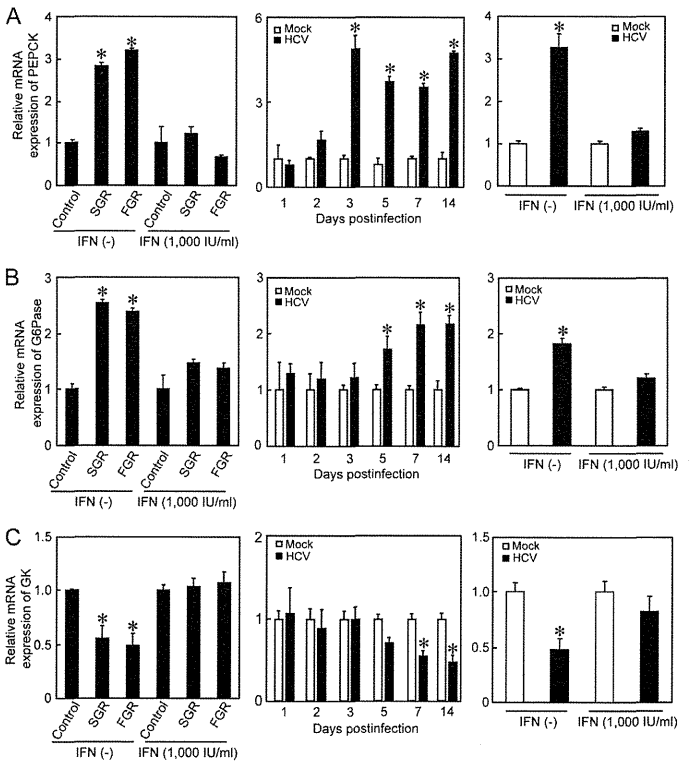

FIG. 1. HCV upregulates gene expressions of PEPCK and G6Pase and downregulates gene expression of GK. Quantitative RT-PCR analysis was performed to quantify PEPCK (A), G6Pase (B), and GK (C) mRNA expression levels in SGR- and FGR-harboring cells and HCV-infected cells (MOI = 2), and the results were normalized to β-glucuronidase mRNA expression levels. In parallel, SGR- and FGR-harboring cells and HCV-infected cells (at 5 dpi) were treated with IFN (1,000 IU/ml) for 10 days to eliminate HCV replication before being subjected to quantitative RT-PCR. Data represent means ± SEM of data from three independent experiments, and the values for the control cells were arbitrarily expressed as 1.0. *, $P < 0.01$ compared with the control.

Next, we tested whether HCV indeed promoted FoxO1 nuclear accumulation. The majority of FoxO1 was accumulated in the nuclear fraction in HCV-infected cells (Fig. 3C, second panel, lanes 2 and 4), whereas in control cells FoxO1 was distributed in both the nuclear and cytoplasmic fractions (lanes 1 and 3). Taken together, these results suggest that HCV suppressed FoxO1 phosphorylation, leading to the nuclear accumulation of FoxO1.

HCV-induced JNK activation is involved in the suppression of FoxO1 phosphorylation. Recent studies demonstrated that a signaling pathway that involves the stress-sensitive serine/threonine kinase JNK regulates FoxO at multiple levels (36, 66). We therefore investigated whether HCV induced JNK activation in Huh-7.5 cells. As shown in Fig. 4A, the amount of phosphorylated (activated) JNK markedly increased in HCV-infected cells in a time-dependent manner, similar to that observed for the suppression of FoxO1 phosphorylation, while the total expression levels of JNK were unchanged. As a result, c-Jun, a key substrate for JNK, was phosphorylated (activated) in HCV-infected cells but not in the mock-infected control cells. It should also be noted that the total expression levels of c-Jun in HCV-infected cells were significantly higher than those in the mock-infected control cells, suggesting that c-Jun activation through its phosphorylation stabilizes c-Jun protein expression in HCV-infected cells, as was proposed previously by Zhang et al (71).

We next sought to determine whether JNK activation was involved in the HCV-induced suppression of FoxO1 phosphorylation. HCV-infected cells at 5 days after virus infection were treated with the specific JNK inhibitor SP600125 (20 μM) (6)

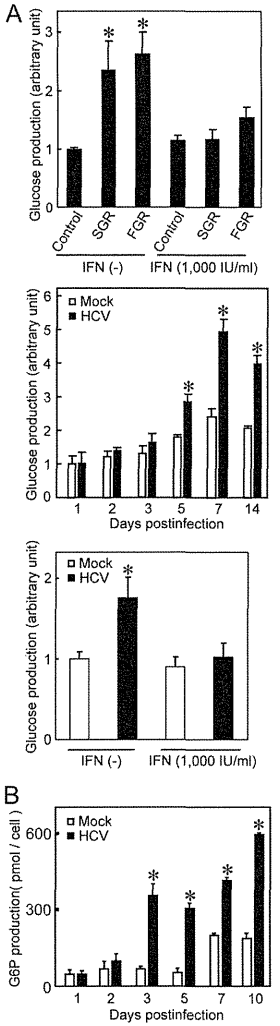

FIG. 2. HCV promotes the production of glucose and G6P. (A) Extracellular glucose production was measured in SGR- and FGR-harboring cells and HCV-infected cells (MOI = 2) and normalized to total cellular protein expression levels. In parallel, SGR- and FGR-harboring cells and HCV-infected cells (at 5 dpi) were treated with IFN (1,000 IU/ml) for 10 days to eliminate HCV replication before being subjected to glucose production analysis. Data represent means ± SEM of data from three independent experiments, and the value for the control cells was arbitrarily expressed as 1.0. *, $P < 0.01$ compared with the control. (B) Cellular G6Pase production was measured in HCV-infected cells (MOI = 2), and the results were normalized to cell numbers. Data represent means ± SEM of data from three independent experiments. *, $P < 0.01$ compared with the control.

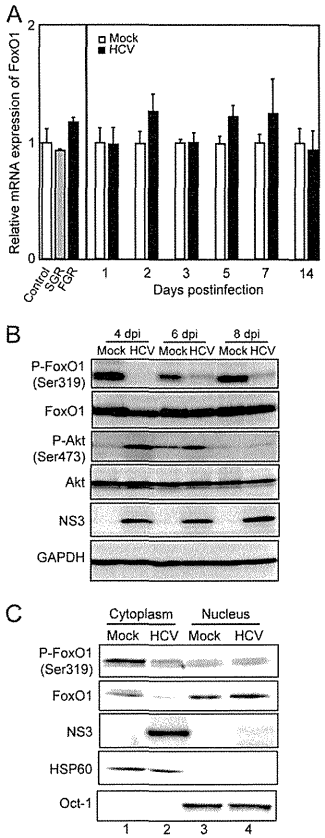

FIG. 3. HCV suppresses FoxO1 phosphorylation, leading to nuclear accumulation of FoxO1. (A) Quantitative RT-PCR analysis was performed to determine FoxO1 mRNA expression levels in SGR- and FGR-harboring cells and HCV-infected cells (MOI = 2), and expression levels were normalized to β-glucuronidase mRNA expression levels. (B) The expression levels of FoxO1, phospho-FoxO1 (Ser319) (P-FoxO1), Akt, and phospho-Akt (Ser473) were analyzed by immunoblotting of HCV-infected cells and mock-infected control cells. Blots were reprobed with antibodies recognizing NS3 and GAPDH. The amounts of GAPDH were measured as an internal control to verify equal amounts of sample loading. (C) Cytoplasmic and nuclear fractions were prepared from HCV-infected cells and mock-infected control cells at 4 dpi and were analyzed by immunoblotting using antibodies against FoxO1, phospho-FoxO1 (Ser319), NS3, Hsp60, and Oct-1. The amounts of Hsp60 and Oct-1 were measured to verify that they were equal to the amounts of cytoplasmic and nuclear fractions, respectively.

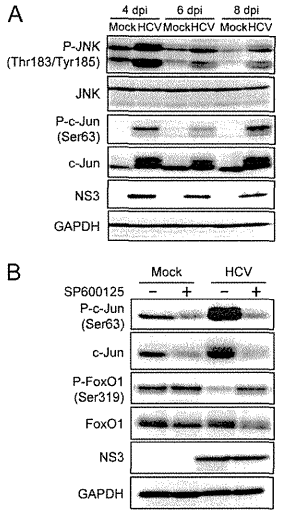

FIG. 4. HCV-induced JNK activation is required for the suppression of FoxO1 phosphorylation. (A) HCV activates the JNK/c-Jun signaling pathway. The activation (phosphorylation) of JNK (Thr183/Tyr185) and c-Jun (Ser63) in whole-cell lysates of HCV-infected cells and mock-infected control cells was analyzed by immunoblotting. Blots were reprobed with antibodies recognizing total JNK and c-Jun, NS3, and GAPDH. The amounts of GAPDH were measured as an internal control to verify equal amounts of sample loading. (B) Pretreatment with the JNK inhibitor SP600125 abrogates HCV-induced c-Jun activation and FoxO1 phosphorylation suppression. The phosphorylation of c-Jun (Ser63) and that of FoxO1 (Ser319) were analyzed by immunoblotting at 6 dpi in HCV-infected cells and mock-infected control cells with or without SP600125 pretreatment (20 μM for 24 h). Blots were reprobed with antibodies recognizing total c-Jun and FoxO1, NS3, and GAPDH. The amounts of GAPDH were measured as an internal control to verify equal amounts of sample loading.

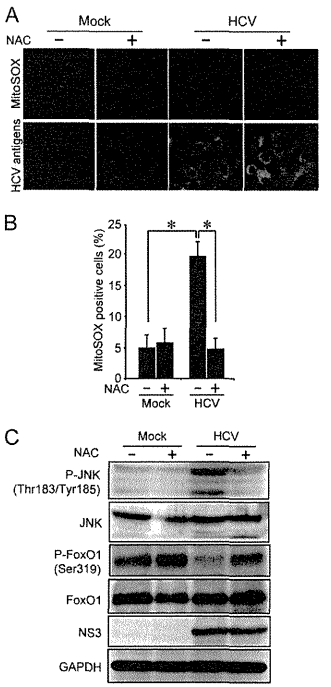

FIG. 5. HCV-induced production of mitochondrial ROS suppresses FoxO1 phosphorylation through activation of JNK. (A) Pretreatment with NAC abrogates the HCV-induced increased production of mitochondrial ROS. HCV-infected cells and mock-infected controls were pretreated with 5 mM NAC for 2 h at 6 dpi. The cells were then incubated with MitoSOX (top) and then stained for HCV antigens by using serum from an HCV-infected patient, followed by FITC-conjugated goat anti-human IgG (bottom). (B) Quantification of MitoSOX-stained cells. The percentages of cells stained with MitoSOX were determined for HCV-infected cells and mock-infected controls with or without NAC pretreatment. Data represent means ± SEM of data from two independent experiments. *, $P < 0.01$. (C) NAC pretreatment abrogates HCV-induced JNK activation and FoxO1 phosphorylation suppression. The phosphorylation of JNK (Thr183/Tyr185) and that of FoxO1 (Ser319) were analyzed by immunoblotting at 6 dpi in HCV-infected cells and mock-infected controls with or without NAC pretreatment (5 mM for 2 h). The blots were reprobed with antibodies recognizing total JNK and FoxO1, NS3, and GAPDH. The amounts of GAPDH were measured as an internal control to verify equal amounts of sample loading.

HCV-infected cells. These results suggest that HCV activates the JNK/c-Jun signaling pathway, which induces the nuclear accumulation of FoxO1 by reducing its phosphorylation status.

HCV-induced mitochondrial ROS production is involved in FoxO1 phosphorylation suppression, FoxO1 nuclear accumulation, and increased glucose production through JNK activation. We previously reported that HCV infection increases mitochondrial ROS production (14). JNK is known to be activated by ROS (35). We therefore sought to determine whether the HCV-induced increase in ROS production is an event occurring upstream of JNK activation by HCV. The pretreatment of HCV-infected cells (at 6 dpi) with 5 mM *N*-acetyl cysteine (NAC) (a general antioxidant) for 2 h significantly reduced the HCV-induced increase in ROS levels (Fig. 5A and B), as revealed by using MitoSOX, a fluorescent probe specific for superoxide that selectively accumulates in the mitochondrial compartment. As shown in Fig. 5C, NAC clearly prevented the phosphorylation of JNK and concomitantly recovered the suppression of FoxO1 phosphorylation in HCV-infected cells. These results suggest that HCV-induced ROS production is involved in JNK activation, which results in the inhibition of FoxO1 phosphorylation.

We next investigated the effects of JNK activation and ROS production on the subcellular localization of FoxO1 in HCV-infected cells by indirect immunofluorescence staining. As shown in Fig. 6A and B, FoxO1 was localized predominantly in the cytoplasm of mock-infected control cells. On the other

for 24 h. The catalytic JNK activity was assayed by monitoring the phosphorylation of c-Jun. As shown in Fig. 4B, SP600125 clearly prevented the phosphorylation of c-Jun and concomitantly recovered the suppression of FoxO1 phosphorylation in

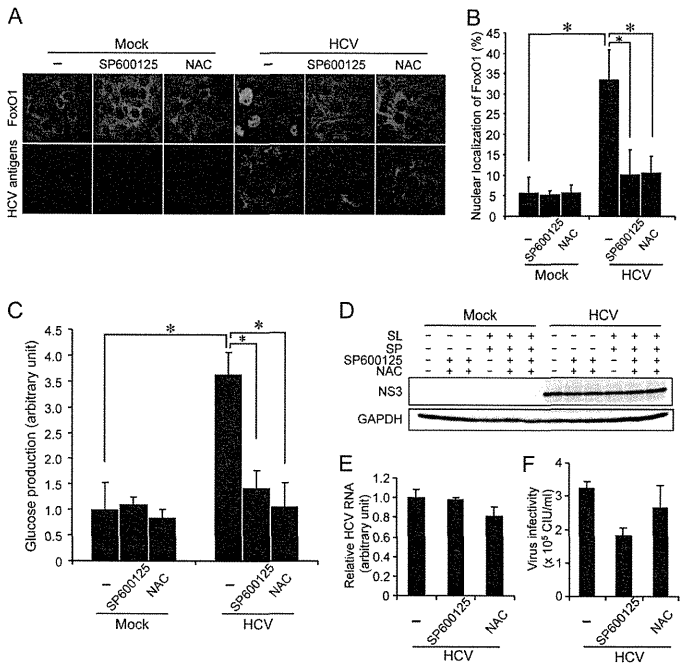

FIG. 6. HCV-induced JNK activation and ROS production are involved in FoxO1 nuclear accumulation and increased glucose production. (A) Subcellular localization of FoxO1 in HCV-infected cells and mock-infected controls with or without JNK inhibitor (SP600125 at 20 μM for 24 h) or antioxidant (NAC at 5 mM for 2 h) pretreatment at 5 dpi was examined by confocal microscopy. After fixation and permeabilization, the cells were incubated with an anti-FoxO1 rabbit monoclonal antibody followed by Alexa Fluor 488-conjugated goat anti-rabbit IgG (top) and with serum from an HCV-infected patient followed by Alexa Fluor 594-conjugated goat anti-human IgG (bottom). (B) The percentages of cells with FoxO1 nuclear localization were determined for HCV-infected cells and mock-infected controls with or without SP600125 or NAC pretreatment. Data represent means ± SEM of data from two independent experiments. *, $P < 0.01$. (C) Extracellular glucose production was measured in HCV-infected cells and mock-infected controls with or without SP600125 or NAC pretreatment at 7 dpi and normalized to total cellular protein expression levels. Data represent means ± SEM of data from two independent experiments, and the value for the control cells was arbitrarily expressed as 1.0. *, $P < 0.01$. (D) Cellular expression levels of NS3 in HCV-infected cells and mock-infected control cells with or without sodium lactate (SL), sodium pyruvate (SP), SP600125, or NAC are shown. The amounts of GAPDH were measured as an internal control to verify equal amounts of sample loading. (E) Amounts of HCV RNA were measured by quantitative RT-PCR analysis of HCV-infected cells treated with SP600125 or NAC or left untreated at 6 dpi. The amounts were normalized to GAPDH mRNA expression levels. Data represent means ± SEM of data from two independent experiments, and the value for the nontreated HCV-infected cells was arbitrarily expressed as 1.0. (F) Virus infectivity in the culture supernatants of HCV-infected cells treated with SP600125 or NAC or left untreated at 6 dpi was measured. Data represent means ± SEM of data from two independent experiments. CIU, cell-infecting units.

hand, the nuclear accumulation of FoxO1 was clearly observed in approximately 35% of HCV-infected cells at 5 dpi. The treatment of HCV-infected cells with a JNK inhibitor (SP600125 at 20 μM for 24 h) or an antioxidant (NAC at 5 mM for 2 h) significantly inhibited HCV-induced FoxO1 nuclear accumulation.

To further verify the role played by JNK activation and ROS production in HCV-induced hepatic gluconeogenesis, the glucose production in SP600125- or NAC-treated HCV-infected cells was assessed. Treatment with SP600125 or NAC significantly impaired the HCV-induced increased glucose production at 7 dpi (Fig. 6C) but did not affect the overall abundance of the HCV NS3 protein (Fig. 6D). We also examined the possible effects of SP600125 or NAC on HCV RNA replication and infectious-virus production. The results obtained revealed that treatment with SP600125 (20 μM for 24 h) or NAC (5 mM for 2 h) barely affected HCV RNA replication (Fig. 6E). On the other hand, we noted a tendency for infectious-virus production to be only slightly suppressed by SP600125 but not by NAC (Fig. 6F). A short-term inhibition of glucose production might not sufficiently affect HCV RNA replication or virus production.

Taken together, these results indicate that ROS-mediated JNK activation plays a key role in the suppression of FoxO1

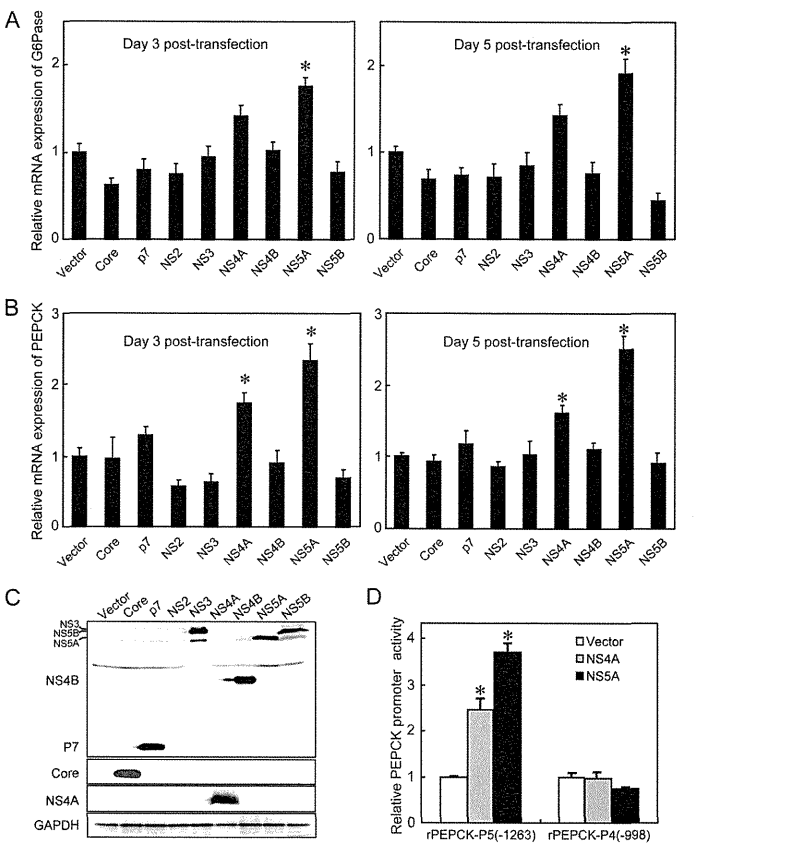

FIG. 7. HCV NS5A is involved in increased mRNA expression levels for G6Pase and PEPCK. Huh-7.5 cells were transfected with the indicated HCV viral protein expression plasmids. (A and B) At 3 and 5 days posttransfection, quantitative RT-PCR analyses of mRNA for G6Pase (A) and PEPCK (B) were conducted, and the results were normalized to β-glucuronidase mRNA expression levels. Data represent means ± SEM of data from three independent experiments, and the values for the control cells were arbitrarily expressed as 1.0. *, $P < 0.01$ compared with the control. (C) At 3 days posttransfection, the expression levels of each of the HCV proteins were examined by immunoblot analysis using antibodies against c-Myc, core, NS4A, and GAPDH. The amounts of GAPDH served as an internal control to verify equal amounts of sample loading. (D) NS5A and NS4A enhance PEPCK promoter activity. NS5A and NS4A expression plasmids were each cotransfected with rPEPCK-P5(−1263)-pGL3basic or rPEPCK-P4(−998)-pGL3basic in Huh-7.5 cells. At 48 h after transfection, the PEPCK promoter activities were measured by using a luciferase reporter assay. Data represent means ± SEM of data from three independent experiments, and the values for the control cells were arbitrarily expressed as 1.0. *, $P < 0.05$ compared with the control.

phosphorylation, the nuclear accumulation of FoxO1, and the enhancement of glucose production in HCV-infected cells.

HCV NS5A is involved in the enhancement of glucose production. To examine which HCV protein(s) is involved in the enhancement of gluconeogenesis, expression constructs of each of the HCV viral proteins were transfected into Huh-7.5 cells, and the gene expression levels of PEPCK and G6Pase were examined by real-time quantitative RT-PCR analysis. We observed that NS5A significantly promoted G6Pase gene expression (Fig. 7A). Moreover, both the NS5A and NS4A proteins significantly enhanced PEPCK gene expression at 3 and 5 days posttransfection, respectively (Fig. 7B). The expression of each of the HCV proteins except NS2 was verified by immunoblot analysis (Fig. 7C). NS2 was reported previously to be unstable and rapidly degraded by the proteasome (22).

Next, we performed a luciferase reporter assay to examine

the possible effects of NS5A and NS4A on PEPCK promoter activities. The construct rPEPCK-P5(−1263)-pGL3basic carries 1,263 bp of the PEPCK 5′-flanking region (−1263 PEPCK) and is used to monitor PEPCK promoter activity. The results demonstrated that the levels of PEPCK promoter activities were significantly higher in both NS5A- and NS4A-expressing cells than in the control cells (Fig. 7D). Interestingly, when the region of the PEPCK promoter from positions −1263 to −998 was deleted, the activation of PEPCK promoter activity in cells expressing NS5A and NS4A was abolished. These results confirmed that NS5A and NS4A activate the PEPCK promoter, leading to an increase in PEPCK mRNA expression levels. Database searches of the deleted sequence did not reveal any potential binding sequences for transcription factors (data not shown).

Recently reported data suggest that ROS production is induced in NS5A-expressing cells (17) or in hepatocytes of NS5A transgenic mice (68). We therefore sough to determine whether NS5A contributes to increased hepatic gluconeogenesis through the induction of ROS production. The NS5A expression plasmid was transfected into Huh-7.5 cells, and ROS production was assessed by MitoSOX at 3 days posttransfection. As shown in Fig. 8A and B, approximately 30% of NS5A-expressing cells displayed a much stronger signal than that observed for vector-transfected control cells.

We then examined whether NS5A mediated JNK/c-Jun activation and FoxO1 phosphorylation inhibition. The results obtained revealed that both the phosphorylation level at Ser63 and the total expression level of c-Jun were upregulated in NS5A-expressing cells compared to the control cells transfected with the vector plasmid or cells expressing the other HCV proteins (Fig. 8C and D, top two panels). Concomitantly, FoxO1 phosphorylation at Ser319 was clearly suppressed in NS5A- and NS4A-expressing cells compared to the control cells (Fig. 8C, compare lanes 6, 5, and 1, respectively, in the third panel). NS4A, a small protein of ca. 7 kDa, forms a stable complex with NS3 to function as a cofactor for NS3 serine protease and RNA helicase activities (51). We previously reported that NS4A caused mitochondrial damage when expressed alone but not when coexpressed with NS3 (47). We therefore speculated that the otherwise observed decrease in FoxO1 phosphorylation levels in NS4A-expressing cells might be canceled when NS4A is coexpressed with NS3. To verify this notion, we tested FoxO1 phosphorylation in cells coexpressing NS3 and NS4A. As had been expected, FoxO1 phosphorylation levels did not differ between NS3/4A-coexpressing cells and vector-transfected control cells (Fig. 8C, compare lanes 4 and 1, respectively).

Notably, we observed that the HCV core protein did not alter the phosphorylation status of c-Jun and FoxO1 (Fig. 8C, compare lanes 1 and 2), with the result being consistent with what was observed for gene expression levels of PEPCK and G6Pase in HCV core-expressing cells (Fig. 7A and B). These results imply that core is not primarily involved in HCV-induced increased gluconeogenesis under our experimental conditions. Similarly, other HCV nonstructural proteins, such as NS4B and NS5B, did not significantly influence the phosphorylation status of c-Jun and FoxO1 (Fig. 8D).

In order to further verify the effect of NS5A on the nuclear accumulation of FoxO1, we examined the subcellular localization of FoxO1 in NS5A-expressing cells by indirect immunofluorescence staining. As shown in Fig. 8E and F, the nuclear accumulation of FoxO1 was clearly observed for approximately 25% of NS5A-expressing cells but not the vector-transfected control. These results suggest that NS5A activates the JNK/c-Jun signaling pathway via increased ROS production, which results in the decreased phosphorylation and nuclear accumulation of FoxO1.

Finally, we examined the effects of NS5A and NS4A on glucose production. As shown in Fig. 9, the amounts of glucose were significantly increased in culture supernatants of NS5A- and NS4A-expressing cells, compared with the amounts of glucose in control cells, at 5 days posttransfection. Again, it is reasonable to assume that the observed increase in glucose production in NS4A-expressing cells might be canceled when NS4A is coexpressed with NS3.

These results collectively suggest that NS5A plays a role, at least to some extent, in the HCV-induced enhancement of hepatic gluconeogenesis.

DISCUSSION

Hepatocytes play an important role in maintaining plasma glucose homeostasis by adjusting the balance between hepatic glucose production and utilization via the gluconeogenic and glycolytic pathways, respectively. We previously reported that HCV suppresses cellular glucose uptake by downregulating the surface expression of the glucose transporters GLUT1 and GLUT2 (37). In this study, we have demonstrated that HCV promotes FoxO1-mediated hepatic gluconeogenesis, as evidenced by the increased accumulation of FoxO1 in the nucleus via the reduction of its phosphorylation status (Fig. 3 and 6A and B), which leads to increased PEPCK and G6Pase gene expression levels (Fig. 1A and B) and the subsequent upregulation of G6P and glucose production (Fig. 2). Moreover, our results indicate that HCV-induced ROS production causes JNK activation, which results in the decreased phosphorylation and nuclear accumulation of FoxO1, leading eventually to increased glucose production (Fig. 4 to 6). Our results thus suggest that FoxO1 is a prime transcription factor in the HCV-mediated progression of hepatic gluconeogenesis through an ROS/JNK-dependent mechanism, as summarized in the schema in Fig. 10. Our results also suggest that HCV NS5A plays a role in enhanced hepatic gluconeogenesis by promoting ROS production and JNK activation (Fig. 7 to 9). In line with our observations, the NS5A-mediated induction of ROS production (68) and JNK activation (49) was reported previously by other investigators.

Increasing evidence suggests that mitochondrial dysfunction is causative of insulin resistance and type 2 diabetes. Mitochondrial dysfunction causes the upregulation of PEPCK and G6Pase, leading to increased gluconeogenesis and insulin resistance (42, 46). We previously reported that HCV causes mitochondrial damage and mitochondrion-mediated apoptosis (14, 47). Our current data further support the concept that altered mitochondrial function plays a role in the development of increased glucose production in hepatocytes.

We and other groups have reported that HCV infection increases the production of mitochondrial ROS, which plays an important role in the development and progression of inflam-

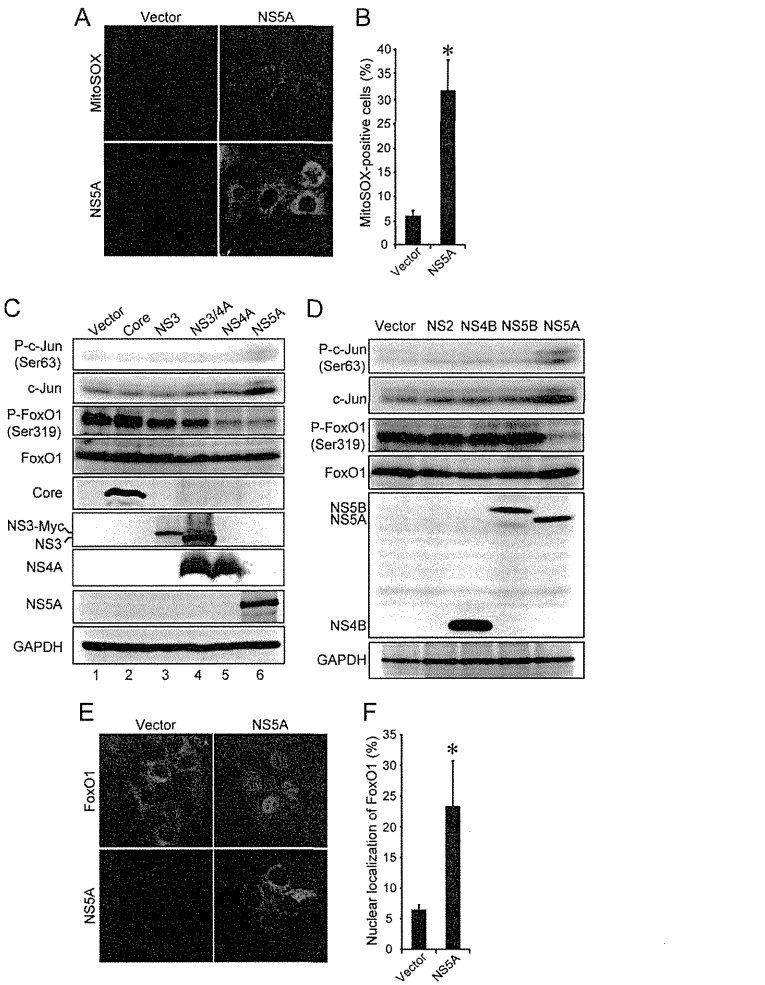

FIG. 8. HCV NS5A is involved in increased ROS production, JNK activation, FoxO1 phosphorylation suppression, and FoxO1 nuclear accumulation. (A) NS5A promotes ROS production. Huh-7.5 cells transfected with an NS5A expression plasmid or the empty control (vector) were incubated with MitoSOX (top) at 3 days posttransfection and then stained for NS5A by using anti-NS5A mouse monoclonal antibody, followed by FITC-conjugated goat anti-mouse IgG (bottom). (B) Quantification of MitoSOX-stained cells. The percentages of cells stained with MitoSOX were determined for NS5A-expressing cells and control cells. Data represent means ± SEM of data from two independent experiments. *, $P < 0.01$. (C and D) HCV NS5A activates c-Jun phosphorylation and suppresses FoxO1 phosphorylation. Huh-7.5 cells transfected with the indicated HCV viral protein expression plasmids were harvested at 3 days posttransfection, and the whole-cell lysates were subjected to immunoblot analysis using antibodies against phospho-c-Jun (Ser63), c-Jun, phospho-FoxO1 (Ser319), FoxO1, GAPDH, core, NS3, NS4A, and NS5A (C) or c-Myc (D). The amounts of GAPDH were measured as an internal control to verify equal amounts of sample loading. (E) NS5A facilitates FoxO1 nuclear accumulation. Huh-7.5 cells transfected with an NS5A expression plasmid or the empty control (vector) were fixed and permeabilized at 3 days posttransfection. The cells were incubated with an anti-FoxO1 rabbit monoclonal antibody followed by Alexa Fluor 488-conjugated goat anti-rabbit IgG (top) or with anti-NS5A mouse monoclonal antibody followed by Alexa Fluor 594-conjugated goat anti-mouse IgG (bottom). (F) The percentages of cells with a nuclear localization of FoxO1 were determined for NS5A-expressing cells and control cells. Data represent means ± SEM of data from two independent experiments. *, $P < 0.01$.

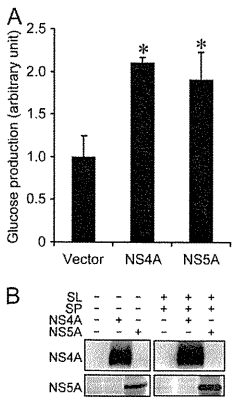

FIG. 9. HCV NS5A and NS4A enhance glucose production. (A) Huh-7.5 cells were transfected with either an NS5A or NS4A expression plasmid. At 5 days posttransfection, extracellular glucose production was measured and normalized to the total cellular protein expression level. Data represent means ± SEM of data from two independent experiments, and the values for the control cells were arbitrarily expressed as 1.0. *, $P < 0.05$ compared with the control. (B) Cellular expression levels of NS4A and NS5A in the absence and presence of sodium lactate (SL) and sodium pyruvate (SP) are shown.

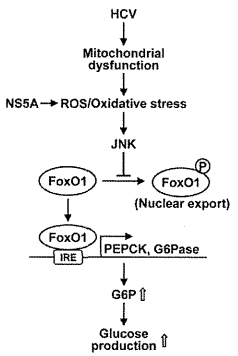

FIG. 10. Schematic representation of the HCV-dysregulated hepatic gluconeogenesis signaling pathway. HCV induces mitochondrial dysfunction (14). This results in increased ROS production and JNK activation, which induces the nuclear accumulation of FoxO1 by reducing its phosphorylation status. Consequently, PEPCK and G6Pase gene expressions are upregulated, leading to an upregulation of G6P and glucose production. NS5A plays a role in HCV-induced gluconeogenesis via the induction of ROS production. IRE, insulin response element.

matory liver disease mediated by HCV (12, 14). Increased mitochondrial ROS generation was also shown previously to be an underlying mediator of multiple forms of insulin resistance, including inflammation- or glucocorticoid-induced insulin resistance (27, 29). Moreover, a significant correlation was observed between oxidative stress and insulin resistance in patients infected with HCV genotype 1 or 2 (44). ROS have also been shown to regulate the activity of the FoxO transcription factor by posttranslational modifications, including phosphorylation (21), deacetylation (8), and ubiquitylation (67).

Although this study showed that JNK induces the nuclear accumulation of FoxO1 by reducing its phosphorylation status under oxidative stress conditions in HCV-infected cells, the precise mechanism(s) of the interplay between JNK and FoxO1 still remains to be addressed. It was reported previously that activated JNK phosphorylates IRS-1 at Ser307, which results in attenuated insulin signal transduction through the inhibition of the tyrosine phosphorylation of IRS-1 (1). Akt is a major downstream signaling protein for insulin/IRS-1 signaling and is activated through its phosphorylation on Thr308 and Ser473, the latter of which is believed to be more crucial (53). Therefore, an impairment of the insulin/IRS-1 signaling pathway should involve the downregulation of Akt phosphorylation. However, our present data showed that Akt phosphorylation on Ser473 was upregulated in HCV-infected cells at 4 and 6 dpi (Fig. 3B), suggesting that an Akt-independent pathway is involved in the JNK-mediated suppression of FoxO1 phosphorylation. Regarding this connection, it should be noted that the 14-3-3 protein, a binding partner for phosphorylated FoxO1 that mediates its nuclear export (72), is phosphorylated by JNK and that the phosphorylated 14-3-3 protein releases its binding partners, which would facilitate the nuclear accumulation of FoxO (63, 65, 70). Further studies are needed to elucidate this issue.

Another trigger that causes excessive JNK activation and insulin resistance is endoplasmic reticulum (ER) stress (28, 48). Several previous studies reported that HCV infection induces ER stress (34, 55). Under our experimental conditions, however, we did not detect significant ER stress in HCV-infected cells (14). It is thus likely that ER stress was not the primary cause of the increased gluconeogenesis in our experimental system using Huh-7.5 cells and the P-47 strain of HCV J6/JFH-1 (9, 14).

Notably, our present data showed that cells harboring the SGR or FGR and HCV-infected cells produced greater amounts of glucose than did the control cells (Fig. 2A); however, the changes in the phosphorylation status of FoxO1 and JNK in SGR- and FGR-harboring cells were not so significant compared to those in virus-infected cells (data not shown). One of the reasons for this difference is that SGR- and FGR-harboring cells were obtained through a longer cultivation in a selection medium for a month or more and that the balance of host gene induction may be somewhat different from that in virus-infected cells. Therefore, it is possible that, in addition to the JNK-FoxO1 pathway, another signaling pathway(s) is involved in the increased gluconeogenesis in SGR- and FGR-harboring cells. Studies on this issue are now under way in our laboratory.

We observed that HCV infection modulated, either positively or negatively, the transcription of the PEPCK, G6Pase, and GK genes at 3 to 5 dpi (Fig. 1). Virus infection, in general, causes dynamically changing induction and the suppression of a wide variety of host genes. For example, expression levels of certain genes, such as interferon genes, increase during an early phase of virus infection, e.g., at 1 dpi, but return to normal levels within a few days in a cell culture system. On the other hand, the virus-infection-induced expression of other genes, such as the extracellular signal-regulated kinase (ERK) gene, remains for a prolonged period of time (data not shown). Also, some of the gene products induced in the acute phase may suppress the expression of other genes. Under these balanced conditions, it is quite possible that certain genes are induced only at a later time, e.g., 3 to 5 dpi, but not immediately after virus infection.

It was reported previously that HCV core protein-expressing transgenic mice exhibit marked insulin resistance by inhibiting IRS-1 tyrosine phosphorylation and Akt phosphorylation (45, 58). However, our present results showed that HCV NS5A, but not the core protein, was associated with increased gluconeogenesis. Moreover, it was recently reported that HCV infection significantly inhibited cellular glucose levels at 10 dpi (69), which is quite the opposite of what we observed in the present study. These results collectively suggest the possibility that multiple pathways are involved in glucose metabolism in HCV-infected cells. Also, the possible effect(s) of the dysregulation of hepatic gluconeogenesis on the HCV life cycle needs to be clarified.

In conclusion, our present results collectively suggest that HCV promotes hepatic gluconeogenesis, resulting in increased glucose production in hepatocytes via an NS5A-mediated, FoxO1-dependent pathway.

ACKNOWLEDGMENTS

We are grateful to C. M. Rice (Rockefeller University, New York, NY) for providing Huh-7.5 cells and pFL-J6/JFH1, R. Bartenschlager (University of Heidelberg, Heidelberg, Germany) for providing an HCV subgenomic RNA replicon (pFK5B/2884Gly), and N. Kato (Okayama University, Okayama, Japan) for providing an HCV full-length RNA replicon (pON/C-5B). We also thank T. Adachi (Kyoto Prefectural University of Medicine, Kyoto, Japan), K. Igarashi, K. Kashikura, and A. Suzuki (Keio University, Yamagata, Japan) for their technical assistance.

This work was supported in part by grants-in-aid for research on hepatitis from the Ministry of Health, Labor, and Welfare, Japan, and the Japan Initiative for Global Research Network on Infectious Diseases (J-GRID) program of the Ministry of Education, Culture, Sports, Science, and Technology, Japan. This study was also carried out as part of the Global Center of Excellence program of the Kobe University Graduate School of Medicine and the Science and Technology Research Partnership for Sustainable Development (SATREPS) program of the Japan Science and Technology Agency (JST) and the Japan International Cooperation Agency (JICA).

REFERENCES

1. **Aguirre, V., T. Uchida, L. Yenush, R. Davis, and M. F. White.** 2000. The c-Jun NH(2)-terminal kinase promotes insulin resistance during association with insulin receptor substrate-1 and phosphorylation of Ser(307). J. Biol. Chem. **275:**9047–9054.
2. **Alaei, M., and F. Negro.** 2008. Hepatitis C virus and glucose and lipid metabolism. Diabetes Metab. **34:**692–700.
3. **Aytug, S., D. Reich, L. E. Sapiro, D. Bernstein, and N. Begum.** 2003. Impaired IRS-1/PI3-kinase signaling in patients with HCV: a mechanism for increased prevalence of type 2 diabetes. Hepatology **38:**1384–1392.
4. **Banerjee, A., K. Meyer, B. Mazumdar, R. B. Ray, and R. Ray.** 2010. Hepatitis C virus differentially modulates activation of forkhead transcription factors and insulin-induced metabolic gene expression. J. Virol. **84:**5936–5946.
5. **Baron, A. D., L. Schaeffer, P. Shragg, and O. G. Kolterman.** 1987. Role of hyperglucagonemia in maintenance of increased rates of hepatic glucose output in type II diabetics. Diabetes **36:**274–283.
6. **Bennett, B. L., et al.** 2001. SP600125, an anthrapyrazolone inhibitor of Jun N-terminal kinase. Proc. Natl. Acad. Sci. U. S. A. **98:**13681–13686.
7. **Blight, K. J., J. A. McKeating, and C. M. Rice.** 2002. Highly permissive cell lines for subgenomic and genomic hepatitis C virus RNA replication. J. Virol. **76:**13001–13014.
8. **Brunet, A., et al.** 2004. Stress-dependent regulation of FOXO transcription factors by the SIRT1 deacetylase. Science **303:**2011–2015.
9. **Bungyoku, Y., et al.** 2009. Efficient production of infectious hepatitis C virus with adaptive mutations in cultured hepatoma cells. J. Gen. Virol. **90:**1681–1691.
10. **Burdette, D., M. Olivarez, and G. Waris.** 2010. Activation of transcription factor Nrf2 by hepatitis C virus induces the cell-survival pathway. J. Gen. Virol. **91:**681–690.
11. **Caronia, S., et al.** 1999. Further evidence for an association between non-insulin-dependent diabetes mellitus and chronic hepatitis C virus infection. Hepatology **30:**1059–1063.
12. **Choi, J., and J. H. Ou.** 2006. Mechanisms of liver injury. III. Oxidative stress in the pathogenesis of hepatitis C virus. Am. J. Physiol. Gastrointest. Liver Physiol. **290:**G847–G851.
13. **Clore, J. N., J. Stillman, and H. Sugerman.** 2000. Glucose-6-phosphatase flux in vitro is increased in type 2 diabetes. Diabetes **49:**969–974.
14. **Deng, L., et al.** 2008. Hepatitis C virus infection induces apoptosis through a Bax-triggered, mitochondrion-mediated, caspase 3-dependent pathway. J. Virol. **82:**10375–10385.
15. **Deng, L., et al.** 2006. NS3 protein of hepatitis C virus associates with the tumour suppressor p53 and inhibits its function in an NS3 sequence-dependent manner. J. Gen. Virol. **87:**1703–1713.
16. **Diamond, D. L., et al.** 2010. Temporal proteome and lipidome profiles reveal hepatitis C virus-associated reprogramming of hepatocellular metabolism and bioenergetics. PLoS Pathog. **6:**e1000719.
17. **Dionisio, N., et al.** 2009. Hepatitis C virus NS5A and core proteins induce oxidative stress-mediated calcium signalling alterations in hepatocytes. J. Hepatol. **50:**872–882.
18. **Doi, H., C. Apichartpiyakul, K. I. Ohba, M. Mizokami, and H. Hotta.** 1996. Hepatitis C virus (HCV) subtype prevalence in Chiang Mai, Thailand, and identification of novel subtypes of HCV major type 6. J. Clin. Microbiol. **34:**569–574.
19. **Dunning, B. E., and J. E. Gerich.** 2007. The role of alpha-cell dysregulation in fasting and postprandial hyperglycemia in type 2 diabetes and therapeutic implications. Endocr. Rev. **28:**253–283.
20. **Eslam, M., M. A. Khattab, and S. A. Harrison.** 2011. Insulin resistance and hepatitis C: an evolving story. Gut **60:**1139–1151.
21. **Essers, M. A., et al.** 2004. FOXO transcription factor activation by oxidative stress mediated by the small GTPase Ral and JNK. EMBO J. **23:**4802–4812.
22. **Franck, N., J. Le Seyec, C. Guguen-Guillouzo, and L. Erdtmann.** 2005. Hepatitis C virus NS2 protein is phosphorylated by the protein kinase CK2 and targeted for degradation to the proteasome. J. Virol. **79:**2700–2708.
23. **Galossi, A., R. Guarisco, L. Bellis, and C. Puoti.** 2007. Extrahepatic manifestations of chronic HCV infection. J. Gastrointestin. Liver Dis. **16:**65–73.
24. **Gottwein, J. M., et al.** 2009. Development and characterization of hepatitis C virus genotype 1-7 cell culture systems: role of CD81 and scavenger receptor class B type I and effect of antiviral drugs. Hepatology **49:**364–377.
25. **Gross, D. N., A. P. van den Heuvel, and M. J. Birnbaum.** 2008. The role of FoxO in the regulation of metabolism. Oncogene **27:**2320–2336.
26. **Hirota, K., et al.** 2008. A combination of HNF-4 and Foxo1 is required for reciprocal transcriptional regulation of glucokinase and glucose-6-phosphatase genes in response to fasting and feeding. J. Biol. Chem. **283:**32432–32441.
27. **Hoehn, K. L., et al.** 2009. Insulin resistance is a cellular antioxidant defense mechanism. Proc. Natl. Acad. Sci. U. S. A. **106:**17787–17792.
28. **Hotamisligil, G. S.** 2005. Role of endoplasmic reticulum stress and c-Jun NH2-terminal kinase pathways in inflammation and origin of obesity and diabetes. Diabetes **54**(Suppl. 2)**:**S73–S78.
29. **Houstis, N., E. D. Rosen, and E. S. Lander.** 2006. Reactive oxygen species have a causal role in multiple forms of insulin resistance. Nature **440:**944–948.
30. **Huang, H., and D. J. Tindall.** 2007. Dynamic FoxO transcription factors. J. Cell Sci. **120:**2479–2487.
31. **Ikeda, M., et al.** 2005. Efficient replication of a full-length hepatitis C virus genome, strain O, in cell culture, and development of a luciferase reporter system. Biochem. Biophys. Res. Commun. **329:**1350–1359.
32. **Inubushi, S., et al.** 2008. Hepatitis C virus NS5A protein interacts with and negatively regulates the non-receptor protein tyrosine kinase Syk. J. Gen. Virol. **89:**1231–1242.
33. **Iynedjian, P. B., et al.** 1989. Differential expression and regulation of the glucokinase gene in liver and islets of Langerhans. Proc. Natl. Acad. Sci. U. S. A. **86:**7838–7842.
34. **Joyce, M. A., et al.** 2009. HCV induces oxidative and ER stress, and sensitizes infected cells to apoptosis in SCID/Alb-uPA mice. PLoS Pathog. **5:**e1000291.
35. **Kamata, H., et al.** 2005. Reactive oxygen species promote TNFalpha-induced death and sustained JNK activation by inhibiting MAP kinase phosphatases. Cell **120:**649–661.
36. **Karpac, J., and H. Jasper.** 2009. Insulin and JNK: optimizing metabolic homeostasis and lifespan. Trends Endocrinol. Metab. **20:**100–106.
37. **Kasai, D., et al.** 2009. HCV replication suppresses cellular glucose uptake

through down-regulation of cell surface expression of glucose transporters. J. Hepatol. **50:**883–894.
38. **Kops, G. J., and B. M. Burgering.** 1999. Forkhead transcription factors: new insights into protein kinase B (c-akt) signaling. J. Mol. Med. **77:**656–665.
39. **Lindenbach, B. D., et al.** 2005. Complete replication of hepatitis C virus in cell culture. Science **309:**623–626.
40. **Lindenbach, B. D., and C. M. Rice.** 2005. Unravelling hepatitis C virus replication from genome to function. Nature **436:**933–938.
41. **Lohmann, V., F. Korner, A. Dobierzewska, and R. Bartenschlager.** 2001. Mutations in hepatitis C virus RNAs conferring cell culture adaptation. J. Virol. **75:**1437–1449.
42. **Lowell, B. B., and G. I. Shulman.** 2005. Mitochondrial dysfunction and type 2 diabetes. Science **307:**384–387.
43. **Mehta, S. H., et al.** 2000. Prevalence of type 2 diabetes mellitus among persons with hepatitis C virus infection in the United States. Ann. Intern. Med. **133:**592–599.
44. **Mitsuyoshi, H., et al.** 2008. Evidence of oxidative stress as a cofactor in the development of insulin resistance in patients with chronic hepatitis C. Hepatol. Res. **38:**348–353.
45. **Miyamoto, H., et al.** 2007. Involvement of the PA28gamma-dependent pathway in insulin resistance induced by hepatitis C virus core protein. J. Virol. **81:**1727–1735.
46. **Morino, K., K. F. Petersen, and G. I. Shulman.** 2006. Molecular mechanisms of insulin resistance in humans and their potential links with mitochondrial dysfunction. Diabetes **55**(Suppl. 2):S9–S15.
47. **Nomura-Takigawa, Y., et al.** 2006. Non-structural protein 4A of hepatitis C virus accumulates on mitochondria and renders the cells prone to undergoing mitochondria-mediated apoptosis. J. Gen. Virol. **87:**1935–1945.
48. **Ozcan, U., et al.** 2004. Endoplasmic reticulum stress links obesity, insulin action, and type 2 diabetes. Science **306:**457–461.
49. **Park, K. J., et al.** 2003. Hepatitis C virus NS5A protein modulates c-Jun N-terminal kinase through interaction with tumor necrosis factor receptor-associated factor 2. J. Biol. Chem. **278:**30711–30718.
50. **Puigserver, P., et al.** 2003. Insulin-regulated hepatic gluconeogenesis through FOXO1-PGC-1alpha interaction. Nature **423:**550–555.
51. **Reed, K. E., and C. M. Rice.** 2000. Overview of hepatitis C virus genome structure, polyprotein processing, and protein properties. Curr. Top. Microbiol. Immunol. **242:**55–84.
52. **Rozance, P. J., et al.** 2008. Chronic late-gestation hypoglycemia upregulates hepatic PEPCK associated with increased PGC1alpha mRNA and phosphorylated CREB in fetal sheep. Am. J. Physiol. Endocrinol. Metab. **294:** E365–E370.
53. **Sale, E. M., and G. J. Sale.** 2008. Protein kinase B: signalling roles and therapeutic targeting. Cell. Mol. Life Sci. **65:**113–127.
54. **Schmoll, D., et al.** 2000. Regulation of glucose-6-phosphatase gene expression by protein kinase Balpha and the forkhead transcription factor FKHR. Evidence for insulin response unit-dependent and -independent effects of insulin on promoter activity. J. Biol. Chem. **275:**36324–36333.
55. **Sekine-Osajima, Y., et al.** 2008. Development of plaque assays for hepatitis C virus-JFH1 strain and isolation of mutants with enhanced cytopathogenicity and replication capacity. Virology **371:**71–85.
56. **Seo, H. Y., et al.** 2010. Endoplasmic reticulum stress-induced activation of activating transcription factor 6 decreases cAMP-stimulated hepatic gluconeogenesis via inhibition of CREB. Endocrinology **151:**561–568.
57. **Shepard, C. W., L. Finelli, and M. J. Alter.** 2005. Global epidemiology of hepatitis C virus infection. Lancet Infect. Dis. **5:**558–567.
58. **Shintani, Y., et al.** 2004. Hepatitis C virus infection and diabetes: direct involvement of the virus in the development of insulin resistance. Gastroenterology **126:**840–848.
59. **Simmonds, P., et al.** 2005. Consensus proposals for a unified system of nomenclature of hepatitis C virus genotypes. Hepatology **42:**962–973.
60. **Soga, T., et al.** 2006. Differential metabolomics reveals ophthalmic acid as an oxidative stress biomarker indicating hepatic glutathione consumption. J. Biol. Chem. **281:**16768–16776.
61. **Soga, T., et al.** 2009. Metabolomic profiling of anionic metabolites by capillary electrophoresis mass spectrometry. Anal. Chem. **81:**6165–6174.
62. **Streeper, R. S., et al.** 1997. A multicomponent insulin response sequence mediates a strong repression of mouse glucose-6-phosphatase gene transcription by insulin. J. Biol. Chem. **272:**11698–11701.
63. **Sunayama, J., F. Tsuruta, N. Masuyama, and Y. Gotoh.** 2005. JNK antagonizes Akt-mediated survival signals by phosphorylating 14-3-3. J. Cell Biol. **170:**295–304.
64. **Takashima, M., et al.** 2010. Role of KLF15 in regulation of hepatic gluconeogenesis and metformin action. Diabetes **59:**1608–1615.
65. **Tsuruta, F., et al.** 2004. JNK promotes Bax translocation to mitochondria through phosphorylation of 14-3-3 proteins. EMBO J. **23:**1889–1899.
66. **van der Horst, A., and B. M. Burgering.** 2007. Stressing the role of FoxO proteins in lifespan and disease. Nat. Rev. Mol. Cell Biol. **8:**440–450.
67. **van der Horst, A., et al.** 2006. FOXO4 transcriptional activity is regulated by monoubiquitination and USP7/HAUSP. Nat. Cell Biol. **8:**1064–1073.
68. **Wang, A. G., et al.** 2009. Non-structural 5A protein of hepatitis C virus induces a range of liver pathology in transgenic mice. J. Pathol. **219:**253–262.
69. **Woodhouse, S. D., et al.** 2010. Transcriptome sequencing, microarray, and proteomic analyses reveal cellular and metabolic impact of hepatitis C virus infection in vitro. Hepatology **52:**443–453.
70. **Yoshida, K., T. Yamaguchi, T. Natsume, D. Kufe, and Y. Miki.** 2005. JNK phosphorylation of 14-3-3 proteins regulates nuclear targeting of c-Abl in the apoptotic response to DNA damage. Nat. Cell Biol. **7:**278–285.
71. **Zhang, S., J. Liu, G. MacGibbon, M. Dragunow, and G. J. Cooper.** 2002. Increased expression and activation of c-Jun contributes to human amylin-induced apoptosis in pancreatic islet beta-cells. J. Mol. Biol. **324:**271–285.
72. **Zhao, X., et al.** 2004. Multiple elements regulate nuclear/cytoplasmic shuttling of FOXO1: characterization of phosphorylation- and 14-3-3-dependent and -independent mechanisms. Biochem. J. **378:**839–849.

Microbiology and Immunology

Microbiol Immunol 2011; **55:** 774–782
doi:10.1111/j.1348-0421.2011.00382.x

ORIGINAL ARTICLE

Inhibition of hepatitis C virus replication through adenosine monophosphate-activated protein kinase-dependent and -independent pathways

Kenji Nakashima[1], Kenji Takeuchi[1,2], Kazuyasu Chihara[1,2], Hak Hotta[3] and Kiyonao Sada[1,2]

[1]Division of Microbiology, Department of Pathological Sciences, Faculty of Medical Sciences, [2]Organization for Life Science Advancement Programs, University of Fukui, Fukui and [3]Division of Microbiology, Center for Infectious Diseases, Kobe University Graduate School of Medicine, Kobe, Japan

ABSTRACT

Persistent infection with hepatitis C virus (HCV) is closely correlated with type 2 diabetes. In this study, replication of HCV at different glucose concentrations was investigated by using J6/JFH1-derived cell-adapted HCV in Huh-7.5 cells and the mechanism of regulation of HCV replication by AMP-activated protein kinase (AMPK) as an energy sensor of the cell analyzed. Reducing the glucose concentration in the cell culture medium from 4.5 to 1.0 g/L resulted in suppression of HCV replication, along with activation of AMPK. Whereas treatment of cells with AMPK activator 5-aminoimidazole-4-carboxamide 1-β-D-ribofuranoside (AICAR) suppressed HCV replication, compound C, a specific AMPK inhibitor, prevented AICAR's effect, suggesting that AICAR suppresses the replication of HCV by activating AMPK in Huh-7.5 cells. In contrast, compound C induced further suppression of HCV replication when the cells were cultured in low glucose concentrations or with metformin. These results suggest that low glucose concentrations and metformin have anti-HCV effects independently of AMPK activation.

Key words 5-aminoimidazole-4-carboxamide 1-β-D-ribofuranoside (AICAR), adenosine monophosphate-activated protein kinase (AMPK), diabetes, metformin.

Hepatitis C virus, which is classified within the family *Flaviviridae*, is a small enveloped virus that possesses a positive-sense single-stranded RNA genome. HCV infection proceeds to a persistent stage at a high rate, leading to cirrhosis and hepatocellular carcinoma. Despite recent advances in the development of antiviral therapies, certain patient populations are difficult to treat (1) due to host factors such as obesity, hyperglycemia and insulin resistance (2–4).

Adenosine monophosphate-activated protein kinase is a major cellular energy sensor that is activated by cellular stresses that increase intracellular AMP (5). ZMP, which mimics AMP, also activates AMPK (6). AMPK is a heterotrimer composed of a catalytic α subunit and regulatory β and γ subunits (7). Phosphorylation of Thr^{172} in its activation loop of α subunit by upstream kinases, namely, LKB1 (8,9) and Ca^{2+}/calmodulin-dependent kinase kinase (10,11) can increase its kinase activity (12). Activated AMPK inhibits the synthesis of fatty acids, cholesterol, proteins and gluconeogenesis in hepatocytes (13–16). Phosphorylation of $Ser^{485/491}$ by protein kinase B is known to inhibit AMPK activity (17).

Hepatitis C virus infection suppresses cellular glucose uptake through down-regulation of cell surface expression

Correspondence
Kiyonao Sada, Division of Microbiology, Department of Pathological Sciences, Faculty of Medical Sciences, University of Fukui, 23-3 Matsuoka-Shimoaizuki, Eiheiji, Fukui, 910-1193, Japan.
Tel: +81 776 61 8323; email: ksada@u-fukui.ac.jp

Received 29 June 2011; revised 4 August 2011; accepted 21 August 2011.

List of Abbreviations: AICAR, 5-aminoimidazole-4-carboxamide 1-β-D-ribofuranoside; AMP, adenosine monophosphate; AMPK, AMP-activated protein kinase; compound C, 6-(4-[2-piperidin-1-yl-ethoxy])-phenyl)-3-pyridin-4-yl-pyrrazolo(1,5-a)-pyrimidine; GAPDH, glyceraldehyde-3-phosphate dehydrogenase; HCV, hepatitis C virus; LKB1, liver kinase B1; MOI, multiplicity of infection; NS3, non-structural protein 3; PRPP, phosphoribosyl pyrophosphate; ZMP, 5-aminoimidazole-4-carboxamide ribonucleotide; ZTP, 5-aminoimidazole 4-carboxamide ribonucleoside 5-triphosphate.

of glucose transporters (18). Our preliminary experiments demonstrated that HCV infection alters the expression of 5-aminoimidazole-4-carboxamide ribonucleotide formyltransferase/inosine monophosphate cyclohydrolase, which catalyzes ZMP in purine nucleotide synthesis. ZMP is known to mimic the activating effects of AMP on AMPK (6). We postulated that glucose usage and/or activation of AMPK might affect the infection and replication of HCV.

In this study, we have investigated HCV replication with different glucose concentrations in the culture medium, with treatment of cells with AMPK activators (AICAR, metformin) or with the AMPK inhibitor compound C in the cell culture medium.

MATERIALS AND METHODS

Cells

The Huh-7.5 cell line used in this study, a highly HCV-susceptible subclone of Huh7 cells, was a kind gift from Dr. C. M. Rice (Center for the Study of Hepatitis C, The Rockefeller University, New York, NY, USA) (19). The cells were propagated in Dulbecco's modified Eagle medium supplemented with 10% heat-inactivated FBS and 0.1 mM nonessential amino acids.

Viruses

The virus stock was prepared as described previously (20,21). The pFL-J6/JFH1 plasmid that encodes the entire viral genome of a chimeric strain of HCV-2a, J6/JFH1, was kindly provided by Dr. C. M. Rice. The HCV RNA genome was transcribed *in vitro* from pFL-J6/JFH1 and transfected to Huh-7.5 cells. The supernatant was harvested as a virus stock. In this study we used an adapted strain of the virus obtained by passaging the HCV genotype 2a, J6/JFH1, infected cells 47 times (20,22). Virus infection was performed at a MOI of three. Culture supernatants of uninfected cells were used as controls (mock preparation). Virus infectivity was measured by indirect immunofluorescence analysis as described previously (20).

Reagents

5-aminoimidazole-4-carboxamide 1-β-D-ribofuranoside and uridine were purchased from Sigma (St. Louis, MO, USA), compound C from Chemdea (Ridgewood, NJ, USA), metformin from Enzo Life Sciences (Plymouth Meeting, PA, USA) and Hoechst 33258 from Wako (Osaka, Japan).

Immunoblotting

Immunoblotting was essentially as described previously (23). Cells were solubilized in a lysis buffer (50 mM Tris-HCl, pH 7.4, 150 mM NaCl, 100 mM NaF, 0.1 mM Na_3VO_4, 10 mM EDTA, 1% Triton-X, and protease inhibitor cocktail [Sigma]). Cell debris was removed by centrifugation and resulted supernatants were diluted 1:2 (v/v) with 3×sampling buffer. Protein quantification was carried out using a bicinchoninic acid protein assay kit (Thermo Fisher Scientific, Rockford, IL, USA). Equal amounts of soluble proteins were subjected to SDS-PAGE and transferred onto a polyvinylidene difluoride transfer membrane (Millipore, Billerica, MA, USA). After blocking in 5% milk in TBST (25 mM Tris, pH 8.0, 150 mM NaCl, and 0.1% Tween 20), the blots were reacted with the respective primary antibodies. The primary antibodies used were anti-phospho-AMPKα (Thr172) monoclonal antibody (clone D79.5E, Cell Signaling Technology, Danvers, MA, USA), anti-AMPKα antibody (Cell Signaling Technology), anti-HCV core monoclonal antibody (clone C7–50, Thermo Fisher Scientific), anti-AMPKα antibody (Phospho-Ser$^{485/491}$) (anti-pAMPK [Ser485/491]) (GenScript, Piscataway, NJ, USA), and anti-HCV NS3 monoclonal antibody (Millipore). Horseradish peroxidase-conjugated goat anti-mouse IgG or goat anti-rabbit IgG (Jackson ImmunoResearch Laboratories, West Grove, PA, USA) were used as secondary antibodies. The respective protein bands were visualized by enhanced chemiluminescence (PerkinElmer, Waltham, MA, USA) (24,25). Protein loading was normalized by probing with anti-GAPDH monoclonal antibody (clone 6C5, Millipore).

Indirect immunofluorescence

Cells seeded in 96-well plates were infected with HCV at a MOI of 3.0 for 4 hr or left uninfected. The cells were incubated for 30 hr and fixed with cold methanol for 10 min at room temperature. After being washed with PBS twice, the cells were stained with anti-HCV core monoclonal antibody and visualized by using horseradish peroxidase-conjugated goat anti-mouse IgG (Bio-Rad Laboratories, Hercules, CA, USA) and the tyramide signal amplification cyanine 3 system (Perkin Elmer). Stained cell samples were examined by fluorescence microscopy (Olympus IX70 microscope system, Tokyo, Japan).

Statistical analysis

The one-tailed Student *t*-test was applied to evaluate the statistical significance of differences found. A P value of <0.05 was considered statistically significant.

RESULTS

Glucose shortage in the culture medium suppresses the replication of hepatitis C virus along with activation of adenosine monophosphate-activated protein kinase

Any virus requires an energy source for replication. We surmised that glucose shortage in the cell culture medium would have a harmful effect on energy metabolism in HCV-infected Huh-7.5 cells. We used Huh-7.5 cells and a J6/JFH1-derived, cell-adapted strain of HCV throughout this study. First, we examined the effect of alterations in glucose concentration in the cell culture medium on the replication of HCV. Reducing the glucose concentration from 4.5 to 1.0 g/L resulted in a significant decrease in HCV replication, as demonstrated by decreased virus infectivity in culture supernatants (Fig. 1a), and decreased production of HCV core protein (Fig. 1b, third panel). In order to estimate the intracellular energy status, we examined the kinase activity of AMPK by the immunoblotting of phosphorylated Thr^{172} in AMPK. Reducing the glucose concentration from 4.5 to 2.0 g/L resulted in a dramatic increase in phosphorylation of Thr^{172} in AMPK, suggesting that Huh-7.5 cells sensed poor nutrition when cultured with 2.0 g/L of glucose in the medium, irrespective of infection with HCV (Fig. 1b). Phosphorylation of Ser$^{485/491}$ of AMPK was not affected by infection with HCV (Fig. 1c). Phosphorylation of AMPK was not affected by infection with HCV, although almost all of the cells were infected in this experiment (Fig. 1d). These results demonstrate that glucose shortage in the cell culture medium suppresses replication of HCV along with activation of AMPK in Huh-7.5 cells. Glucose shortage activates AMPK regardless of HCV infection.

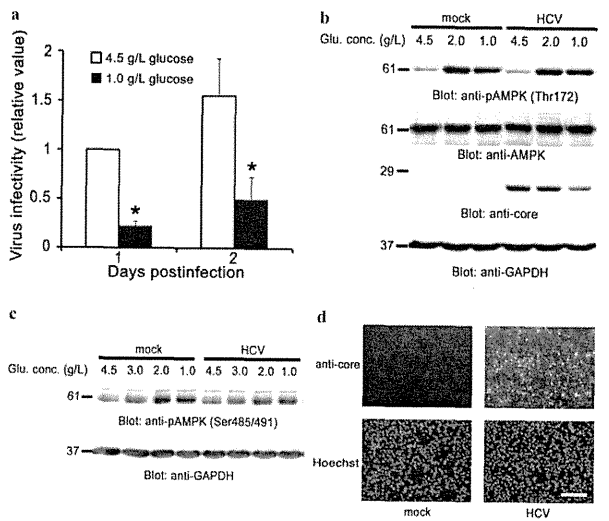

Fig. 1. Glucose shortage suppresses HCV replication and activates AMPK. (a) Huh-7.5 cells were infected with HCV at a MOI of 3.0 for 4 hr and then incubated at the indicated concentration of glucose in serum-free DMEM. Infectivity titer in culture supernatants of HCV-infected cells cultured in medium containing 4.5 g/L glucose at day 1 postinfection was arbitrarily expressed as 1.0. Data are expressed as means ± standard deviations (SD) of three independent experiments. *, $P < 0.05$, compared with the control. (b and c) Huh-7.5 cells were mock infected or infected with HCV at a MOI of 3.0 for 4 hr and then incubated at the indicated concentrations of glucose in serum-free DMEM for 30 hr. (b) Cell lysates were separated by SDS-PAGE and analyzed by immunoblotting with anti-phospho-AMPKα (Thr172) (anti-pAMPK (Thr172)), anti-AMPK, anti-HCV core, anti-GAPDH antibodies as indicated. (c) Cell lysates were analyzed by immunoblotting with anti-AMPKα antibody (anti-pAMPK (Ser485/491)) and anti-GAPDH monoclonal antibody. (d) Huh-7.5 cells mock infected or infected with HCV at a MOI of 3.0 for 4 hr were subjected to indirect immunofluorescence analysis by anti-HCV core antibody. Nuclei were stained with Hoechst 33258. Scale bar, 200 μm. Molecular size markers are indicated at the left in kilodaltons. The results are representative of three independent experiments. Conc., concentration; glu., glucose.

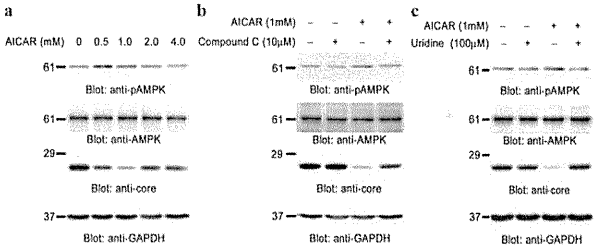

Fig. 2. AICAR suppresses HCV replication by activating AMPK. Huh-7.5 cells were infected with HCV at a MOI of 3.0 for 4 hr. (a) The cells were treated with the indicated concentrations of AICAR for 20 hr. (b) 10 μM compound C was added to the cells 30 min prior to the addition of AICAR and was present in the medium during the entire 20 hr of incubation with AICAR. (c) The cells were treated with 1 mM AICAR for 20 hr with or without supplementation with 100 μM uridine. Cell lysates were separated by SDS-PAGE and analyzed by immunoblotting as Figure 1. The results are representative of three independent experiments.

5-aminoimidazole-4-carboxamide 1-β-D-ribofuranoside suppresses the replication of hepatitis C virus by activating adenosine monophosphate-activated protein kinase in Huh-7.5 cells

Activated AMPK inhibits the synthesis of fatty acids, cholesterol, proteins and gluconeogenesis (13–16). Imbalance of these metabolic pathways in liver cells might affect the replication of HCV. Therefore we next examined whether activated AMPK suppresses the replication of HCV by using an activator (AICAR) and an inhibitor (compound C) of AMPK. Mankauri J. *et al.* have previously reported that treatment of Huh-7 parental cells with AICAR suppresses the replication of JFH-1 (26). In this study, we adopted a more efficient HCV replication system, Huh-7.5 cells and a J6/JFH1-derived, cell-adapted strain of HCV. Similar to the previous finding, activation of AMPK by AICAR suppressed the expression of HCV core protein in Huh-7.5 cells (Fig. 2a, lanes 1–3). Activation of AMPK by AICAR was observed when the cells were treated with relatively low concentrations (0.5 or 1.0 mM), but not with higher concentrations (2.0 or 4.0 mM). Possible reasons for the latter effect are that higher concentrations of AICAR could suppress the synthesis of purine nucleotides and/or increase the concentration of ZTP, thus inhibiting AMPK (6,27).

To examine whether the inhibitory effect of AICAR on HCV replication is mediated by activation of AMPK, we tested an AMPK inhibitor (compound C) in this experiment. We found that pretreatment of cells with 10 μM compound C attenuates AICAR-mediated suppression of HCV core protein expression (Fig. 2b, lane 4). This suggests that AICAR-mediated suppression of HCV replication is mediated by activation of AMPK. Addition of compound C to the cell culture medium without AICAR did not affect the expression of HCV core protein, suggesting that this inhibitor does not affect the replication of HCV under nutritious condition in which AMPK is inactive (Fig. 2b, lane 2).

In the presence of AICAR, the amounts of uridine triphosphate and cytidine triphosphate are decreased in the cultured cells as a result of PRPP depletion (27). PRPP is an important precursor for pyrimidine nucleotide synthesis. PRPP-derived pyrophosphate can increase ZTP/ZMP which are then no longer able to activate AMPK (6,28). To complement the pyrimidine shortage in Huh-7.5 cells treated with AICAR, the cells were co-incubated with 100 μM uridine in the presence of 1 mM AICAR. This resulted in the complete prevention of AICAR-mediated activation of AMPK and the resulting suppression of HCV (Fig. 2c, lane 4). Taken together, these data demonstrate that AICAR suppresses the replication of HCV by activating AMPK in Huh-7.5 cells.

Glucose shortage and metformin have an anti-hepatitis C virus effect independently of adenosine monophosphate-activated protein kinase activation

It is important to note that glucose shortage activates AMPK because of cellular energy limitations, whereas AICAR can activate AMPK regardless of cellular energy status. Therefore we tried another AMPK activator, metformin, which activates AMPK by impairing complex I of the mitochondrial respiratory chain (29,30). In addition, in mice metformin has a LKB1/AMPK-independent

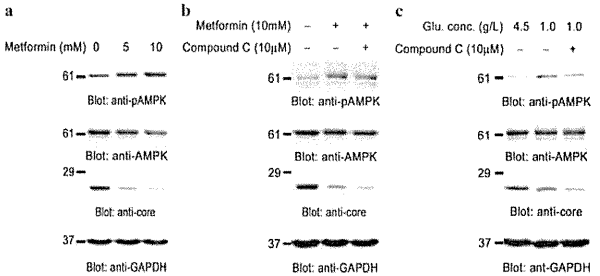

Fig. 3. Compound C, an AMPK inhibitor, stimulates the anti-HCV effects of glucose shortage or metformin. Huh-7.5 cells were infected with HCV at a MOI of 3.0 for 4 hr. (a) The cells were treated with the indicated concentration of metformin for 20 hr. (b) 10 μM compound C was added to the cells 30 min prior to the addition of metformin and present in the medium during the entire 20 hr of incubation with metformin. (c) The cells were incubated with or without 10 μM compound C at the indicated glucose concentrations in serum-free DMEM for 15 hr. Cell lysates were separated by SDS-PAGE and analyzed by immunoblotting as Figure 1. The results are representative of three independent experiments. Conc., concentration; glu., glucose.

inhibitory role on gluconeogenesis by decreasing the hepatic energy state (31). Treatment of cells with metformin activated AMPK and suppressed replication of HCV in a concentration-dependent manner in Huh-7.5 cells (Fig. 3a). However, co-incubation of cells with compound C, an inhibitor of AMPK, did not prevent metformin-mediated suppression of HCV replication (Fig. 3b, lane 3). Relatively speaking, compound C enhances the suppression of HCV replication induced by metformin. Likewise, compound C promoted suppression of HCV replication when the cells were cultured under conditions of glucose shortage (Fig. 3c, lane 3). These results demonstrate that glucose shortage and metformin inhibit HCV replication independently of AMPK activation.

The effects of adenosine monophosphate-activated protein kinase activators/inhibitor on hepatitis C virus non-structural protein 3

Finally, we tested the effects of AMPK activators/inhibitor on the expression of other HCV protein besides core protein (Fig. 4). As shown, treatment of cells with AICAR, metformin or glucose shortage suppressed the expression of NS3 protein. In addition, compound C attenuated the anti-HCV effect of AICAR, whereas it enhanced the anti-HCV effect of metformin or glucose shortage. These results support the conclusion that AMPK activators/inhibitor affect the replication of HCV, as demonstrated by the expression of HCV core protein (Figs. 1–3).

DISCUSSION

Previous reports have suggested that HCV infection directly causes insulin resistance, resulting in the progression of diabetes (32,33). Moreover it has been reported that insulin resistance is a negative predictor of the response to antiviral therapy in chronic hepatitis C patients treated with peginterferon plus ribavirin (4). However, the association between virus proliferation and hyperglycemia due to insulin resistance remains elusive. In this study, we have demonstrated that HCV proliferation is promoted in Huh-7.5 cells cultured at 4.5 g/L glucose, the equivalent of the blood glucose concentrations of diabetes patients (Fig. 1). This result suggests that intensive control of glucose concentrations would aid antiviral therapy in hepatitis C patients with diabetes.

We have demonstrated that activation of AMPK suppresses HCV replication (Fig. 2). This result suggests that AMPK as a potential target for the treatment of chronic hepatitis C. Therapeutic interest has recently been increased by the findings that hepatic AMPK is activated by adiponectin (34) and by thiazolidinedione-type antidiabetic drugs (35). Pharmacological activation of AMPK may provide a new strategy for both the management of chronic hepatitis C itself and metabolic hepatic disorders linked to HCV infection.

Adenosine monophosphate-activated protein kinase, a major energy sensor, is activated by energy depletion. AMPK is directly activated by AICAR, being metabolized to ZMP in the cell, regardless of the cellular energy status (6). We have demonstrated that AICAR-mediated suppression of HCV proliferation is AMPK-dependent

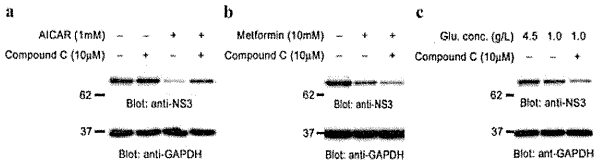

Fig. 4. AMPK activators/inhibitors' effect on the expression of HCV NS3 protein. Huh-7.5 cells were infected with HCV at a MOI of 3.0 for 4 hr. The cells were treated with the indicated reagents. Cell lysates were separated by SDS-PAGE and analyzed by immunoblotting with anti-HCV NS3 and anti-GAPDH antibodies. The results are representative of three independent experiments.

(Fig. 2). In terms of phosphorylation of AMPK, the most effective concentration of AICAR was 0.5 mM, whereas the most effective concentration of AICAR for suppression of HCV replication was clearly 1.0 mM. One of the possible explanations of this discrepancy is that the former immunoblot shows the state of AMPK phosphorylation at the endpoint of the experiment, whereas the latter immunoblot reflects the accumulation of the expression of core protein during the whole period of the experiment. Compound C, a specific AMPK inhibitor that competes with ATP (36), could inhibit the effect of AICAR on HCV proliferation (Fig. 2b). Compound C did not completely reverse the suppressive effect of AICAR treatment on HCV replication. In general, inhibitors do not completely suppress the effect of reagents or enzymes; however it is still possible that the suppression of HCV replication by AICAR cannot be explained purely by activation of AMPK. Uridine as a source of pyrimidine could also prevent the effect of AICAR (Fig. 2c). Moreover, we focused on another mechanism of AICAR-mediated inhibition of HCV replication. Activated AMPK causes inhibitions of fatty acids and cholesterol synthesis. Recent reports have shown a crucial involvement of fatty acids, cholesterol and lipid droplets in infectious virion production (37–40). Therefore, we predicted that AICAR-mediated inhibition of HCV replication might be due to lipid depletion. To investigate this possibility, we added mevalonolactone and/or oleic acid in the presence of AICAR to the cell culture medium, and then examined the replication of HCV. However, the addition of lipids had almost no effect on AICAR-mediated suppression of HCV (Fig. S1). This suggests that HCV replication does not require additional lipids when the cells are treated with AICAR, which shifts cellular metabolism from energy expenditure to energy production by activating AMPK.

Cell confluency is known to activate AMPK, and LKB1 is a major kinase that activates AMPK. Replication of the HCV replicon is known to be inhibited in confluent Huh-7 cells (41). Replication of HCV replicon in HeLa cells, a known LKB1-deficient cell line, is not affected by their confluence (42). These data suggest that confluence-mediated suppression of HCV replication requires the LKB1-AMPK pathway. Our experiments demonstrated that confluence of cells can activate AMPK and suppress replication of HCV in Huh-7.5 cells (Fig. S2). It is still not clear whether this anti-HCV effect is due to relative undernutrition resulting from increased cell numbers or the activation of AMPK by the confluence itself.

Culturing cells under a shortage of glucose or with metformin can activate cellular AMPK and suppress replication of HCV in the cells (Fig. 1 and 3). Under such low energy conditions, compound C, a specific AMPK inhibitor, can induce further suppression of HCV replication. The explanation of this phenomenon is as follows: AMPK is activated in order to restore energy status. In the presence of glucose depletion or energy limitations by metformin, compound C-induced AMPK inhibition may lead to failure to maintain ATP concentrations. Various compensatory mechanisms may maintain intracellular ATP concentrations. In other words, under energy limitations the breakdown of the fuel gauge, AMPK, may proceed to imbalance in metabolism leading to poor replication of HCV. Recent reports have shown that metformin therapy is associated with a reduced hepatocarcinogenesis risk in type 2 diabetes patients (43) and an improvement of sustained virological response in chronic hepatitis C patients (44). The present study provides evidence for the possibility that not only metformin monotherapy, but also AMPK inhibitor and metformin combination therapy, may be helpful in the treatment of chronic hepatitis C.

In a previous study using JFH-1 strain of HCV and Huh-7 cells, it was reported that HCV-infection causes $Ser^{485/491}$ phosphorylation of AMPK and inhibits the kinase activity of AMPK. Inhibition of AMPK facilitates HCV replication (26). In the present study using Huh-7.5 cells and a J6/JFH1-derived, cell-adapted strain of HCV, inhibition of AMPK by HCV replication was not observed. Moreover, phosphorylation of $Ser^{485/491}$ was not affected by HCV-infection (Fig. 1c). Since this experimental system using Huh-7.5 and the cell-adapted HCV strain produces

infectious HCV particles efficiently, inhibition of AMPK by HCV replication may play a minor role in efficient HCV replication. In addition, a previous study having shown that AMPK activators suppress HCV replication, we further investigated the mechanisms of AMPK involvement in HCV replication by using a specific AMPK inhibitor. AICAR-induced AMPK activation plays a critical role in the suppression of HCV (Fig. 2), meanwhile AMPK inhibitor rather potentiates the anti-HCV effects of metformin or glucose shortage (Fig. 3). These data suggest that AMPK activation does not simply lead to an anti-HCV effect.

In conclusion, we have shown the replication of HCV by AMPK-dependent and -independent mechanisms in Huh-7.5 cells. HCV does not replicate efficiently under the low energy conditions that activate AMPK. Hence, correction of hyperglycemia in hepatitis C patients should have a beneficial effect on anti-HCV therapy and the clinical course of hepatitis C. We suggest that AMPK is a therapeutic target for the treatment of chronic hepatitis C patients.

ACKNOWLEDGMENTS

The authors are grateful to Dr. C. M. Rice (The Rockefeller University, New York, NY, USA) for providing pFL-J6/JFH1 and Huh7.5 cells, to Dr. Takaji Wakita (National Institute of Infectious Diseases, Tokyo, Japan) for providing pSGR-JFH1 and to Ms. Satomi Nishibata and Ms. Kuniyo Miyagoshi for their assistance. This work was supported in part by Grant-in-Aids from the Japan Society for the Promotion of Science; the Ministry of Education, Culture, Sports, Science and Technology, Japan; the Ministry of Health, Labor and Welfare, Japan; JST/JICA SATREPS; the Yakult Foundation; and research grants from the University of Fukui, and Organization for Life Science Advancement Programs, University of Fukui.

DISCLOSURE

The authors who have taken part in this study declare that they do not have anything to disclose regarding funding or conflict of interest with respect to this manuscript.

REFERENCES

1. Manns M.P., Foster G.R., Rockstroh J.K., Zeuzem S., Zoulim F., Houghton M. (2007) The way forward in HCV treatment–finding the right path. *Nat Rev Drug Discov* **6**: 991–1000.
2. Inoue M., Kurahashi N., Iwasaki M., Tanaka Y., Mizokami M., Noda M., Tsugane S. (2009) Metabolic factors and subsequent risk of hepatocellular carcinoma by hepatitis virus infection status: a large-scale population-based cohort study of Japanese men and women (JPHC Study Cohort II). *Cancer Causes Control* **20**: 741–50.
3. Bressler B.L., Guindi M., Tomlinson G., Heathcote J. (2003) High body mass index is an independent risk factor for nonresponse to antiviral treatment in chronic hepatitis C. *Hepatology* **38**: 639–44.
4. Romero-Gomez M., Del Mar Viloria M., Andrade R.J., Salmeron J., Diago M., Fernandez-Rodriguez C.M., Corpas R., Cruz M., Grande L., Vazquez L., Munoz-De-Rueda P., Lopez-Serrano P., Gila A., Gutierrez M.L., Perez C., Ruiz-Extremera A., Suarez E., Castillo J. (2005) Insulin resistance impairs sustained response rate to peginterferon plus ribavirin in chronic hepatitis C patients. *Gastroenterology* **128**: 636–41.
5. Carling D., Clarke P.R., Zammit V.A., Hardie D.G. (1989) Purification and characterization of the AMP-activated protein kinase. Copurification of acetyl-CoA carboxylase kinase and 3-hydroxy-3-methylglutaryl-CoA reductase kinase activities. *Eur J Biochem* **186**: 129–36.
6. Corton J.M., Gillespie J.G., Hawley S.A., Hardie D.G. (1995) 5-aminoimidazole-4-carboxamide ribonucleoside. A specific method for activating AMP-activated protein kinase in intact cells? *Eur J Biochem* **229**: 558–65.
7. Dyck J.R., Gao G., Widmer J., Stapleton D., Fernandez C.S., Kemp B.E., Witters L.A. (1996) Regulation of 5'-AMP-activated protein kinase activity by the noncatalytic beta and gamma subunits. *J Biol Chem* **271**: 17798–803.
8. Hawley S.A., Boudeau J., Reid J.L., Mustard K.J., Udd L., Makela T.P., Alessi D.R., Hardie D.G. (2003) Complexes between the LKB1 tumor suppressor, STRAD alpha/beta and MO25 alpha/beta are upstream kinases in the AMP-activated protein kinase cascade. *J Biol* **2**: 28
9. Woods A., Johnstone S.R., Dickerson K., Leiper F.C., Fryer L.G., Neumann D., Schlattner U., Wallimann T., Carlson M., Carling D. (2003) LKB1 is the upstream kinase in the AMP-activated protein kinase cascade. *Curr Biol* **13**: 2004–8.
10. Hawley S.A., Pan D.A., Mustard K.J., Ross L., Bain J., Edelman A.M., Frenguelli B.G., Hardie D.G. (2005) Calmodulin-dependent protein kinase kinase-beta is an alternative upstream kinase for AMP-activated protein kinase. *Cell Metab* **2**: 9–19.
11. Woods A., Dickerson K., Heath R., Hong S.P., Momcilovic M., Johnstone S.R., Carlson M., Carling D. (2005) Ca2+/calmodulin-dependent protein kinase kinase-beta acts upstream of AMP-activated protein kinase in mammalian cells. *Cell Metab* **2**: 21–33.
12. Hawley S.A., Davison M., Woods A., Davies S.P., Beri R.K., Carling D., Hardie D.G. (1996) Characterization of the AMP-activated protein kinase kinase from rat liver and identification of threonine 172 as the major site at which it phosphorylates AMP-activated protein kinase. *J Biol Chem* **271**: 27879–87.
13. Munday M.R., Campbell D.G., Carling D., Hardie D.G. (1988) Identification by amino acid sequencing of three major regulatory phosphorylation sites on rat acetyl-CoA carboxylase. *Eur J Biochem* **175**: 331–8.
14. Clarke P.R., Hardie D.G. (1990) Regulation of HMG-CoA reductase: identification of the site phosphorylated by the AMP-activated protein kinase *in vitro* and in intact rat liver. *EMBO J* **9**: 2439–46.
15. Horman S., Browne G., Krause U., Patel J., Vertommen D., Bertrand L., Lavoinne A., Hue L., Proud C., Rider M. (2002) Activation of AMP-activated protein kinase leads to the phosphorylation of elongation factor 2 and an inhibition of protein synthesis. *Curr Biol* **12**: 1419–23.
16. Lochhead P.A., Salt I.P., Walker K.S., Hardie D.G., Sutherland C. (2000) 5-aminoimidazole-4-carboxamide riboside mimics the effects of insulin on the expression of the 2 key gluconeogenic genes PEPCK and glucose-6-phosphatase. *Diabetes* **49**: 896–903.